

②  
AD A 123468

SAI DOCUMENT NO. SAI-067-83R-006

# **MANEUVERING AEROTHERMAL TECHNOLOGY (MAT) PROGRAM**

## **A METHOD FOR COUPLED THREE--DIMENSIONAL INVISCID AND INTEGRAL BOUNDARY LAYER CALCULATIONS**

SCIENCE APPLICATIONS, INC.  
APPLIED MECHANICS OPERATION  
WAYNE, PENNSYLVANIA 19087

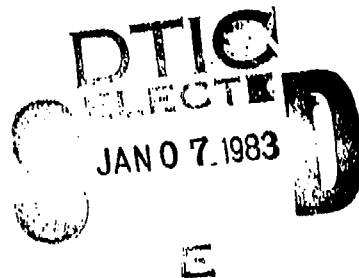
MAY 1982

FINAL REPORT FOR PERIOD 16 MAY 1980 - 15 FEBRUARY 1982

CONTRACT NO. F04701-80-C-0033

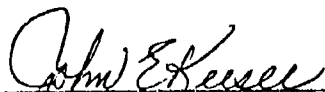
APPROVED FOR PUBLIC RELEASE; DISTRIBUTION UNLIMITED

AIR FORCE BALLISTIC MISSILE OFFICE  
NORTON AIR FORCE BASE, CALIFORNIA 92409

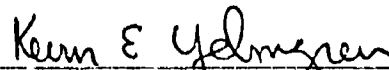


83 1 7 069

This Final Report was submitted by Science Applications, Inc., 994 Old Eagle Road, Valley Forge PA 19087 under Contract Number FO4701-80-C-0033, with the Ballistic Missile Office, AFSC, Norton AFB, California. Capt John E. Keesee, BMO/SYMS, was the Project Officer in charge. This Technical Report has been reviewed and is approved for publication.



JOHN E. KEESEE, Capt, USAF  
Project Officer  
Advanced Systems  
Advanced Strategic Missile Systems



KEVIN E. YELMGREN, Major, USAF  
Chief, Advanced Systems Division  
Advanced Strategic Missile Systems

FOR THE COMMANDER



RICHARD T. WILLIAMS, Lt Col, USAF  
Director, Missile Systems  
Advanced Strategic Missile Systems

UNCLASSIFIED

SECURITY CLASSIFICATION OF THIS PAGE (When Data Entered)

REPORT DOCUMENTATION PAGE		READ INSTRUCTIONS BEFORE COMPLETING FORM
1. REPORT NUMBER BMO-TR-82-37	2. GOVT ACCESSION NO. <i>A123 468</i>	3. RECIPIENT'S CATALOG NUMBER
4. TITLE (and Subtitle) Maneuvering Aerothermal Technology (MAT) Program: A Method for Coupled Three-Dimensional Inviscid and Integral Boundary Layer Calculations		5. TYPE OF REPORT & PERIOD COVERED Final Report for Period 16 May 1980 - 15 Feb. 1982
7. AUTHOR(s) Darryl W. Hall Calvin J. Wolf Thomas B. Harris Alvin L. Murray		6. PERFORMING ORG. REPORT NUMBER SAI-067-83R-006
9. PERFORMING ORGANIZATION NAME AND ADDRESS Science Applications, Inc. 994 Old Eagle School Road, Suite 1018 Wayne, Pennsylvania 19087		8. CONTRACT OR GRANT NUMBER(s) F04701-80-C-0033
11. CONTROLLING OFFICE NAME AND ADDRESS Ballistic Missile Office (BMO/SYMST) Norton Air Force Base, California 92409		10. PROGRAM ELEMENT, PROJECT, TASK AREA & WORK UNIT NUMBERS Tasks 3.1 - 3.3
14. MONITORING AGENCY NAME & ADDRESS (if different from Controlling Office)		12. REPORT DATE May 1982
		13. NUMBER OF PAGES 138
		15. SECURITY CLASS. (of this report) Unclassified
		15a. DECLASSIFICATION/DOWNGRADING SCHEDULE
16. DISTRIBUTION STATEMENT (of this Report)  Approved for Public Release: Distribution Unlimited.		
17. DISTRIBUTION STATEMENT (of the abstract entered in Block 20, if different from Report)		
18. SUPPLEMENTARY NOTES		
19. KEY WORDS (Continue on reverse side if necessary and identify by block number) Flow Field Boundary Layers Inviscid Flows Maneuvering Reentry Vehicles		
20. ABSTRACT (Continue on reverse side if necessary and identify by block number)  ➤ A procedure is developed for computing the complete flow field over maneuvering reentry vehicles by coupling a finite difference inviscid flow field code to an integral boundary layer procedure. Viscous calculations are performed along inviscid surface streamlines, which are explicitly computed in the inviscid code. The detailed inviscid flow field solution is used to accurately define the required boundary layer edge properties. The boundary layer procedure can treat laminar, transitional, or turbulent flows, and surface (over)		

UNCLASSIFIED

SECURITY CLASSIFICATION OF THIS PAGE(When Data Entered)

→ roughness and mass addition effects. Approximate techniques are provided to define the wall temperatures and mass addition rates of ablating heatshields.  
↑

UNCLASSIFIED

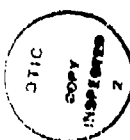
SECURITY CLASSIFICATION OF THIS PAGE(When Data Entered)

# FOREWORD

This report describes the coupling of an inviscid flow field code (3IS) to an integral boundary layer procedure (3DMEIT) to provide a complete flow field prediction capability for maneuvering reentry vehicles. This effort was performed as part of Task 3 (Flow Field Effects) of the Maneuvering Aerothermal Technology (MAT) Program, Contract Number F04701-80-C-0033, for the Air Force Ballistic Missile Office. The project officer for this effort is Captain John Keese, BMO/SYMST.

This study was conducted by personnel of Science Applications, Inc., Valley Forge, Pennsylvania, with work on the 3DMEIT integral boundary layer code being performed by personnel of the Aerotherm Division of the Acurex Corporation, Mountain View, California, on a subcontract from SAI.

Accession For	
DTIC GRANT	<input checked="" type="checkbox"/>
DTIC TAB	<input type="checkbox"/>
Unannounced	<input type="checkbox"/>
Justification	
By	
Distribution/	
Availability Codes	
Dist	Approved/or
	Special
<i>A</i>	



RE: Classified References, Distribution  
Unlimited  
No change per Mr. F. A. Gridley, BMO/AWD

# TABLE OF CONTENTS

	<u>Page</u>
DD1473 (ABSTRACT) . . . . .	i
FOREWORD . . . . .	iii
TABLE OF CONTENTS . . . . .	1
LIST OF FIGURES . . . . .	3
LIST OF TABLES . . . . .	4
NOMENCLATURE . . . . .	5
SECTION 1 INTRODUCTION . . . . .	7
SECTION 2 APPROACH AND ASSUMPTIONS . . . . .	10
SECTION 3 INVISCID FLOW FIELD SOLUTION . . . . .	14
3.1 BLUNT BODY CODE DESCRIPTION . . . . .	14
3.2 AFTERBODY CODE DESCRIPTION . . . . .	15
3.3 INVISCID SURFACE STREAMLINE CALCULATION . . . . .	15
3.3.1 Spherical Nosetip Streamline Calculation . . . . .	16
3.3.2 Afterbody Streamline Calculation . . . . .	19
3.4 USER INSTRUCTIONS . . . . .	20
3.4.1 Input and Output . . . . .	20
3.4.2 Inviscid Flow Field File Description . . . . .	21
SECTION 4 BOUNDARY LAYER SOLUTION . . . . .	23
4.1 INTRODUCTION . . . . .	23
4.2 3DMEIT METHODOLOGY . . . . .	24
4.2.1 Basic Equations . . . . .	24
4.2.2 Shape Factor, Recovery Factor, Stanton Number and Friction Coefficient . . . . .	26
4.2.3 Transition Criteria . . . . .	37
4.2.4 Surface Roughness Modeling . . . . .	37
4.2.5 Surface Temperature and Ablation Modeling . . . . .	38
4.2.5.1 Wall Gas Enthalpy . . . . .	39
4.2.5.2 Graphite Ablation Option . . . . .	40
4.2.5.3 Carbon Phenolic Ablation Option . . . . .	42
4.2.5.4 Teflon Ablation Option . . . . .	42

# TABLE OF CONTENTS (Cont'd)

	<u>Page</u>
4.2.6 Edge Entropy Models . . . . .	43
4.2.7 Induced Pressure Models . . . . .	46
4.2.8 Solutions of the Boundary Layer Integral Equations . . . . .	46
4.3 GEOMETRIC ANALYSES . . . . .	50
4.4 USER INSTRUCTIONS . . . . .	55
4.4.1 Input Instructions . . . . .	55
4.4.2 Output Description . . . . .	77
4.4.2.1 Printout of Input Data . . . . .	77
4.4.2.2 Calculation Output . . . . .	77
4.4.3 Sample Problem . . . . .	84
SECTION 5 RESULTS . . . . .	118
SECTION 6 CONCLUSIONS . . . . .	131
SECTION 7 REFERENCES . . . . .	133

# LIST OF FIGURES

<u>No.</u>	<u>Title</u>	<u>Page</u>
3.1	2IT and 3IS Coordinate Systems . . . . .	17
4.1	Schematic of Boundary Layer Entrainment . . . . .	44
4.2	Schematic of Viscous and Inviscid Profiles Used in Mass Flux Balance . . . . .	45
4.3	Patch Input Geometry . . . . .	53
4.4	Illustrations of Geometry Descriptions . . . . .	63
4.5	Geometry Descriptions for Option 3 . . . . .	64
4.6	View Orientation Angles . . . . .	76
5.1	Comparison of 3DMEIT with HYTAC Data Group 159, Laminar, $M = 10$ , $\alpha = 0$ . . . . .	120
5.2	Axial Heat Transfer Distributions, Groups 96, 97, 136 to 158 Laminar, $M = 10$ , $\alpha = 5$ . . . . .	122
5.3	Circumferential Heat Transfer Distributions, Groups 96, 97, 136 to 158 Laminar, $M = 10$ , $\alpha = 5^\circ$ . . . . .	123
5.4	Circumferential Heat Transfer Distributions, Phase IV, Turbulent, $M = 8$ , $\alpha = 10^\circ$ . . . . .	124
5.5	Axial Heat Transfer Distributions, Phase IV, Turbulent, $M = 8$ , $\alpha = 10^\circ$ . . . . .	125
5.6	Inviscid Surface Pressure Distribution Compared with HYTAC Data, $M = 8$ , $\alpha = 10^\circ$ . . . . .	126
5.7	Inviscid Surface Pressure Distributions Compared with HYTAC Data, $M = 8$ , $\alpha = 10^\circ$ . . . . .	127
5.8	Flight Case Geometry with Yaw Stabilizers . . . . .	128
5.9	Predicted Axial Heating Distributions at Flight Con- ditions, 10.4/6.0 Biconic with Yaw Stabilizers, $M = 16$ , $\alpha = 5^\circ$ . . . . .	129
5.10	Predicted Circumferential Heating Distributions at Flight Conditions, 10.4/6.0 Biconic with Yaw Stabilizers, $M = 16$ , $\alpha = 5^\circ$ . . . . .	130



# LIST OF TABLES

<u>No.</u>	<u>Title</u>	<u>Page</u>
4.1	Notation for Influence Coefficients . . . . .	29
4.2	Coefficient for the Turbulent Wall Shear Roughness Influence Coefficient . . . . .	34
4.3	Functions $f_2$ and $f_3$ for the Turbulent Heat Transfer Roughness Influence Coefficient . . . . .	35
5.1	Test Case Conditions . . . . .	119

# NOMENCLATURE

$B'$	Blowing parameters
$C_m$	Stanton number for mass transfer
$h$	Enthalpy
$h_c$	Solid (graphite or char layer) enthalpy
$h_g$	Phenolic resin gas enthalpy
$h_\beta$	Streamline metric coefficient
$\dot{m}$	Mass flux
$\dot{m}_c$	Thermochemical graphitic blowing rate
$\dot{m}_g$	Phenolic resin gas blowing rate
$M$	Mach number
$p$	Pressure
$Pr$	Prandtl number
$\dot{q}$	Heat flux
$\dot{q}_c$	Convective heat flux
$\dot{q}_R$	Re-radiative heat flux
$r$	Radial coordinate
$Re$	Reynolds number
$R_N$	Nose radius
$s$	Stream length measured from the stagnation point
$T$	Temperature
$u$	Streamwise velocity component (3DMEIT); radial velocity component (3IS)
$U$	Radial velocity component (2IT)
$v$	Body normal velocity component (3DMEIT); circumferential velocity component (3IS)
$w$	Axial velocity component (3IS)
$y$	Distance in surface normal direction

$Y$	Polar coordinate (2IT)
$z$	Axial coordinate (3IS)
$\alpha$	Angle of attack
$\theta$	Boundary layer momentum thickness; circumferential coordinate (3IS)
$\theta_b$	Body angle relative to the centerline
$\theta'$	Circumferential coordinate (2IT)
$\mu$	Viscosity
$\rho$	Density
$\phi$	Boundary layer energy thickness

#### Subscripts

$e$	Boundary layer edge
$i$	Inviscid flow
$\ell$	Laminar flow
$r$	Recovery state
$t$	Turbulent flow or stagnation conditions
$te$	Stagnation conditions at the boundary layer edge
$tiw$	Inviscid stagnation conditions at the wall
$tr$	Transition point
$w$	Wall

## SECTION 1

### INTRODUCTION

For most reentry vehicles and missions, the aerothermal environment of primary concern for vehicle design is the lower altitude flight regime ( $h \leq 120$  KFT), where peak aerodynamic loads and heating are experienced. Successful design and analysis of maneuvering reentry vehicles require the ability to accurately predict this aerothermal environment, where the Reynolds number is sufficiently large that the shock layer flow is primarily inviscid, with viscous effects confined to the thin boundary layer adjacent to the vehicle surface and to leeside regions of separated flow at high angles of attack.

Sophisticated flow field prediction techniques have been developed that directly compute the entire shock layer, both inviscid and viscous regions, eliminating the need for explicit coupling between the inviscid and viscous portions of the flow. These techniques, the parabolized Navier-Stokes (PNS) procedures, are thus capable of rigorously treating higher altitudes (where the boundary layer is not thin), as well as leeside separated flow regions. (A review of the current PNS methods was performed as part of the MAT program and is documented in Reference 1.)

These detailed PNS solutions, however, generally require a large amount of computer time and presently do not constitute a design technique. Consequently, more efficient inviscid flow field techniques are often used to predict the aerodynamic forces and moments (e.g., normal force, pitching moment, and inviscid contribution to the axial force). Boundary layer calculations are used to determine both the heat transfer

to the body and the viscous shear forces, with the required boundary layer edge conditions being obtained from the inviscid solution. This coupled inviscid-boundary layer solution procedure has been widely used to obtain accurate flow field predictions for both ballistic and maneuvering re-entry vehicles.

For engineering calculations, the most appropriate approach for boundary layer predictions is the technique in which integral boundary layer equations are obtained by integrating the fundamental boundary layer equations across the layer. The solution of the resulting equations determines the viscous parameters of primary interest - shear stress, heat transfer, boundary layer thicknesses, etc. - but does not provide definition of specific details such as velocity and temperature profiles across the viscous layer. For three-dimensional problems, the integral boundary layer method is usually applied by integrating the axisymmetric integral equations along inviscid surface streamlines. Although this approach, termed the "small cross-flow approximation," neglects the cross-flow profiles in the boundary layer at angle of attack, it has been successfully applied to many RV configurations, providing reasonably accurate boundary layer solutions with great efficiency.

As part of the BMO Maneuvering Aerothermal Technology (MAT) program, an existing state-of-the-art three-dimensional inviscid flow field code has been coupled to an extension of an existing integral boundary layer solution procedure in order to provide the capability for efficient inviscid/viscous flow field solutions on maneuvering reentry vehicles, while taking maximum advantage of the inherent capabilities of the codes being coupled. The inviscid code used in this coupling procedure is the

BMO/3IS code, which is described in References 2-4. (The review of inviscid flow field codes for application to MaRV configurations conducted under the MAT program is documented in Reference 5.) The integral boundary layer code used is an extension of the Momentum-Energy Integral Technique (MEIT), described in References 6-10, which, unlike many integral boundary layer techniques, solves both the momentum and energy integral equations rather than invoking the Reynolds analogy to relate heat transfer and skin friction.

The approach taken in this coupling effort is described in Section 2 of this report, which also details the assumptions made. The inviscid flow field code used in this effort is briefly described in Section 3, as is the procedure developed in this effort to compute the inviscid surface streamlines. Details on the 3DMEIT integral boundary layer solution technique are provided in Section 4.

## SECTION 2

### APPROACH AND ASSUMPTIONS

The goal of this effort is the development of an efficient, robust, reliable procedure for computing complete flow fields on maneuvering reentry vehicles in the high Reynolds number flight regime, where the thin boundary layer assumption is valid. In this regime, the inviscid portion of the shock layer can be accurately computed without regard to the boundary layer, and the boundary layer solution can be determined using edge conditions obtained from the inviscid solution.

In this task, the BMO/3IS three-dimensional flow field code is used to define the inviscid shock layer, and an extension to the MEIT integral boundary layer procedure is used to determine the viscous flow. This extension, called 3DMEIT, solves the integral boundary layer equations along inviscid surface streamlines to efficiently model the three-dimensional boundary layer using the "small cross-flow" assumption. The coupling procedure developed in this effort provides definition of the inviscid surface streamlines and flow field properties obtained from the inviscid solution in a format compatible with the 3DMEIT boundary layer procedure.

A unique feature of this coupling procedure is the method used to define the inviscid surface streamlines. In previous 3-D integral boundary layer solutions, such as those described in References 11 and 12, the inviscid streamlines were determined in an approximate manner using the surface pressure distribution obtained from the inviscid flow field solution. In the current effort, the inviscid surface streamlines are

computed explicitly as part of the inviscid flow field procedure; this technique is described in Section 3.

Another unique feature of the coupled 3IS/3DMEIT flow field procedure is the method used for defining boundary layer edge properties. Rather than determining the edge entropy from a stream tube entrainment procedure (which works well for axisymmetric configurations at zero angle of attack, but is difficult to apply in three dimensional problems), the edge conditions are determined using a mass balance between the inviscid and boundary layer flows, using the detailed information available from the finite difference inviscid solution. This procedure is described in Section 4.2.6.

A buffer code has been developed to handle the coupling between the 3IS and 3DMEIT codes. This buffer code accepts as input the 3IS solution output file and defines the inviscid surface streamlines to be used by 3DMEIT in the boundary layer calculations. The format of the buffer code output is described in Section 3.4.

Several requirements were established for the 3DMEIT code in this effort. These requirements were:

- the ability to treat equilibrium air thermodynamics, in a manner consistent with the 3IS inviscid code
- the ability to automatically determine the wall temperature and mass addition rates for ablating heatshields using steady state ablation models (or, as an option, allow values of  $T_w$  and  $\dot{m}$  to be input by the user)
- the ability to treat laminar, transitional, or fully turbulent flows.

These capabilities of the 3DMEIT code, and others that have been implemented, are described in Section 4 of this report.



The coupled 3IS/3DMEIT procedure is applicable to any vehicle geometry which the inviscid (3IS) code is capable of treating. 3IS is formulated in a cylindrical coordinate system and allows the definition of generated afterbody cross-sections. Special geometry procedures are included to allow simple specification of multi-conics with slices, cuts and flaps. (Short-comings do exist in the current ability of 3IS to execute calculations over moderate to large flap deflection angles; however, activities are now underway to eliminate this limitation.) The ability of the 3IS/3DMEIT technique to treat control surfaces is partially demonstrated in the sample calculation in Section 4.4.3 which involves a fixed yaw stabilizer (FYS).

The intended emphasis of this effort was to develop and demonstrate a valid 3IS/3DMEIT coupling for afterbody applications. Therefore it was decided to initially restrict attention to spherical nosetip shapes. The axisymmetric 2IT nosetip code is currently used to determine the inviscid flow profiles associated with the streamlines on a sphere. This limitation can be removed by using the CM3DT blunt body code for the treatment of non-spherical, asymmetric nosetip shapes. It is necessary to simply calculate the streamlines paths from a converged CM3DT solution and transmit the corresponding inviscid flow field information to the buffer code.

In addition, the coupled 3IS/3DMEIT flow field procedure currently cannot treat non-zero sideslip angles because the 3DMEIT geometry routine is restricted to the description of bodies over a half-plane. The inviscid codes (blunt body and afterbody) which are used to provide the inviscid flow field information necessary to drive

the boundary layer solutions are fully capable of performing calculations for bodies at yaw. Thus, the current limitation to zero sideslip is not due to fundamental restrictions on the techniques themselves, but is simply a consequence of the 3DMEIT geometry description.

## SECTION 3

### INVISCID FLOW FIELD SOLUTION

The inviscid frustum flow field technique used in this effort is the BMO/3IS code. Since spherical nosetips are assumed in this initial effort, the required initial data for the 3IS afterbody calculations are obtained from the axisymmetric 2IT nosetip flow field code. Both the 2IT and 3IS codes are documented in References 2-4 and are briefly described in Sections 3.1 and 3.2 below.

Sections 3.3 and 3.4 describe the buffer code developed to handle the interface between the inviscid codes and the 3DMEIT boundary layer procedure and the user instructions for this buffer code.

#### 3.1 BLUNT BODY CODE DESCRIPTION

Inviscid flow field solutions on spherical nosetips are readily obtained with the time-dependent axisymmetric 2IT code. This code obtains the steady state solution as the asymptotic limit of an unsteady flow, starting from an assumed initial flow field. The time-dependent inviscid flow equations are solved using the MacCormack finite difference procedure.

Formulated in a spherical coordinate system, the 2IT code is ideally suited to the calculation of flows on spherical nosetips, since the grid is perfectly aligned with the body geometry. Calculations on spheres with 2IT are always performed in wind-fixed coordinates; appropriate initial data for the 3IS afterbody code at angle of attack are determined by interpolation and rotation of the 2IT solution. The 2IT code can treat either ideal gas or equilibrium air thermodynamics.

### 3.2 AFTERBODY CODE DESCRIPTION

Inviscid afterbody flow field solutions are obtained for this effort with the 3IS code. This code is a forward marching, steady, finite difference flow field solution procedure, and requires only that the axial component of the flow in the frustum shock layer be supersonic at all points.

3IS is formulated in a cylindrical coordinate system and allows the definition of generalized afterbody cross-sections. Alternatively, special geometry procedures have been implemented in the code to allow simple specification of multi-conics with slices, cuts, and flaps. Coordinate stretching can be used in the 3IS code to circumferentially concentrate mesh points in either the pitch or yaw planes. In addition, recent modifications to this code<sup>13</sup> also permit radial clustering of mesh points near the body to improve resolution of the flow gradients near the wall. Either ideal gas or equilibrium air thermodynamics can be used in the 3IS calculation procedure.

### 3.3 INVISCID SURFACE STREAMLINE CALCULATION

Inviscid surface streamlines are defined for the coupled 3IS/3DMEIT procedure through explicit streamline calculations in the 3IS inviscid afterbody code. The inviscid streamlines on the spherical nose-tip are readily defined by noting that the streamlines remain in meridional planes in wind-fixed coordinates on the sphere.

It is critical in this coupled inviscid-boundary layer approach to ensure that the selected inviscid streamlines along which boundary layer solutions are to be obtained provide complete coverage of the body. To accomplish this goal, the selected streamlines include those

streamlines that are equally spaced circumferentially at the initial afterbody plane (at the nosetip tangency point) as well as those that are equally spaced circumferentially at the end of the body. This choice allows complete coverage of the body, since at angle of attack the equally spaced streamlines at the initial plane will be swept around the body and will be concentrated near the lee plane at the end of the body, while those streamlines equally spaced at the end of the body will all originate near the wind plane at the initial plane.

The details on the streamline calculation procedures used on the nosetip and the frustum are provided in Sections 3.3.1 and 3.3.2, respectively, below.

### 3.3.1 SPHERICAL NOSETIP STREAMLINE CALCULATION

The relationship between the 3IS ( $r, \theta, z$ ) cylindrical coordinate system and the 2IT ( $R, \theta', Y$ ) wind-fixed spherical coordinate system is depicted in Figure 3.1. The locations of the required inviscid surface streamlines at the 3IS initial data plane are assumed to be known, and are defined by specifying the appropriate value of  $\theta$  for each streamline. The track of each of these streamlines on the nosetip is readily defined by  $\theta' = \text{constant}$  on the sphere. The problem thus reduces to determining the relationship between  $\theta$  (3IS coordinates) and  $\theta'$  (2IT coordinates) at the initial data plane.

The relationship between  $\theta$  and  $\theta'$  may be written as

$$\tan \theta' = \frac{R_N \cos \theta_{b1} \sin \theta}{\frac{R_N}{\sin \theta_{b1}} - z_1 \sin \alpha + R_N \cos \theta_{b1} \cos \theta \cos \alpha} \quad (3.1)$$

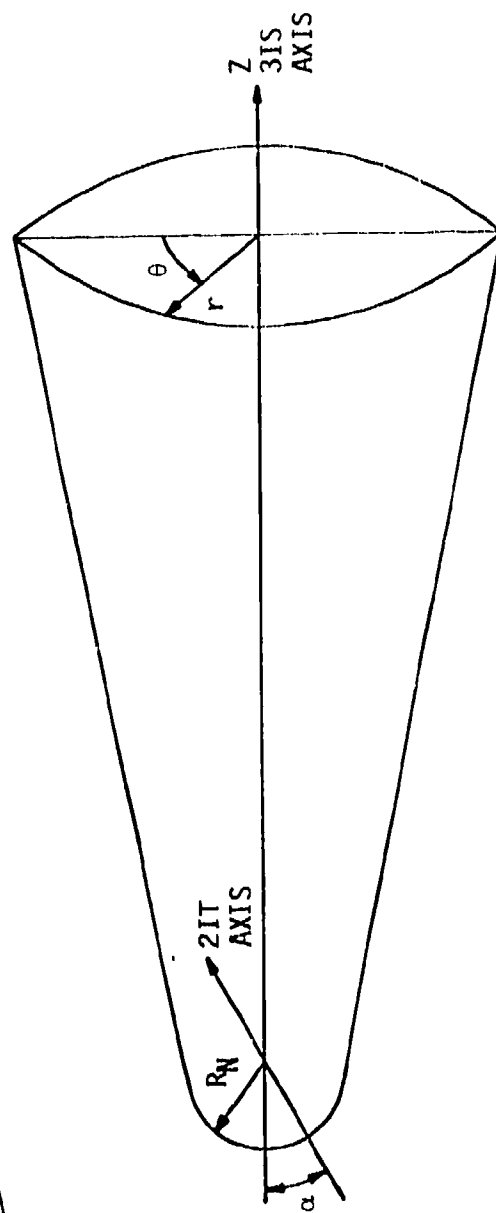
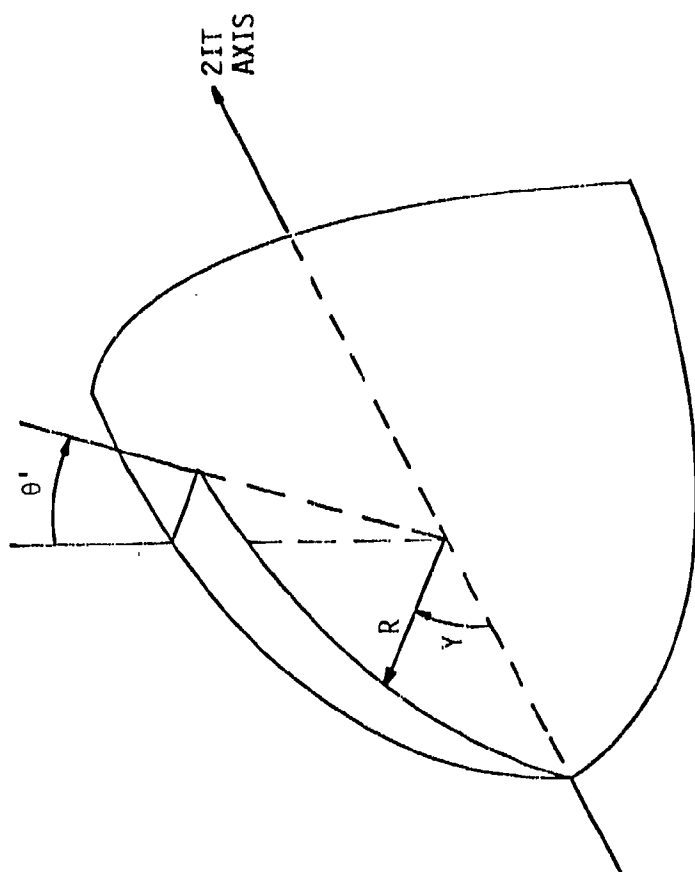


Figure 3.1.1. 2IT and 3IS Coordinate Systems

where  $\theta_{b1}$  is the body angle at the initial data plane,  $R_N$  is the nose radius, and  $z_1$  is the distance of the initial data plane from the virtual apex.

Knowing the appropriate value of  $\theta'$  for each desired streamline, the inviscid nosetip flow field parameters may then be defined at the desired axial stations (in 3IS coordinates), requiring only transforming the 2IT velocity components to the appropriate 3IS velocity components. Given the  $U, V$  velocity components of the 2IT solution (defined in References 2 and 3), the 3IS velocity components ( $u, v, w$ ) may be written at a given station ( $z$ ) as

$$u = -V [\sin\phi \cos\theta \sin\alpha + \cos\phi (\sin\theta \sin\theta' + \cos\theta \cos\theta' \sin\alpha)] + U [-\cos\phi \cos\theta \sin\alpha + \sin\phi (\sin\theta \sin\theta' + \cos\theta \cos\theta' \cos\alpha)] \quad (3.2)$$

$$v = -V [-\sin\phi \sin\theta \sin\alpha + \cos\phi (\cos\theta \sin\theta' - \sin\theta \cos\theta' \cos\alpha)] + U [\cos\phi \sin\theta \sin\alpha + \sin\phi (\cos\theta \sin\theta' - \sin\theta \cos\theta' \cos\alpha)] \quad (3.3)$$

$$w = -V (\sin\phi \cos\alpha - \cos\phi \cos\theta' \sin\alpha) - U (\sin\phi \cos\theta' \sin\alpha + \cos\phi \cos\alpha) \quad (3.5)$$

where

$$\cos \phi = \cos\alpha \cos\psi - \sin\alpha \sin\psi \cos\theta$$

$$\cos \psi = 1 - \frac{z - z_0}{R_N}$$

$$\tan \theta = \frac{\sin\phi \sin\theta'}{\sin\phi \cos\theta' \cos\alpha - \cos\phi \sin\alpha}$$

with  $z_0$  being the intersection of the 3IS axis with the spherical nose.

The nosetip flow field data obtained using this procedure is structured in the format described in Section 3.4.2 for use by the 3DMEIT code.

### 3.3.2 AFTERBODY STREAMLINE CALCULATION

On the afterbody, as noted earlier, a procedure has been developed in this effort to allow the explicit calculation of inviscid surface streamlines within the 3IS code. This procedure takes advantage of the fact that functions which are conserved along streamlines can be readily computed in an inviscid flow field code using convective finite difference schemes. The calculation of entropy in the 3IS code is an example of such a procedure. (Since inviscid flows are isentropic, the value of entropy does not change along a streamline in inviscid flows.)

The attributes of such "convective" functions can readily be used to simplify the calculation of inviscid surface streamlines. In the 3IS code, each surface streamline is identified by a unique value of a function  $f$ , which is chosen to represent the value of  $\theta$  in the initial data plane through which that streamline passes. The "conservation of  $f$ " along streamlines can then be expressed mathematically as

$$\vec{V} \cdot \nabla f = 0 \quad (3.5)$$

which can be expressed in terms of the 3IS variables at the body surface as

$$\frac{\partial f}{\partial Z} = -B \frac{\partial f}{\partial Y} \quad (3.6)$$

where  $Y$  is the transformed circumferential coordinate and



$$B = \frac{v}{rw} \frac{dY}{d\theta} .$$

(For more detail on the 3IS equations and transformations, see References 2 and 3.)

Equation (3.6) is then solved using second-order accurate differences in a predictor-corrector scheme, simultaneously with the other flow equations being solved in 3IS, to define the appropriate value of  $f$  at all grid points located on the body.

Given the computed  $f$  distribution over the entire afterbody surface, the track of any given streamline ( $f = \text{constant}$ ) can rapidly be determined by interpolation, along with the rest of the flow field information to be passed to 3DMEIT by the buffer code.

### 3.4 USER INSTRUCTIONS

#### 3.4.1 INPUT AND OUTPUT

As input, the buffer code between the 3IS and 3DMEIT procedures requires only two parameters to be input: the nose radius (RN) and the body angle at the nosetip tangency point (THB1), in degrees. These parameters are input in NAMELIST format. All other required inputs are provided either through the 2IT output file (which must be assigned to logical unit 23) and the 3IS output file (which must be assigned to logical unit 21). The formats of the 2IT and 3IS output files are described in Reference 3.

The output of the buffer code is written to a formatted file assigned to logical unit 22. The format of this file, which will be read as input to the 3DMEIT code, is described in the following section.

### 3.4.2 INVISCID FLOW FIELD FILE DESCRIPTION

The first record on the output file of the buffer code contains:

$M_\infty$	Mach number
$\alpha$	Angle of attack
MMAX	Number of streamlines
NMAX	Number of points through the shock layer.

The format of this record is 2E13.6,2I3,48X.

The second record contains the axial location on the body, Z, in the format E13.6,67X.

The third record contains values for

$\theta$	Circumferential angle
$r_b$	Body radius
$rb_z$	$\partial r_b / \partial z$
$rb_\theta$	$\partial r_b / \partial \theta$
$\omega$	$\tan^{-1}(v/w)$ , where v and w are the circumferential and axial velocity components, respectively
SF	Stream function, used to identify individual streamlines

for each of the MMAX streamlines at the axial station defined in the preceding record. These data are written in the format 6E13.6,2X.

The next NMAX records contain values for

p	Pressure
T	Temperature
u	Radial velocity component
v	Circumferential velocity component

w      Axial velocity component  
y      Distance from the body surface, measured  
         radially

for each streamline, written in the format 6E13.6,2X. Each of these records corresponds to a different value of N, where  $N = 1$  corresponds to the body surface and  $N = NMAX$  corresponds to the bow shock.

This sequence of records, starting with the second record, is repeated for each axial station at which the 3IS solution produced complete field output.

## SECTION 4

### BOUNDARY LAYER SOLUTION

#### 4.1 INTRODUCTION

The 3DMEIT code is a solution procedure for the boundary layer integral momentum and energy equations in a streamline-body normal coordinate system over a general three-dimensional body. The flow may be laminar, transitional or turbulent, and the procedure accounts for compressibility, real gas effects and surface ablation. The usual inputs to the code are the geometry of the body and the streamlines, a specification of inviscid flowfield data near the body surface and selection of a wall boundary condition.

Closure of the set of integral equations is accomplished by specifying the local shape factor, the recovery factor, the Stanton number and the friction coefficient as functions of the momentum and energy thickness Reynolds numbers. These basic "laws" are modified to account for the effects of surface roughness, transpiration, acceleration, and compressibility by influence coefficients, which are multiplicative factors on the local Stanton number and friction laws. The numerical solution procedure is an implicit finite difference scheme.

In Section 4.2.1 the basic equations are presented. This is followed by the formulation of local shape factor, recovery factor, Stanton number, friction coefficient and influence coefficients in Section 4.2.2. The transition criteria and surface roughness modeling are presented in

Sections 4.2.3 and 4.2.4, respectively. Section 4.2.5 describes the models used to approximate the ablation effects while Sections 4.2.6 and 4.2.7 detail the entropy swallowing and induced pressure models. The solution procedure is described in Section 4.2.8

## 4.2 3DMEIT METHODOLOGY

### 4.2.1 Basic Equations

The two equations that are basic to 3DMEIT are the integral momentum equation,

$$\frac{\partial \theta}{\partial s} = \theta \left\{ \frac{H}{\rho_e u_e} \frac{1}{2} \frac{\partial p}{\partial s} - \frac{1}{h_\beta} \frac{\partial h_\beta}{\partial s} - \frac{1}{\rho_e u_e} \frac{\partial}{\partial s} (\rho_e u_e^2) \right\} + \frac{C_f}{2} + \frac{\rho_w v_w u_{iw}}{\rho_e u_e} \quad (4.1)$$

and the integral energy equation,

$$\begin{aligned} \frac{\partial \phi}{\partial s} = & C_h \frac{h_r - h_w}{h_{te} - h_w} + \frac{\rho_w v_w (h_{tiw} - h_w)}{\rho_e u_e (h_{te} - h_w)} \\ & - \theta \left\{ \frac{1}{h_\beta} \frac{\partial h_\beta}{\partial s} + \frac{1}{\rho_e u_e (h_{te} - h_w)} \frac{\partial}{\partial s} [\rho_e u_e (h_{te} - h_w)] \right\} \end{aligned} \quad (4.2)$$

where  $s$  is distance along a streamline and  $h_\beta$  is the body surface metric. These forms of the boundary layer equations result from neglecting the crossflow velocity; 3DMEIT is therefore most appropriate for regions where the crossflow is "small." However, a simplified form of the crossflow momentum equation can be added to 3DMEIT without changing the parabolic nature of the system of equations. This addition is a relatively simple change to the code and should be considered in predictions at the next level of detail in the flow are necessary.

The other variables in these equations are the momentum and energy thicknesses, which are respectively:

$$\theta = \int_0^{\infty} \frac{\rho u}{\rho_e u_e} \left( \frac{u_e - u}{u_e} \right) dy \quad (4.3)$$

$$\phi = \int_0^{\infty} \left( \frac{\rho u}{\rho_e u_e} \frac{h_{te} - h_t}{h_{te} - h_w} \right) dy \quad (4.4)$$

and the boundary layer shape factor,  $H$ , is defined as:

$$H = \frac{\delta^*}{\theta} \quad (4.5)$$

where  $\delta^*$ , the displacement thickness, is given by:

$$\delta^* = \int_0^{\infty} \left( 1 - \frac{\rho u}{\rho_e u_e} \right) dy \quad (4.6)$$

The total enthalpy at the boundary layer edge is defined by:

$$h_{te} = h_e + \frac{u_e^2}{2} \quad (4.7)$$

while the recovery enthalpy is given by:

$$h_r = h_e + F \frac{u_e^2}{2} \quad (4.8)$$

where  $F$  is the recovery factor.

The heat transfer rate and skin friction are related to the Stanton number and friction coefficient, respectively, by:

$$\tau_w = \rho_e u_e^2 \frac{C_f}{2} \quad (4.9)$$

$$\dot{q}_w = \rho_e u_e C_h (h_r - h_w) \quad (4.10)$$

Closure of this system of equations is described in the following subsection.

#### 4.2.2 SHAPE FACTOR, RECOVERY FACTOR, STANTON NUMBER AND FRICTION COEFFICIENT

The shape and recovery factors are evaluated in 3DMEIT by the following relation for laminar flow:

$$H_\lambda = 3.029 \frac{T_w}{T_e} - 0.614 \quad (4.11)$$

$$F_\lambda = Pr^{1/2} \quad (4.12)$$

and for turbulent flow:

$$H_t = H_{ref} [1 + D(6 - \log_{10} Re_\theta)] \quad (4.13)$$

where

$$H_{ref} = A e^{BM^C} \quad (4.14)$$

$$A = \left\{ A_0 + A_1 \right\} \left\{ 0.0064 + 0.0231 (T_w/T_{te}) \right\} / A_0 \quad (4.15)$$

$$A_0 = -0.02 + 1.20 (T_w/T_{te}) \quad (4.16)$$

$$A_1 = (0.0372 + 0.0322 (T_w/T_{te})) f_4 \quad (4.17)$$

$$f_4 = \begin{cases} 0 & \text{for } k_s^+ < 3 \\ \log_{10}(k_s^+/3) & \text{for } k_s^+ \geq 3 \end{cases} \quad (4.18)$$

$$B = \begin{cases} 0.35 (T_w/T_{te})^{-0.5} & \text{for } M < 1.5 \\ 3.817 & \text{for } M > 1.5 \end{cases} \quad (4.19)$$

$$C = \begin{cases} 1.25 & \text{for } M < 1.5 \\ 0.29 & \text{for } M > 1.5 \end{cases} \quad (4.20)$$

$$M = M_e \sqrt{\frac{\gamma_e - 1}{0.4}} \quad (4.21)$$

$$D = \begin{cases} 0.05 & \text{for } k_s^+ < 3 \\ 0.05 + 0.04 \log_{10}(k_s^+/3) & \text{for } k_s^+ \geq 3 \end{cases} \quad (4.22)$$

and

$$F_t = Pr^{1/3} \quad (4.23)$$

where  $k_s^+$  is the local roughness Reynolds number.

The friction coefficient and the Stanton number are determined by the basic wall shear and heat flux laws respectively. The basic form of these laws comes from theory and data for incompressible flow along a smooth, isothermal, impervious, flat plate. The friction coefficient and Stanton number for laminar flow are:

$$\frac{C_{f,l,0}}{2} = \frac{0.245}{Re_\theta} \quad (4.24)$$



$$C_{h,\ell,o} = \frac{0.22}{Pr^{4/3} Re_\phi} \quad (4.25)$$

and for turbulent flow:

$$\frac{C_{f,t,o}}{2} = \frac{0.245}{Re_\phi} + \frac{0.010742 Re_\phi}{100 + Re_\phi} (\log_{10} Re_\phi)^{-1.5262} \quad (4.26)$$

$$C_{h,t,o} = \frac{0.22}{Pr^{4/3} Re_\phi} + \frac{a Re_\phi}{(100 + Re_\phi)} (\log_{10} Re_\phi)^{-b} \quad (4.27)$$

where

$$\left. \begin{aligned} a &= 0.0993 e^{(0.0648 Pr)/(1 + 9.6 Pr)} \\ b &= 1.954 e^{(0.273 Pr)/(1 + 0.71 Pr)} \end{aligned} \right\} Pr \geq 0.6 \quad (4.28)$$

or

$$\left. \begin{aligned} a &= 0.1256 e^{(0.2435 Pr)/(1 + 14.2 Pr)} \\ b &= 2.217 e^{(0.6313 Pr)/(1 + 1.677 Pr)} \end{aligned} \right\} Pr < 0.6 \quad (4.29)$$

The Stanton number and friction coefficient laws given above are modified by corresponding influence coefficients to account for various boundary layer effects:

$$C_{x,y} = C_{x,y,o} \prod_z I_{x,y,z} \quad \begin{aligned} &\text{for } x = h, f \\ &\quad y = \ell, t \end{aligned} \quad (4.30)$$

The influence coefficients are shown by  $I_{x,y,z}$  where the subscripts  $x$  and  $y$  indicate whether the influence coefficient pertains to heat or momentum transfer ( $x = h$  or  $f$ ) and laminar or turbulent flow

(y = l or t), respectively. The subscript z indicates the type of phenomenon for which the basic laws are being modified.

Five phenomena are considered by 3DMEIT. These phenomena and their corresponding z-subscripts are given in Table 4.1. The influence coefficients corresponding to each of these effects are given below.

#### Acceleration

In laminar flow:

$$I_{f,l,\beta} = \begin{cases} (1 + 3\beta)^{1/3}, & \beta > 0 \\ 1.0, & \beta < 0 \end{cases} \quad (4.31)$$

$$I_{h,l,\beta} = \begin{cases} (1 + 4\beta)^{1/6}, & \beta > 0 \\ 1.0, & \beta < 0 \end{cases} \quad (4.32)$$

where

$$\beta \equiv \frac{2\xi}{u_e} \frac{du_e}{d\xi} \quad (4.33)$$

$$\xi \equiv \int_0^s \rho_e u_e u_e r^2 ds \quad (4.34)$$

Table 4.1. Notation for Influence Coefficients

Phenomena	z-Subscript of Influence Coefficient
Acceleration	$\beta$
Transpiration	$\beta'$
Boundary layer properties	$p$
Roughness	$r$
Transition proximity	$tr$

In turbulent flow, only the first terms of the appropriate basic turbulent laws are modified by the above influence coefficients.

### Transpiration

Blowing effects on the wall shear are modeled by adaptations of film theory (Reference 14).

$$I_{f,y,B'} = \frac{\ln(1 + 2\lambda_{f,y} R' R B')}{2\lambda_{f,y} R R' B'} , \quad y = l, t \quad (4.35)$$

where:

$$B' \equiv \dot{m} / \rho_e u_e C_m \quad (4.36)$$

and

$$R = C_h / C_f / 2 = \text{Reynolds Analogy Factor}$$

$$R' = \text{Mass to heat transfer coefficient ratio} = C_m / C_h$$

$$\lambda_{f,y} = \text{Blowing reduction parameter.}$$

R is a dependent variable which is evaluated during the solution process. Both R' and  $\lambda_{f,y}$  are input; 3DMEIT, however, does provide built-in default values for  $\lambda_{f,y}$ . These default values are:

$$\lambda_{f,l} = 0.5 \quad (4.37)$$

$$\lambda_{f,t} = 0.35$$

The variables B' and R' are, in effect, definitions for the mass transfer coefficient, which, in 3DMEIT, are obtained from the analogy between heat and mass transfer. Therefore,  $C_m$  is the mass transfer analog of the Stanton number and  $\dot{m} / \rho_e u_e C_m$ .

Ordinarily,  $R' = 1$  and the default values of  $\lambda$  are used because these are the theoretical values for unity Prandtl and Lewis numbers in laminar flow. Also, the default values for turbulent flow have been chosen to fit available data. Other input values of  $R'$  and  $\lambda$  can be developed from finite difference calculations for chemically reacting boundary layers or by fits to mass transfer data. (A detailed description of these procedures is given in "An Evaluation of a Transfer Coefficient Approach for Unequal Diffusion Coefficients" by E. P. Bartlett and R. G. Grose, Aerotherm Report 69-50, June 30, 1969.)

There are two blowing correlation options for the heat transfer:

(1) Aerotherm option and (2) GE option. The Aerotherm option utilizes the expression (Reference 15):

$$I_{h,y,B'} = \frac{C_h}{C_{h_0}} = \frac{\ln(1 + 1.4 B')}{1.4 B'}, \quad y = \ell, t \quad (4.38)$$

The GE option employs the Costello correlation (Reference 16) for laminar flow:

$$I_{h,\ell,B'} = \frac{C_h}{C_{h_0}} = (1 + 0.69 B')^{-1} \quad (4.39)$$

and another correlation (Reference 17) for turbulent flow

$$I_{h,t,B'} = \frac{C_h}{C_{h_0}} = \left[ \frac{2}{B'} \left( \sqrt{1 + B'} - 1 \right) \right]^{1.6} (1 + B')^{0.2(\omega-1)} \quad (4.40)$$

where

$$\omega = \left( \frac{T_w}{T_e} \right)^{-1/8} + 1/8 M_e \quad (4.41)$$

#### Boundary Layer Properties

Boundary layer properties of density, viscosity, and Prandtl number are evaluated at a reference enthalpy  $h'$  as follows for laminar flow:

$$h' = 0.42 h_e + 0.19 h_r + 0.58 h_w \quad (4.42)$$

and the property influence coefficients are:

$$I_{f,l,p} = 1 \quad (4.43)$$

$$I_{h,l,p} = \left( \frac{\rho'}{\rho_e} \right) \left( \frac{\mu'}{\mu_e} \right) \left( \frac{h_{te} - h_w}{h_r - h_w} \right) \quad (4.44)$$

For turbulent flows:

$$h' = 0.353 h_e + 0.19 h_r + 0.45 h_w + f_5 f(h_e, h_r, h_w) \quad (4.45)$$

where

$$f(h_e, h_r, h_w) \text{ is the greater of zero or } (-0.609 h_e + 0.332 h_r + 0.277 h_w) \quad (4.46)$$

and

$$f_5 = \begin{cases} 0 & \text{for } k_s^+ \leq 3 \\ \frac{(k_s^+ - 3)^2}{400 + (k_s^+ - 3)^2} & \text{for } k_s^+ > 3 \end{cases} \quad (4.47)$$

where  $k_s^+$  is the local roughness Reynolds number.

The influence coefficients are:

$$I_{x,t,p} = \left( \frac{\rho'}{\rho_e} \right) \left( \frac{\mu'}{\mu_e} \right)^{0.25}, \quad x = f, h \quad (4.48)$$

#### Surface Roughness

In laminar flow:

$$I_{h,\ell,r} = I_{f,\ell,r} = 1 \quad (4.49)$$

The turbulent influence coefficient for the wall shear due to roughness is:

$$I_{f,t,r} = \frac{a(\log_{10} Re_\theta)^{-e}}{0.010742 (\log_{10} Re_\theta)^{-1.5262}} \quad (4.50)$$

where

$$a = b + c(k_s^+)^d \quad (4.51)$$

$$e = f + g(k_s^+)^h \quad (4.52)$$

The values of  $b$ ,  $c$ ,  $d$ ,  $f$ ,  $g$  and  $h$  are dependent on the local roughness Reynolds number ( $k_s^+ \triangleq u_\tau k_s / \nu_w$ ) and are listed in Table 4.2.  $Re_\theta$  is the local momentum thickness Reynolds number for the rough wall,  $u_\tau$  is the local shear velocity ( $u_\tau \triangleq \sqrt{\tau_w / \rho_w}$ ),  $k_s$  is the equivalent sand-grain roughness height and  $\nu_w$  is the wall kinematic viscosity.

The turbulent heat transfer influence coefficient is:

$$I_{h,t,r} = 1 + R(I_{f,t,r} - 1) \quad (4.53)$$

where

$$R = f_1 \left\{ [1 + g_2(g_3 - f_2)][1 - f_3] + f_3 \right\} - g_1 h \quad (4.54)$$

Table 4.2. Coefficients for the Turbulent Wall Shear Roughness Influence Coefficient

Range of $k_s^+$	$b \times 10^3$	$c \times 10^3$	$d$	$f$	$g$	$h$
0 - 3	10.742	0	-	1.5262	0	-
3 - 7	10.650	0.00344	3.0340	1.5227	0.000155	2.8460
7 - 17	6.150	1.787	0.6011	1.3070	0.1204	0.3860
17 - 30	9.140	0.556	0.8850	1.3850	0.0710	0.4865
30 - 100	0.987	3.178	0.5324	-2.9459	4.1085	0.0397
100 - 1000	8.143	1.878	0.5997	-3.1856	4.3879	0.0357
1000 - 3000	-22.840	3.657	0.5370	4.7184	-4.6579	-0.1028
> 3000	0	1.301	0.6640	0	1.3560	0.0870

$$h = \begin{cases} \left[ \log_{10}(10,000 k_s/\theta)^2 \right] & \text{for } k_s/\theta > 10^{-4} \\ 0 & \text{for } k_s/\theta \leq 10^{-4} \end{cases} \quad (4.55)$$

$$g_1 = 0.005 \{ 1 + 0.35 \sin [\pi/2 (1 - Pr)] \} \quad (4.56)$$

$$g_2 = 0.142 (Pr - 0.71) \quad (4.57)$$

$$g_3 = (0.121 + 0.053 Pr)^{-1} \quad (4.58)$$

The values  $f_2$  and  $f_3$  are functions of  $k_s^+$  and are given in Table 4.3.

Table 4.3. Functions  $f_2$  and  $f_3$  for the Turbulent Heat Transfer Roughness Influence Coefficient

Range of $k_s^+$	$f_2$	$f_3$
3 - 76	1.8808	$-0.32 \left[ \log_{10}(k_s^+ - 1.8808) \right]$
76 - 1500	$\log_{10}(k_s^+)$	0
1500 - $10^4$	3.176	$0.32 \left[ \log_{10}(k_s^+ - 3.176) \right]$

The function  $f_1$  is the relationship between heat transfer and roughness shear augmentation. The modified correlation is:

$$f_1 = \begin{cases} 0.89 - 0.46(k_s^+ - 3)/(k_s^+ + 47) & \text{for } k_s^+ > 3 \\ 0.89 & \text{for } k_s^+ \leq 3 \end{cases} \quad (4.59)$$

#### Transition Proximity

The transition proximity influence coefficients apply only to the laminar region upstream of the transition point. The present influence coefficients are based on PANT and ART wind tunnel heat transfer data (References 18 and 19). It is assumed that the influence coefficient for momentum is the same as for heat transfer, i.e.,

$$I_{f,l,tr} = I_{h,l,tr} \quad (4.60)$$

and

$$I_{h,l,tr} = \text{the greater of } 1.0 \text{ or}$$

$$7.6(s_{tk})^{-0.366} e^{0.0005 s_{tk}} \quad s_{tk} < 1000 \quad (4.61)$$



where

$$s_{tk} = s_{tr}/\theta_{tr}(I_{h,\ell,tr})^{1.3} \quad (4.62)$$

### Intermittency

The above formulations for  $H$ ,  $F$ ,  $C_h$ ,  $C_{f/2}$  are for entirely laminar or for entirely turbulent flows. To evaluate these four parameters for transitional flow the following relation is used:

$$P = (1 - f) P_\ell + f P_t$$

where  $P$  is one of the four parameters above and  $f$  is the transitional intermittency factor.

The transitional intermittency employed in 3DMEIT is based on the work of Persh (Reference 20), and an interpretation by Dahm (Reference 21):

$$f = 1 - \frac{\alpha}{Re_{\theta}^2 (C_{f,t} - C_{f,\ell})} \quad (4.63)$$

where

$$\alpha = Re_{\theta,tr}^2 (C_{f,t} - C_{f,\ell})_{tr} \quad (4.64)$$

and the subscript  $tr$  refers to conditions at the transition point.

$f$  is set to zero in laminar flow, unity in turbulent flow, and varies between 0 and 1 in transitional flow.

This completes the formulation of the parameters required in the solutions of Equations (4.1) and (4.2).

#### 4.2.3 TRANSITION CRITERIA

The 3DMEIT code has several built-in options to specify the critical flow/material surface parameters that establish transition onset and location. In addition, all laminar or all turbulent (from stagnation point) calculations may be made.

The analytic transition criteria for rough wall calculations available are the Anderson criterion for nose transition and LORN criterion for cone transition (although use of the LORN criterion is not recommended). These are:

##### Anderson Criterion

$$Re_{\theta} \left( \frac{k_i}{\theta} \frac{1}{\psi} \right)^{0.7} = \begin{cases} 255 \text{ onset} \\ 215 \text{ location} \end{cases} \quad (4.65)$$

where

$$\psi = 0.18' + (1 + 0.25 B') \rho_e / \rho_w \quad (4.66)$$

##### LORN Criterion

$$Re_{\theta} = 275 e^{0.134 M_e} \quad (4.67)$$

where  $M_e$  is the boundary layer edge Mach number.

#### 4.2.4 SURFACE ROUGHNESS MODELING

Two types of surface roughness are modeled

- Intrinsic roughness,  $k_i$
- Turbulent or scallop roughness,  $k_t$ .

Intrinsic roughness ( $k_i$ ) is that associated with the basic material granularity and is input as a constant for each material or as a function

of the axial length. The intrinsic roughness is used in the transition criteria and transition proximity influence coefficient.

The turbulent roughness ( $k_t$ ) is the effective sand grain roughness that results from turbulent ablation and is used in the turbulent roughness influence coefficients. The roughness height,  $k_t$ , is specified in one of three ways. A uniform value of  $k_t$  for all turbulent regions may be input by the user; a distribution of  $k_t$  as a function of axial length may be input; or a value may be obtained by using the scallop dimension correlation. From the correlation, the effective turbulent region scallop depth is computed as follows:

$$k_t = K_1 p_e^{-0.77} \quad (4.68)$$

where

$k_t$  = the effective sand grain roughness height

$K_1$  = a material dependent property determined from experimental data and input by the user.

#### 4.2.5 SURFACE TEMPERATURE AND ABLATION MODELING

The technique used in 3DMEIT is an approximation because it assumes steady-state conditions; i.e., no transient conduction in the solid. Under these special conditions of quasi-equilibrium, the energy balance is (excluding mechanical erosion):

$$\dot{q}_{NET} = \dot{q}_C - \dot{q}_R - \dot{m}_T h_w + \dot{m}_C h_C + \dot{m}_g h_g \quad (4.69)$$

where

$$\dot{m}_T = \dot{m}_C + \dot{m}_g \quad (4.70)$$

Since the net heat conducted into the solid is approximately the energy lost due to mass removal, i.e.:

$$\dot{q}_{NET} \approx \dot{m}_c h_c + \dot{m}_g h_g \quad (4.71)$$

The surface energy balance can be further simplified to give:

$$\rho_e u_e C_h (h_r - h_w) - \dot{m}_T h_w - \dot{q}_R = 0 \quad (4.72)$$

This equation is solved iteratively for  $\dot{m}_T$  and  $h_w$  by varying the wall temperature until the recovery enthalpy matches, within a specified limit, the local value derived from mass balance considerations. The above equation is conveniently rewritten for this purpose as:

$$\Delta h_r = 1.0 - \left( \frac{\epsilon \sigma T_w^4 + \dot{m}_T h_w}{\rho_e u_e C_h} + h_w \right) / h_r \quad (4.73)$$

#### 4.2.5.1 Wall Gas Enthalpy

The wall gas enthalpy for graphitic materials is expressed in the functional form:

$$h_w = f(B') \quad (4.74)$$

where  $B'$  is the blowing parameter:

$$B' = \dot{m}_T / \rho_e u_e C_h \quad (4.75)$$

and  $C_h$  is the Stanton number,  $\dot{q}_{convective} / \rho_e u_e (h_r - h_w)$ , with blowing.

$f(B')$  is represented by the following polynomial relationships for the range of indicated pressures:

$$\begin{aligned}
A &= 1.4216 + 0.0293 \log_{10} p_e \\
C &= 0.55993 + 0.00348 \log_{10} p_e \\
D &= -8.1997 - 0.2173 \log_{10} p_e \\
E &= 0.9024 - 0.062 \log_{10} p_e
\end{aligned} \tag{4.76}$$

$$B' \leq 0.19: h_w^* = \frac{2500}{2C} \left[ -E + \sqrt{E^2 - 4C(0.0361A + 0.19D + 1)} \right] \tag{4.77}$$

$$h_{wD} = -172.46 + 76.63 \log_{10} p_e + 20.41 (\log_{10} p_e)^2 \tag{4.78}$$

$$h_w = \left[ (h_{wD}^* - h_w) B' + \frac{0.19}{D} h_w - 0.175 h_w^* \right] / 0.015 \tag{4.79}$$

$$B' > 0.19: h_w = \frac{2500}{2C} \left[ -E + \sqrt{E^2 - 4C(AB'^2 + DB' + 1)} \right] \tag{4.80}$$

These relationships also satisfactorily approximate the wall gas enthalpies for carbon phenolic (Reference 15).

A discussion of the relevant expressions used in the three ablative material options is presented in the following subsections:

#### 4.2.5.2 Graphite Ablation Option

For graphite (carbon/carbon, ATJ, etc.) ablation, the phenolic resin gas blowing rate is zero; i.e.,  $\dot{m}_g = 0$ . The ablation rate expression employed is of the form:

$$B' = B'_c = \exp \left[ \sum_{n=0}^5 b_n T^{*n} \right] \tag{4.81}$$

where

$$T^* = T_w - 6000 - \sum_{n=1}^4 a_n \log_{10} p_e \quad (4.82)$$

and the numerical values for  $a_n$  and  $b_n$  are listed as follows:

Ablation Parameter Correlation Constants

$n$	$a_n$	$b_n$
0	-	-1.3191
1	587.496	$6.5704 (10^{-4})$
2	32.826	$3.6955 (10^{-7})$
3	9.643	$6.7268 (10^{-12})$
4	-2.965	$-2.7179 (10^{-14})$
5	-	$3.3450 (10^{-17})$

$T^*$  is employed as a collapsing function which reduces the data to one curve. The relationship between  $T^*$  and  $B'_C$  is:

$$\begin{aligned} T^* < -4447: \quad B'_C &= 0.175 \\ -4447 < T^* < -939: \quad B'_C &= 0.175 + 4.2759 (10^6) (T^* + 4447) \\ T^* > -939: \quad B'_C &= \exp \left[ \sum_{n=0}^5 b_n T^{*n} \right] \end{aligned} \quad (4.83)$$

#### 4.2.5.3 Carbon Phenolic Ablation Option

In the carbon phenolic option, the total mass loss rate from Equation (4.70) becomes:

$$B' = B'_c \left( 1 + \frac{\dot{m}_g}{\dot{m}_c} \right) \quad (4.84)$$

where the char mass loss rate parameter  $B'_c$  is obtained from Equations (4.81) and (4.82) and the ratio  $\dot{m}_g / \dot{m}_c$  (correlated as a function of the zero-blowing film coefficient  $C_{h_0}$  from results reported in Reference 22) is

$$\frac{\dot{m}_g}{\dot{m}_c} = \begin{cases} 0.22 & C_{h_0} < 1.0 \\ 0.22 - 0.01 C_{h_0} & C_{h_0} > 1.0 \end{cases} \quad (4.85)$$

The wall gas enthalpy for carbon phenolic ablation is satisfactorily approximated (see Reference 23) using Equation (4.74) in the form

$$h_w = f(B'_c) \quad (4.86)$$

This approximation is valid only for  $\dot{m}_g / \dot{m}_c < 10$  which encompasses most reentry applications.

The procedure to compute the blowing rate and wall temperature is identical to that described in the "Graphite Ablation Option" section.

#### 4.2.5.4 Teflon Ablation Option

For Teflon ablation, the empirical "heat of ablation" concept is employed to obtain the mass loss rate. The expression employed in

subroutine ABLATE was obtained from Reference 24 and is utilized in the form:

$$\dot{m}_T = \frac{C_{h_0}}{0.4594 - 0.0027 p_e} \quad (4.87)$$

with the ablation temperature of Teflon set at 1,800°R. Any of the three material options described above may be used at one time.

#### 4.2.6 EDGE ENTROPY MODELS

The 3DMEIT code has four different models for determining the entropy at the edge of the boundary layer. The first two options are very simple and do not account for entrainment into the boundary layer. Option 1 uses a constant entropy equal to that behind a normal shock and Option 2 uses the entropy calculated from the inviscid pressure and temperature at the wall. Options 3 and 4 account for swallowing and use the inviscid flowfield data to calculate the edge entropy. Option 3 is the streamtube entrainment method used in ASCC and is shown schematically in Figure 4.1.

Balancing the mass entering the streamtube with the mass flux in the boundary layer gives:

$$\int_0^{\bar{y}} \rho_\infty u_\infty y dy = 2h_\beta \int_0^\delta \rho u dy - 2 \int_0^s h_\beta (\rho v)_w ds \quad (4.88)$$

where  $h_\beta$  is the spreading metric. In axisymmetric flow,  $h_\beta = r(s)$ , which is the local body radius. Note that  $y$  is the body normal coordinate in the right hand side of this equation. Then, using MEIT's variables, this becomes:

$$\rho_\infty u_\infty \bar{y}^2 = 2h_\beta F \nu_e Re_\theta - 2 \int_0^s h_\beta (\rho v)_w ds \quad (4.89)$$



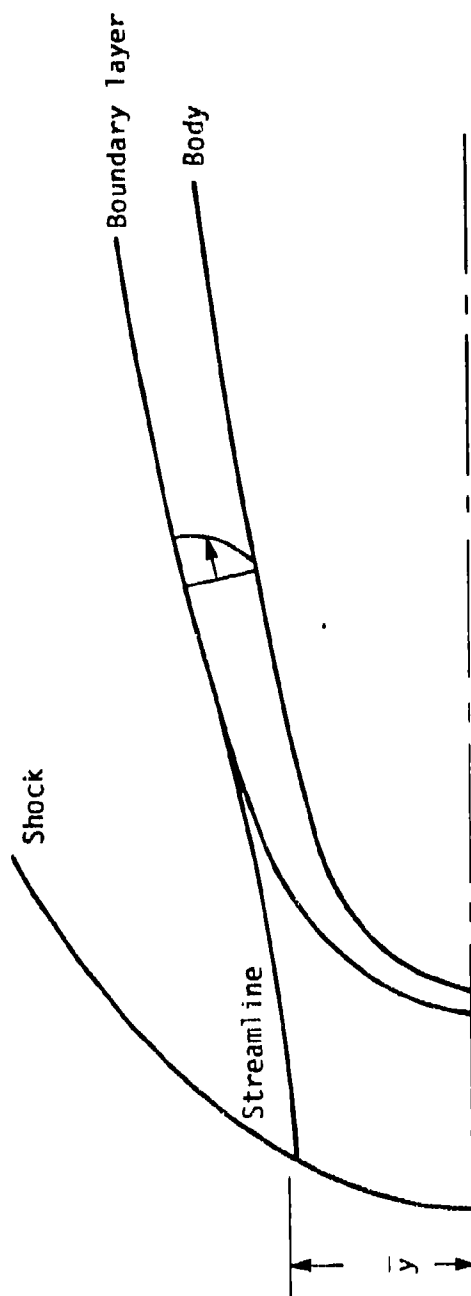


Figure 4.1. Schematic of Boundary Layer Entrainment

Equation (4.89) is solved for  $\bar{y}$  which is then used with the inviscid shock shape and entropy to determine the entropy of the streamline at the edge to the boundary layer. This model works well on axisymmetric configurations at zero angle of attack. However, in three-dimensional problems, the tracking of the streamline at the edge of the boundary layer is difficult because the streamlines curve around the body. Therefore, Option 4 was developed to utilize a mass balance between the inviscid flow, as defined by a finite difference calculation, and the boundary layer flow (Figure 4.2). Balancing the mass fluxes at a local station gives for this case:

$$\int_0^{\delta} (\rho u)_{inv} dy = \int_0^{\delta} (\rho u)_{BL} dy - \int_0^s h_B (\rho v)_w ds \quad (4.90)$$

where  $\delta$  is used as the integration limit for both the inviscid and boundary profiles because the "edge" of the boundary layer must have the same  $\rho$  and  $u$  as that which exists in the inviscid flow at that  $\delta$  and the boundary layer mass flux must include that which is entrained from the entropy layer. This equation effectively defines  $\delta$ , which is otherwise unknown and not needed for an integral boundary layer calculation.

$$\int_0^{\delta} (\rho u)_{inv} dy = u_e Re_{\theta} F - \int_0^s h_B (\rho v)_w ds \quad (4.91)$$

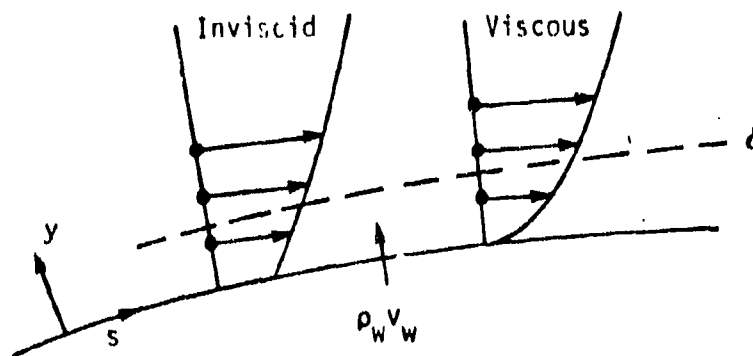


Figure 4.2. Schematic of Viscous and Inviscid Profiles Used in Mass Flux Balance

The right hand side of this equation is known from the boundary layer solution. The solution for  $\delta$  is obtained by constructing the inviscid mass flux as a function of the distance normal to the surface and interpolating in these inviscid data.

#### 4.2.7 INDUCED PRESSURE

The effect of the boundary displacement on the pressure is modeled by a correction to the inviscid values

$$p = p_{inv} + \frac{\Delta p}{\Delta \theta} \frac{d\delta^*}{dx} \quad (4.92)$$

where  $d\delta^*/dx$  is the derivative of the displacement thickness with respect to the axial direction. The term  $\Delta p/\Delta \theta$  models the effect of the angle on the wall pressure. This term is evaluated using Linnell's formula (Reference 25) which may be written as:

$$\frac{p}{p_\infty} = 1 + 0.5 \gamma (\gamma + 1) K^2 \quad (4.93)$$

where  $K$  is the hypersonic similarity parameter,  $K = M_\infty \sin \theta$ .

The term  $\Delta p/\Delta \theta$  is determined by calculating  $p$  at the body angle and at the effective angle:

$$\theta' = \theta + \tan^{-1} (\Delta \delta^*/\Delta s) \quad (4.94)$$

When  $\theta$  is less than zero, limiting values of  $\theta = 1^\circ$  and  $\theta' = 2^\circ$  are used in calculating  $\Delta p/\Delta \theta$ .

#### 4.2.8 SOLUTIONS OF THE BOUNDARY LAYER INTEGRAL EQUATIONS

As mentioned above, the required input to 3DMEIT are surface shape, boundary layer edge conditions, and wall conditions. These quantities are input in terms of body points and inviscid solution points. A finer grid

in terms of integration points, which include all the inviscid points, is generated by the program to ensure adequate solution accuracy of the integral equations. The boundary layer edge conditions, gas properties and wall conditions at each integration point are obtained by interpolation from the input. The solution procedures of the boundary layer integral Equations (4.1) and (4.2) consist of:

- Start-up solutions at the first integration points
- Finite difference numerical solutions for the rest of the integration points.

The starting values of  $\theta$  and  $\phi$  are defined in the code by:

$$\theta_1 = \sqrt{\frac{0.245 \nu_1 (1 + R_1 B_1')}{(3 + H) \left. \frac{du_e}{ds} \right|_1} \frac{z}{\Pi} C_{f,\ell,z}} \quad (4.95)$$

$$\phi_1 = \sqrt{\frac{0.22 \nu_1 (1 + B_1')}{2 \text{Pr}^{4/3} \left. \frac{du_e}{ds} \right|_1} \frac{z}{\Pi} C_{h,\ell,z}} \quad (4.96)$$

The solutions at the second and third integration points are related to the first integration point by:

$$\theta = \theta_1 (1 + a_\psi^2) \quad (4.97)$$

$$\phi = \phi_1 (1 + b_\psi^2) \quad (4.98)$$

where

$$a = \frac{\frac{13 + H_1}{4} \frac{\alpha}{\gamma} + \frac{1}{3} - \frac{0.659 (3 + H_1) \alpha (\gamma - 1)}{\gamma + 2H_1} - \frac{(H_1 - 0.614) \alpha (\gamma - 1)}{\gamma}}{\gamma} \quad (4.99)$$

$$b = \frac{1}{6} \left[ \frac{3\alpha}{\gamma} + \frac{1}{3} - \frac{2 \times 0.659 \alpha (\gamma - 1)}{\gamma} - \frac{2 (1 - F_\ell) (1 + B') \alpha (\gamma - 1)}{(1 - \gamma_w/\gamma_1) \gamma} \right] \quad (4.100)$$

$$\psi = s/R_{\text{ref}} \quad (4.101)$$

and

$$\alpha = \frac{1 - (p_3/p_1)}{\psi_3^2} \quad (4.102)$$

In the above formulation,  $R_{\text{ref}}$  is an arbitrary constant radius and  $\gamma$  is the isentropic exponent. The subscripts 1 and 3 denote the first and third integration point condition, respectively (e.g.,  $H_1$  is the shape factor at point 1).

The following implicit finite difference scheme is used for the rest of the integration points:

$$F_{x,I} = F_{x,I-1} + 0.5 (F'_{x,I-1} + F'_{x,I}) (s_I - s_{I-1}) \times = f, h \quad (4.103)$$

where:

$$F_f = r \rho_e u_e^2 \theta \quad [\text{see Equation (4.1)}] \quad (4.104)$$

$$F_h = r \rho_e u_e (h_{te} - h_w) \phi \quad [\text{see Equation (4.2)}] \quad (4.105)$$

$$F'_f = \frac{dF_f}{ds} \quad (4.106)$$

$$F'_h = \frac{dF_h}{ds}$$

(4.107)

I is the integration point index and  $F'_f$  and  $F'_h$  are both evaluated from Equations (4.1) and (4.2), respectively.

The solution is obtained by iteration since the values of  $F_{x,I}$  depend on  $F'_{x,I}$ . This iteration is local because closure is obtained at each integration point before proceeding down the body to the next integration point. Convergence is based on changes of less than 0.1 percent in both the heat and momentum transfer coefficients between successive iterations. If the iteration fails to converge in 30 tries, a local explicit solution is obtained by setting  $F'_{x,I} = F'_{x,I-1}$ , and subsequently reevaluating  $F'_{x,I}$  based on the resulting value of  $F_{x,I}$ . The algorithm then proceeds to the next integration point.

### 4.3 GEOMETRIC ANALYSES

It is important to describe the geometry with high resolution because the boundary layer integration procedure often needs small step sizes and the surface metrics and normals must be known at each integration step. This surface fitting is accomplished in 3DMEIT by a parametric interpolation method which is described below (Reference 26).

The vehicle surface is separated into a number of basic elements, referred to as patches. Schematically, patches are defined as having four sides, but in some cases one of the sides will be at a single point. The parametric representation of a patch is given by:

$$\vec{r} = [x(u, w), y(u, w), z(u, w)] = \sum_{i=0}^3 \sum_{j=0}^3 \vec{a}_{ij} u^i w^j \quad (4.108)$$

where  $0 \leq u \leq 1$

$0 \leq w \leq 1$

Equation (4.108) transforms the surface of the patch into a unit square in  $(u - w)$  space. The advantage of the parametric interpolation scheme is that, once identified, the patches may be treated independently, and therefore, only a single patch is treated in detail in the following discussion.

The physical identity of the 48 coefficients,  $\hat{a}_{ij}$ , which must be found for each patch, can be described by rewriting Equation (4.108) in the following matrix form:

$$\hat{r} = U M \hat{B} M^T W^T \quad (4.109)$$

where the superscript, T, refers to the matrix transpose, and where U and W are the vectors  $(u^3, u^2, u, 1)$  and  $(w^3, w^2, w, 1)$ , respectively. In this case, the matrix, M is given by:

$$M = \begin{bmatrix} 2 & -2 & 1 & 1 \\ -3 & 3 & -2 & -1 \\ 0 & 0 & 1 & 0 \\ 1 & 0 & 0 & 0 \end{bmatrix} \quad (4.110)$$

The three matrices,  $\hat{B}$ , describe the input quantities, which are specified at the corner points of the patch.

$$B = \begin{bmatrix} \hat{r}(0, 0) & \hat{r}(0, 1) & \frac{\partial \hat{r}}{\partial w}(0, 0) & \frac{\partial \hat{r}}{\partial w}(0, 1) \\ \hat{r}(1, 0) & \hat{r}(1, 1) & \frac{\partial \hat{r}}{\partial w}(1, 0) & \frac{\partial \hat{r}}{\partial w}(1, 1) \\ \frac{\partial \hat{r}}{\partial u}(0, 0) & \frac{\partial \hat{r}}{\partial u}(0, 1) & \frac{\partial^2 \hat{r}}{\partial u \partial w}(0, 0) & \frac{\partial^2 \hat{r}}{\partial u \partial w}(0, 1) \\ \frac{\partial \hat{r}}{\partial u}(1, 0) & \frac{\partial \hat{r}}{\partial u}(1, 1) & \frac{\partial^2 \hat{r}}{\partial u \partial w}(1, 0) & \frac{\partial^2 \hat{r}}{\partial u \partial w}(1, 1) \end{bmatrix} \quad (4.111)$$

Calculating the elements of  $\hat{B}$  for input can be extremely difficult. The first derivatives would require that the parametric form of the curve is explicitly known and cross derivatives would be even more difficult to calculate. Therefore, the 3DMEIT code uses another method which avoids inputting derivatives.



The 48 coefficients  $\vec{a}_{ij}$  in Equation (4.108) are computed in the code using the input locations of 16 points on each patch, which are usually much easier to generate than derivatives. The points are to be uniformly distributed over the patch surface as shown in Figure 4.3, so the input points will map into a uniform grid in the unit square in (u - w) space. Equation(4.109) can be rewritten in the following manner:

$$\vec{r} = U N \vec{P} N^T W^T \quad (4.112)$$

where

$$\vec{P} = \begin{bmatrix} \vec{r}(0, 0) & \vec{r}(0, 1/3) & \vec{r}(0, 2/3) & \vec{r}(0, 1) \\ \vec{r}(1/3, 0) & \vec{r}(1/3, 1/3) & \vec{r}(1/3, 2/3) & \vec{r}(1/3, 1) \\ \vec{r}(2/3, 0) & \vec{r}(2/3, 1/3) & \vec{r}(2/3, 2/3) & \vec{r}(2/3, 1) \\ \vec{r}(1, 0) & \vec{r}(1, 1/3) & \vec{r}(1, 2/3) & \vec{r}(1, 1) \end{bmatrix} \quad (4.113)$$

and

$$N = \begin{bmatrix} -9/2 & 27/2 & -27/2 & 9/2 \\ 9 & -45/2 & 18 & -9/2 \\ -11/2 & 9 & -9/2 & 1 \\ 1 & 0 & 0 & 0 \end{bmatrix} \quad (4.114)$$

Once the network of patch points has been developed, the code gives designation to the curves by requiring that the vector product  $\partial \vec{r} / \partial u \times \partial \vec{r} / \partial w$  produces an outward surface normal.

Where the  $\vec{B}$  matrix input scheme guarantees continuity in slope from one patch to a connecting patch, the  $\vec{P}$  matrix cannot guarantee this. If slope continuity becomes noticeably absent, this is remedied within the 3DMEIT code by matching the unit vectors while retaining the original

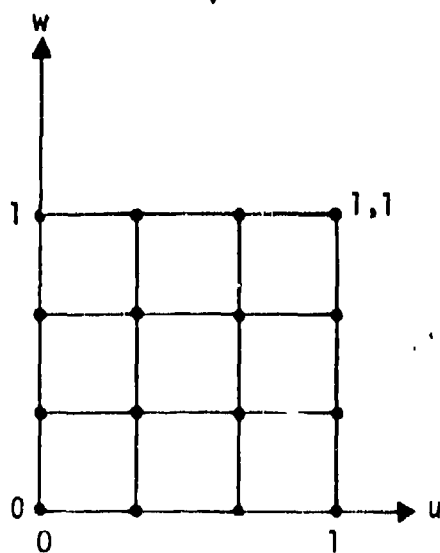
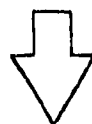
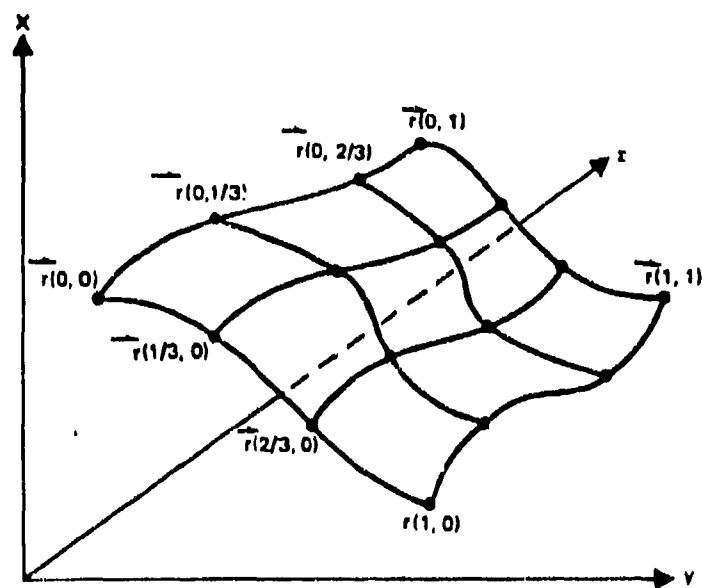


Figure 4.3. Patch Input Geometry

magnitudes. The  $\hat{B}$  matrix for the patch is obtained from the  $\hat{P}$  matrix by the following operation:

$$\hat{B} = M^{-1} N \hat{P} N^T (M^{-1})^T \quad (4.115)$$

If the slopes in the  $u$ -direction at the adjacent corners of two patches do not match, continuity is assured by calculating the unit vector  $\hat{t}$  of the slope at the corner of the first patch and recalculating the value of the new  $\partial \vec{r} / \partial u$  for the second patch. The new value of  $\partial \vec{r} / \partial u$  inserted in the  $\hat{B}$  matrix for the second patch is given by:

$$\left( \frac{\partial \vec{r}}{\partial u} \right)_{\text{new}} = \left| \frac{\partial \vec{r}}{\partial u} \right|_{\text{old}} \hat{t} \quad (4.116)$$

The new  $B$  matrix is then used to determine the coefficients  $\hat{a}_{ij}$  for the patch. Thus, a procedure for generating a parametric interpolation surface from 16 uniformly spaced points has been established.

This procedure allows slope discontinuities to exist in the input data that define the corners of the patches. However, the internal calculations described above remove these slope discontinuities and facilitate reliable boundary layer calculations. This is necessary because boundary layer theory is not generally applicable to bodies with slope discontinuities.

The 3DMEIT computer code limits the number of patches on a vehicle to 60. A vehicle is set up in segments along the  $w$  direction. The maximum number of segments is 15. For each segment a maximum of 10 patches can be put around the body, but the overall limit of 60 patches must be observed. Therefore, when 15 segments have been used to describe the body, only four patches can be used around the body for each segment.

If the vehicle is a body of revolution, four points along a meridional curve can be input for each segment and they will be revolved about the axis to generate the required number of patches. Further automation of patch generation is available for spherical sections and certain maneuvering vehicle shapes (see Section 4.4, Input Table 3).

## 4.4 USER INSTRUCTIONS

This user oriented section describes 3DMEIT inputs and outputs. A complete set of user instructions is presented in Section 4.4.1. The 3DMEIT output format, including variable descriptions, is presented in Section 4.4.2. Section 4.4.3 gives a sample problem and selected listings of input and output.

### 4.4.1 INPUT INSTRUCTIONS

The details of the input are described below. The basic input for a run consists of:

- One title card
- Eight input tables

Not all eight of the input tables are required for every run. Each table is preceded by a single card containing the identifying table number.

The following sections describe the title card, and the eight input tables.

#### Title Information

The first card contains title information in columns 1 through 80. The contents of the card are printed at the beginning of the boundary layer solution.

The following table describes the format for the first card of the data deck.

<u>Card No.</u>	<u>Columns</u>	<u>Format</u>	<u>Description</u>	<u>Units</u>
1	1-80	8A10	BCD -- Title card information	(-)

# INPUT TABLE 1. GENERAL PROGRAM CONSTANTS

This table supplies the code with program flags that indicate which options to be subsequently read and other computation information.

<u>Card No.</u>	<u>Columns</u>	<u>Format</u>	<u>Description</u>	<u>Units</u>
1	1-2	I2	Enter 01 (table number)	(-)
2	1-5	I5	NF(12) Plot output flag	(-)
			0 No plots	
			1 Read Table 8 for plot instructions	
	6-10	I5	NF(13) Output print flag	(-)
			0 Summary table only	
			1 Boundary layer output for streamline points	
			2 Boundary layer output for integration points	
	11-15	I5	IRG Property flag	(-)
			0 Ideal gas properties	
			1 Real gas properties	
	16-20	I5	NF(5) Transition criteria flag	(-)
			1 Laminar flow (Table 04 not required)	
			2 Critical momentum thickness Reynolds number versus edge Mach number	
			3 Critical stream length Reynolds versus edge Mach number	
			4 Axial distance along each streamline	
			5 Anderson nose criterion	
			$Re_e \left( \frac{k}{\theta} \frac{1}{\psi} \right)^{0.7} = \begin{cases} 255 & \text{for onset} \\ 215 & \text{for location} \end{cases}$ $\psi = T_w / T_e$	
			LORN cone criterion	

Table 04  
required

Table not  
required

INPUT TABLE 1. GENERAL PROGRAM CONSTANTS (Continued)

<u>Card No.</u>	<u>Columns</u>	<u>Format</u>	<u>Description</u>	<u>Units</u>
2 (cont.)	Table not required		6 Anderson nose criterion	
			$Re_{\theta} \left( \frac{k}{\theta} \frac{1}{\psi} \right)^{0.7} = \begin{cases} 255 & \text{for onset} \\ 215 & \text{for location} \end{cases}$	
			$\psi = 0.1B' + (0.9 + 0.11CARB)$	
			$(1 + 0.25B')(p_e/p_w)$	
			LORN cone criterion	
			7 Fully turbulent	
			Positive NREYCR -- transitional heating	
			Negative NREYCR -- no transitional heating (abrupt transition)	
21-25	15	NF(6)	Carbon flag in PANT transition criterion (NF(5) = 6)	(-)
		0	Uses 0.9 factor in $\psi$ calculation (recommended for carbon materials)	
		1	Uses 1.0 factor in $\psi$ calculation	
26-30	15	NF(35)	u-integration mesh density for aerodynamic coefficient calculations	(-)
		0	No aerodynamic coefficient calculation	
		1	4 point mesh density	
		2	8 point mesh density	
		3	16 point mesh density	
31-35	15	NF(36)	w-integration mesh density for aerodynamic coefficient calculations	(-)
		0	No aerodynamic coefficient calculation	
		1	4 point mesh density	
		2	8 point mesh density	
		3	16 point mesh density	

# INPUT TABLE 1. GENERAL PROGRAM CONSTANTS (Continued)

Card No.	Columns	Format	Description	Units
2 (cont.)	36-40	I5	IENTRP Entropy swallowing flag 1 Normal shock entropy 2 Inviscid wall entropy 3 Streamtube entrainment option 4 Local mass balance option	(-)
	41-45	I5	ITWFLG Wall temperature flag -1 Wall temperature calculated 0 Constant wall temperature input on next card 1 Wall temperature distribution input in Table 6	(-)
	46-50	I5	IBPFLG Blowing flag -1 B' calculated 0 B' = 0 1 B' distribution input in Table 6	(-)
	51-55	I5	JBLM Heat transfer blowing correction flag 0 Use GE option 1 Use Aerotherm option	(-)
3	1-10	F10.3	SCALF Scale factor for input configuration 1.0 Input in feet 0.08333 Input in inches	
	11-20	F10.3	TW Wall temperature	(°R)
4			This card is necessary only if NF(35) ≠ 0 and NF(36) ≠ 0	
	1-10	F10.4	DATAR(1) Reference area for aerodynamic coefficient calculations	(input <sup>2</sup> units)
	11-20	F10.4	DATAR(2) Reference length for aerodynamic coefficient calculations	(input units)
	21-30	F10.4	DATAR(3) x-coordinate of the center of gravity	(input units)

INPUT TABLE 1. GENERAL PROGRAM CONSTANTS (Concluded)

<u>Card No.</u>	<u>Columns</u>	<u>Format</u>	<u>Description</u>	<u>Units</u>
	31-40	F10.4	DATAR(4) y-coordinate of the center of gravity	(input units)
	41-50	F10.4	DATAR(5) z-coordinate of the center of gravity	(input units)



# INPUT TABLE 2. ENVIRONMENT TABLE

This table inputs environment conditions and the streamlines to be used for the boundary layer solution.

<u>Card No.</u>	<u>Columns</u>	<u>Format</u>	<u>Data</u>	<u>Units</u>
1	1-2	I2	Enter 02 (table number)	(-)
2	1-10	F10.2	T1 Freestream temperature	(°R)
	11-20	F10.2	P1 Freestream pressure	(atm)
	21-30	F10.2	V1 Velocity	(ft/s)
	31-40	F10.2	ALPHAB Angle of attack	(deg)
	41-50	I10	NSTREM Number of streamlines ( $\leq 50$ )	(-)
3	1-80	8F10.2	SANGLE (N), N = 1, NSTREM, Circumferential angles of the streamlines at the sphere-cone tangency point (windward streamline = 180°)	(deg)

INPUT TABLE 3. INITIAL CONFIGURATION

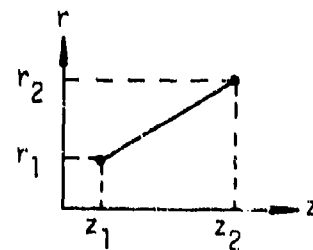
<u>Card No.</u>	<u>Columns</u>	<u>Format</u>	<u>Description</u>	<u>Units</u>
1	1-2	I2	Enter 03 (table number)	(-)
2	1-10	F10.3	RN Initial nose radius	(in.) or (ft)
	11-20	F10.3	THETC Initial cone half angle	(deg)
	21-30	F10.3	BOA Height/span ratio 1.0 for circular cross section ≠ 1.0 for elliptical cross section	
	31-40	F10.3	ZN Distance from apex of afterbody to nosetip	(in.) or (ft)
	41-45	I5	NUMNOS Number of segments on the spherical section of the nosetip	(-)
	46-50	I5	NOSFLG Nosetip generation flag 0 Each segment on nosetip must be individually input 1 Code automatically sets up NUMNOS spherical segments on the nose	(-)
3	1-32	16I2	NC array  NC(1) Total number of segments ( $\leq 15$ )  NC(I), I = 2, NC(1) input mode for each segment $1 \leq NC \leq 5$  If NOSFLG = 1, values must be input for each segment but the code will ignore those for segments 2 through NUMNOS	(-)
4	1-30	15I2	NPATCH(I) I = 1, 15 number of patches around the body on segment I (user should input a constant number at this stage in code development)	(-)

# INPUT TABLE 3. INITIAL CONFIGURATION (Continued)

The optional input modes for the segments are described below. The data for each segment must be ordered to match the mode selection arrangement specified in the NC array. The modes can be separated into three options. For Option 1 ( $NC \leq 3$ ), a single meridian curve  $r(z)$  is described and the code automatically generates NPATCH patches to cover  $180^\circ$  circumferentially as shown in Figure 4.4. Option 2 is used to input completely arbitrary patches as also shown in Figure 4.4. Option 3 is used to describe the afterbody of a vehicle with flat sections and cut sections as illustrated in Figure 4.5. The input formats for each of these options are as follows:

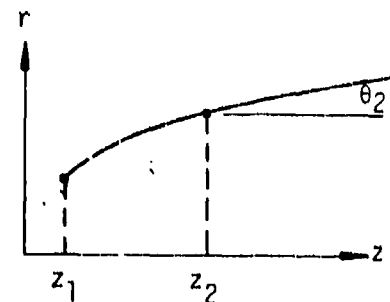
Input Table 3(a). Option 1

<u>NC(I)</u>	<u>Format</u>	<u>Description</u>
1	4F7.3	Conical frustum, input $z_1, r_1, z_2, r_2$



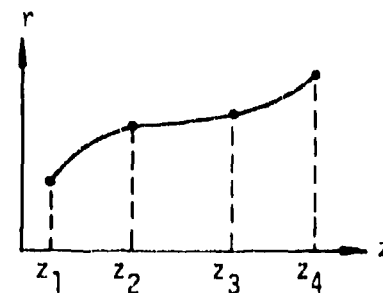
2	5F7.3	Circular arc input $z_1, r_1, z_2, r_2, \theta_2$
---	-------	---

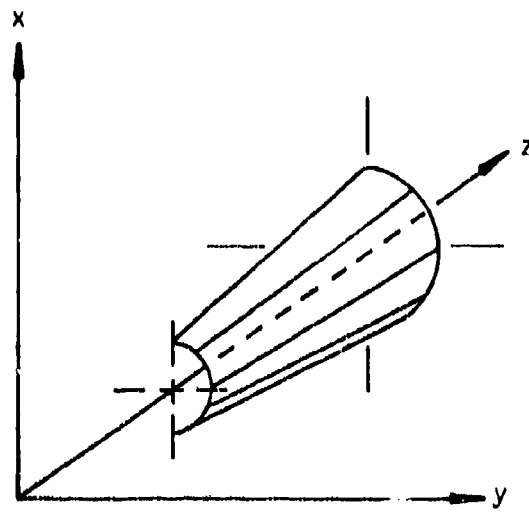
If NOSFLG = 0, each segment cannot turn more than  $45^\circ$



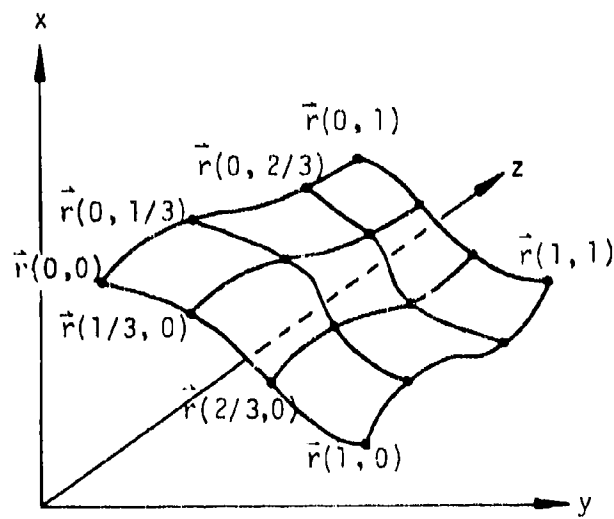
3	8F7.3	Arbitrary curve input $z_1, r_1, z_2, r_2, z_3, r_3, z_4, r_4$
---	-------	--

Note: an attempt should be made to distribute evenly the four points along the curve segment





(a) Patch Rotation for Option 1



(b) Patch Description for Option 2

Figure 4.4. Illustrations of Geometry Descriptions

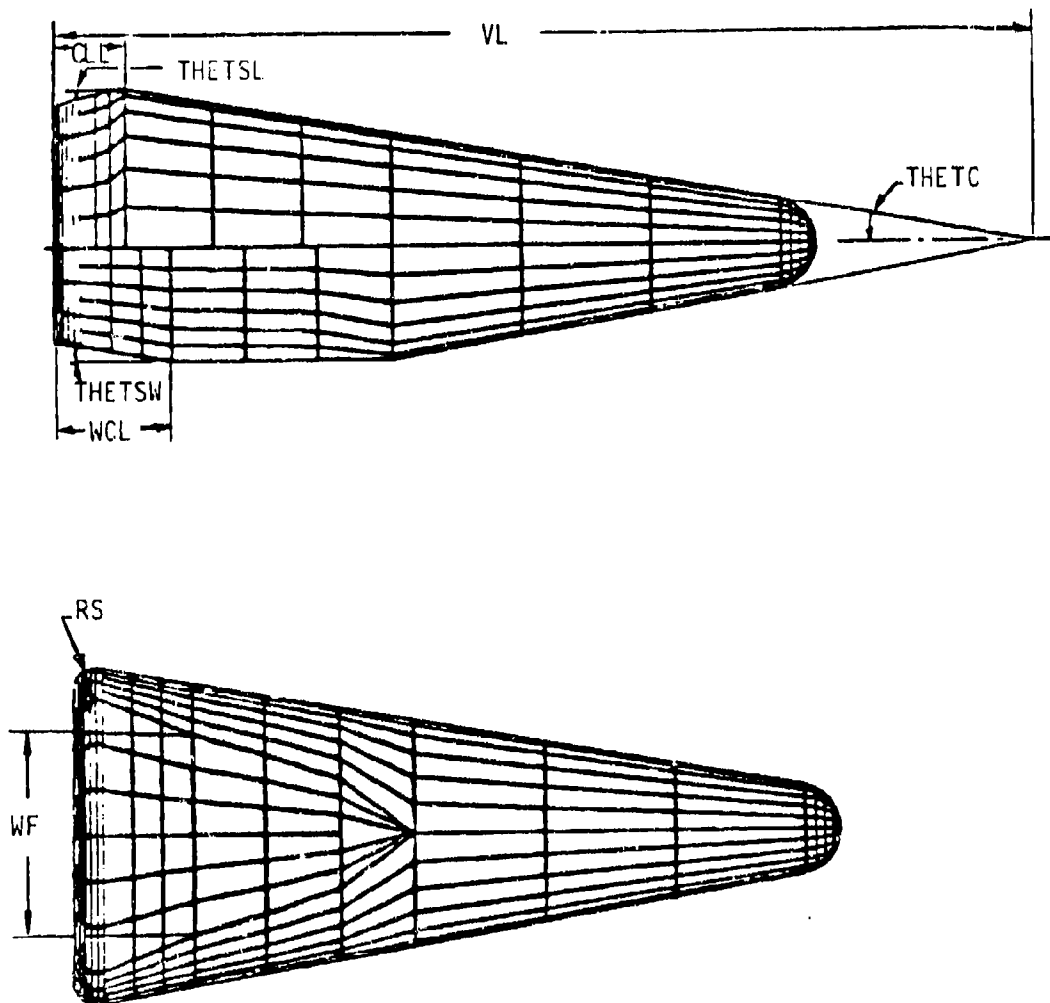


Figure 4.5. Geometry Descriptions for Option 3

# INPUT TABLE 3. INITIAL CONFIGURATION (Continued)

Table 3(b). Option 2: NC(I) = 4

Each patch requires six data cards which are ordered as follows:

<u>Card No.</u>	<u>Format</u>	<u>Description</u>
1	8F9.5	x(0, 0), x(0, 1/3), x(0, 2/3), x(0, 1), x(1/3, 0), x(1/3, 1/3), x(1/3, 2/3), x(1/3, 1)
2	8F9.5	x(2/3, 0), x(2/3, 1/3), x(2/3, 2/3), x(2/3, 1), x(1, 0), x(1, 1/3), x(1, 2/3), x(1, 1)
3	8F9.5	y(0,0), y(0, 1/3), y(0, 2/3), y(0, 1), y(1/3, 0), y(1/3, 1/3), y(1/3, 2/3), y(1/3, 1)
4	8F9.5	y(2/3, 0), y(2/3, 1/3), y(2/3, 2/3), y(2/3, 1), y(1, 0), y(1, 1/3), y(1, 2/3), y(1, 1)
5	8F9.5	z(0,0), z(0, 1/3), z(0, 2/3), z(0, 1), z(1/3, 0), z(1/3, 1/3), z(1/3, 2/3), z(1/3, 1)
6	8F9.5	z(2/3, 0), z(2/3, 1/3), z(2/3, 2/3), z(2/3, 1), z(1, 0), z(1, 1/3), z(1, 2/3), z(1, 1)

Input Table 3(a). Option 3: NC(I) = 5

<u>Columns</u>	<u>Format</u>	<u>Description</u>	<u>Units</u>
1-7	E7.3	THETAC Cone half angle	(deg)
8-14	E7.3	VL Virtual length of the vehicle measured from the apex of the afterbody cone	(in.) or (ft)
15-21	E7.3	WCL Distance from the end of the body to the windshield cut	(in.) or (ft)
22-28	E7.3	WF Width of the flat	(in.) or (ft)

INPUT TABLE 3. INITIAL CONFIGURATION (Continued)

<u>Columns</u>	<u>Format</u>		<u>Description</u>	<u>Units</u>
29-35	E7.3	THETWS	Angle of the windward cut	(deg)
36-42	E7.3	CLL	Distance from the end of the body to the leeward cut	(in.) or (ft)
43-49	E7.3	THETSL	Angle of the leeward cut	(deg)
50-56	E7.3	RS	Radius of curvature for the rounded corner of the base	(in.) or (ft)
57-63	E7.3	BASXP	Exponent describing the cross sectional shape of the base = 2.0 for circular ≠ 2.0 for "super circle"	(-)
64-65	--	Not used		
66-70	I5	KSTART	Patch number where the interpolation between an exponent of 2 and BASXP begins	(-)
71-75	I5	IFLAT	Flat flag 0 No flat surface 1 Flat surface on windward side determined by WF	(-)

The next group of cards control the patch setup to be used to print the boundary layer and surface energy balance results. This option is for future use of 3DMEIT as part of a procedure for predicting shape change. It spline fits a group of patches in a least squares sense and then redefines the coordinates of the body segment patches. It is not operative in the present version of 3DMEIT, but users are advised to enter 1's in all fields to prevent execution errors in the input routines.

<u>Card No.</u>	<u>Columns</u>	<u>Format</u>	<u>Description</u>	<u>Units</u>
4 + NC(1) + 1	1-30	15I2	NDISC(I) I = 1, 15 The number of w stations per spline group to be used in the recession analysis	(-)

INPUT TABLE 3. INITIAL CONFIGURATION (Concluded)

<u>Card No.</u>	<u>Columns</u>	<u>Format</u>	<u>Description</u>	<u>Units</u>
	31-60	15I2	NDISC(I) I = 16, 30 The number of body segments per spline group. Up to 15.	(-)
			Note: it is suggested that the entire nosetip (spherical section) be included in one group and the afterbody in another	
	61-62	I2	NDISC(31) Number of groups describing the body	(-)
4 + NC(1) + 2	1-3	I3	NTBZ Number of w locations where boundary layer and surface energy balance results are saved (30 maximum)	(-)
	4-6	I3	NTBU Number of u locations where boundary layer and surface energy balance results are saved (10 maximum)	(-)
4 + NC(1) + 3	1-80	8F10.4	TBZ(I) I = 1, NTBZ w locations where boundary layer and surface energy balance results are saved	(-)
4 + NC(1) + 4 → n	1-80	8F10.4	Continue TBZ array	(-)
n + 1	1-80	8F10.4	TBU(I) I = 1, NTBU u locations where boundary layer and surface energy balance results are saved	(-)
n + 2 → m	1-80	8F10.4	Continue TBU array input	(-)
m + 1	1-30	30I1	IMAT(I, J) I = 1, NTBZ Surface material flag for shape change points	(-)
m + 2 → l			Continue for J = 2, NTBU	(-)



# INPUT TABLE 4. TRANSITION TABLE

Enter this table only when  $NF(5) = 2, 3$  or  $4$ . Maximum of 50 entries are allowed in this table.

## 1. Input for $Re_\theta$ versus $M_e$ , $NF(5) = 2$

<u>Card No.</u>	<u>Columns</u>	<u>Format</u>	<u>Description</u>	<u>Units</u>
1	1- 2	I2	Enter 04 (table number)	(-)
2	1- 2	I2	Nonzero entry for the last card in the table	(-)
	3-14	E12.5	AM Local edge Mach No. ( $M_e$ )	(-)
	15-26	E1.5	REM Critical momentum thickness Reynolds number ( $Re_\theta$ )	(-)
3 (etc.)	Same as Card 2 for increasing $M_e$			

## 2. Input for $Re_s$ versus $M_e$ , $NF(5) = 3$

<u>Card No.</u>	<u>Columns</u>	<u>Format</u>	<u>Description</u>	<u>Units</u>
1	1- 2	I2	Enter 04 (table number)	(-)
2	1- 2	I2	Nonzero entry for the last card in the table	(-)
	3-14	E12.5	AM Local edge Mach No. ( $M_e$ )	(-)
	15-26	E1.5	REM Critical stream-length Reynolds number ( $Re_s$ )	(-)
3 (etc.)	Same as Card 2 for increasing $M_e$			

### 3. Input for Transition Location, NF(5) = 4

<u>Card No.</u>	<u>Columns</u>	<u>Format</u>	<u>Description</u>	<u>Units</u>
1	1- 2	I2	Enter 04 (table number)	(-)
2	1- 2	I2	Nonzero entry for the last card in the table	(-)
	3-14	E12.5	AM Axial location of transition along each streamline specified in Table 2	(in.)

# INPUT TABLE 5. MATERIAL PROPERTIES

Maximum of three material inputs are allowed in this table. Each material input is treated according to the following format.

Card No.	Columns	Format	Description	Units
1	1- 2	I2	Enter 05 (table number)	(-)
2	1- 5	I5	MAT Material index for following table	(-)
	6-10	I5	JROUGH Laminar heating augmentation flag 0 No augmentation 1 Transition proximity augmentation	(-)
3	1- 2		Blank	
	3-14	E12.5	RUFL Intrinsic roughness height; nonuniform roughness may be input in Table 6	(mil)
	15-26	E12.5	RUFMAX Maximum turbulent roughness height ( $k_{t_{max}}$ )	(mil)
	27-38	E12.5	RUF1 Constant $k_1$ >0 White-Grabow scallop law is used: $k_t = k_1 p_e^{-0.77}$ with $k_{t_{max}} = RUFMAX$ =0 Constant turbulent roughness of RUFMAX is used	(mil-psi <sup>0.77</sup> )
	39-50	E12.5	EMISS Emissivity	(-)
	51-62	E12.5	CMH Ratio of mass to heat transfer coefficients	(-)

# INPUT TABLE 5. MATERIAL PROPERTIES (Concluded)

## Parameters in Blowing Correction to Transfer Coefficients

<u>Card No.</u>	<u>Columns</u>	<u>Format</u>	<u>Description</u>	<u>Default Values</u>	<u>Units</u>
4	1- 2	I2	NC Flag, zero		(-)
	3-14	E12.5	BLS Laminar shear parameter	0.5	(-)
	15-26	E12.5	BLH Laminar heating parameter	0.5	(-)
	27-38	E12.5	BTS Turbulent shear parameter	0.35	(-)
	39-50	E12.5	BTH Turbulent heating parameter	0.35	(-)

If zero is entered, default values are used.

# INPUT TABLE 6. SURFACE DATA

The 3DMEIT code includes approximate techniques to predict surface temperature and blowing rate distributions of ablating surfaces. The user, however, may bypass these computations and enter the desired surface temperature or blowing rate distributions via this table. A nonuniform surface roughness distribution may also be input in this table. Entries for each variable are described in the following subsections. Any combination of one or three subsections can be input.

<u>Card No.</u>	<u>Columns</u>	<u>Format</u>	<u>Description</u>	<u>Units</u>
1	1-2	I2	Enter 06 (table number)	(-)
2	1-5	I5	ITABL Enter 1 (temperature table)	(-)
3	1-80	9F10.5	Surface temperature for NTBZ w points	(°R)
4	1-80	8F10.5	Same as above for each of NTBU u values	(°R)
m	1-5	I5	ITABL Enter 2 (blowing rate table)	
m+1	1-80	8F10.5	Blowing rate ( $B'$ ) = $\rho_w V_w / \rho_e u_e C_m$ for each NTBZ w values	(-)
m+2	1-80	8F10.5	Same as above for each NTBU u value	(-)
n	1-5	I5	ITABL Enter 3 (surface roughness)	
n+1	1-80	8F10.5	Surface roughness for NTBZ w points	(mil)
n+2	1-80	8F10.5	Same as above for each of NTBZ w values	(mil)
Last card	1-5	I5	ITABL < 0 signifies end of Table 6	(-)

# INPUT TABLE 7. INVISCID DATA

The 3DMEIT code reads inviscid data from tape 23 and stores the needed edge conditions and integrated mass fluxes on tape 22. If a calculation is to be done using the same inviscid data as a previous calculation, one may use the stored values on tape 22 and avoid the cost of integrating the velocity fields and calculating the metrics.

<u>Card No.</u>	<u>Columns</u>	<u>Format</u>		<u>Description</u>	<u>Units</u>
1	1- 5	I5	IRSTRT	Inviscid data input flag 0 Read inviscid data from tape 23 1 Read previously defined mass fluxes and metrics from tape 22	(-)

For IRSTRT = 0, the format on tape 23 is given in the following table:

<u>Card No.</u>	<u>Columns</u>	<u>Format</u>		<u>Description</u>	<u>Units</u>
1	1-13	E13.6	AMINF	Freestream Mach number	(-)
	14-26	E13.6	ALPHA	Angle of attack	(deg)
	27-29	I3	MDAT	Number of streamlines	(-)
	30-32	I3	NDAT	Number of points through the shock layer	(-)
2	1-13	E13.6	ZDAT	Axial location	(in.)
3	3 + MDAT				
	1-13	E13.6	PHDAT	Circumferential angle	(rad)
	14-26	E13.6	RB	Body radius	(in.)
	27-39	E13.6	RBZ	$\arg/aZ$	(-)

# INPUT TABLE 7. INVISCID DATA (Concluded)

Card No.	Columns	Format	Description	Units
3 → 3 + MDAT (cont.)				
	40-52	E13.6	RBTH	$\arg/\alpha$ (in.)
	53-65	E13.6	OMEGA	$\tan^{-1}(u_\phi/u_z)$ on the surface (rad)
	66-78	E13.6	SF	Stream function (-)
4 → 4 + (NDAT * MDAT)				
	1-13	E13.6	PF	Flowfield pressure
			$p/p_\infty$ IRG = 0	(-)
			$p$ IRG = 1	(lb <sub>f</sub> /ft <sup>2</sup> )
	14-26	E13.6	T	Temperature
			$T/T_\infty$ IRG = 0	(-)
			$T$ IRG = 1	(°R)
	27-39	E13.6	VR	Radial velocity component
			$u_r \sqrt{p_\infty/\rho_\infty}$ IRG = 0	(-)
			$u_r$ IRG = 1	(ft/s)
	40-52	E13.6	VP	Circumferential velocity component
			$u_\phi \sqrt{p_\infty/\rho_\infty}$ IRG = 0	(-)
			$u_\phi$ IRG = 1	(ft/s)
	53-65	E13.6	VZ	Axial velocity component
			$u_z \sqrt{p_\infty/\rho_\infty}$ IRG = 0	(-)
			$u_z$ IRG = 1	(ft/s)
	66-78	E13.6	YR	Distance from body (in.)

Card sets 2, 3, 4 are repeated for each axial station.

# INPUT TABLE 8. PLOT DATA

Card No.	Format	Description	Units
1	I2	Enter 08 (table number)	(-)
2	F7.3	YL Minimum value of y on the vehicle	(ft or in.)
	F7.3	YR Maximum value of y on the vehicle	(ft or in.)
	F7.3	XB Minimum value of x on the vehicle	(ft or in.)
	F7.3	XT Maximum value of x on the vehicle	(ft or in.)
	F7.3	ZN Minimum value of z on the vehicle	(ft or in.)
	F7.3	ZB Maximum value of z on the vehicle	(ft or in.)

Note: these six dimensions should form a box completely enclosing the vehicle to aid the system in scaling the plot

I2	NU	Number of u-increments to be taken $\leq 10$	(-)
I2	NW	Number of w-increments to be taken $\leq 10$	(-)
I2	NPLOT	Number of views at a given time	(-)
I2	NI	<div> <div>0 draws complete grid</div> <div>1 draws only patch boundaries</div> <div>2 draws profile</div> </div>	(-)
3	F7.3	XBETA View orientation angle defined in Figure 4.6	(deg)
	F7.3	XTHETA View orientation angle defined in Figure 4.6	(deg)
4 → n		Same as card number 3 for NPLOT views	

## End of Input

The end of the input deck is signaled by a single card with a -1 punched in columns 1 and 2.



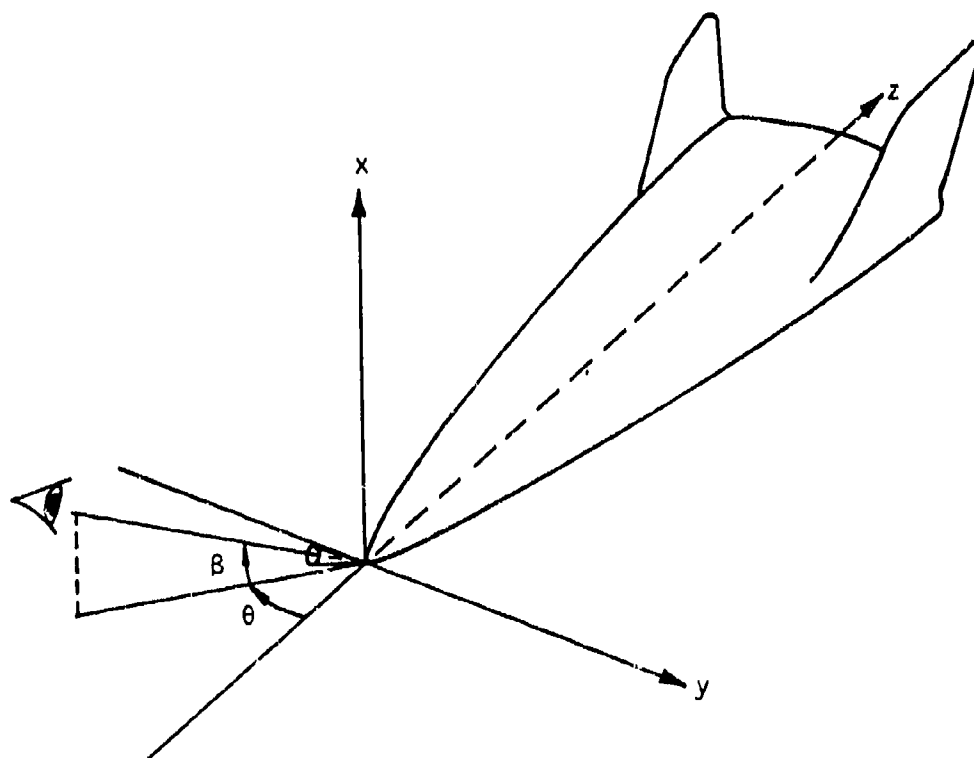


Figure 4.6. View Orientation Angles

#### 4.4.2 OUTPUT DESCRIPTION

This section describes the 3DMEIT code output. There are two classes of output from the 3DMEIT code:

1. Printout of the input data
2. Calculation (results) output

These are described in the following sections.

##### 4.4.2.1 Printout of Input Data

Program output begins with a complete printout of the contents of input Tables 1 through 7. Most of this output is fully labeled and is printed exactly as input by the user.

##### 4.4.2.2 Calculation Output

The results of the calculation are output in one of three formats. All three output formats include up to five separate groups of information. These groups are (1) environment information, (2) fluid properties, (3) boundary layer results, (4) body geometry and surface quantities results, and (5) aerodynamic coefficients. The output formats differ in the degree of detail of the boundary layer results. Also, the aerodynamic coefficients are only printed if NF(35) and NF(36) are nonzero. The following sections describe the variables printed in each of the output groups.

##### ENVIRONMENT INFORMATION

- ENVIRONMENT NUMBER
- DESCRIPTIVE HEADING: input on title card
- MACH NO: current freestream Mach number
- VELOCITY: current freestream velocity (ft/s)
- ANGLE OF ATTACK: current angle of attack (deg)
- UNIT RE NO: current value of freestream unit Reynolds number (per ft)

## FLUID PROPERTIES

The following results are printed for the freestream conditions, the conditions behind the normal shock, and the stagnation point conditions:

- PRESSURE (atm)
- TEMPERATURE ( $^{\circ}\text{R}$ )
- DENSITY ( $\text{lbm}/\text{ft}^3$ )
- ENTHALPY (Btu/lbm)
- ENTROPY (Btu/lbm  $^{\circ}\text{R}$ )
- ISENTROPIC EXPONENT

## BOUNDARY LAYER RESULTS

The summary output (NF(13) = 0) includes only the first of the following sets of information. The rest of the tables are printed for each streamline at either the streamline points (NF(13) = 1) or, in more detail, at the boundary layer integration points (NF(13) = 2).

### Boundary Layer Summary

- STREAMLINE NO: streamline number
- BETA, deg: initial direction of the streamline from the stagnation point
- SONIC POINT LOCATION, in.: streamlength from the stagnation point to the sonic point, and the Cartesian coordinates
- TRANSITION POINT LOCATION, in.: streamlength from the stagnation point to the transition point, and the Cartesian coordinates
- POINT NO: streamline point number or boundary layer integration point number

- STREAMLINE LOCATION, in. and deg: z-coordinate (measured from initial z-location of the nosetip) and PHI -- the angular location on the body (measured from the positive x-axis in the cross sectional plane)
- METRIC COEFFICIENT, in.: metric coefficient for the streamline coordinate system
- BODY ANGLE, deg: angle that a line tangent to the surface and perpendicular to the normal makes with the wind vector
- EDGE PRESSURE, atm: pressure at the edge of the boundary layer
- WALL TEMPERATURE, °R: temperature at the wall
- B-PRIME THERMOCHEM: dimensionless blowing parameter,  
 $B' \equiv (\rho v)_w / M$  due to ablation only, where  $M$  is the mass transfer coefficient
- RECOVERY ENTHALPY, Btu/lbm:  $h_r \equiv h_e + r (h_t - h_e)$   
 where  $h_t$  is the total enthalpy,  $h_e$  is the edge enthalpy, and  $r$  is the recovery factor
- HEAT TRANS COEFFICIENT, lbm/ft<sup>2</sup>-s:  $H = \rho_e u_e C_h = \frac{\dot{q}_w}{h_r - h_w}$ ,  
 where  $C_h$  is the Stanton number and  $\dot{q}_w$  is the surface heat flux

#### Viscous Flow -- Wall and Boundary Layer Recovery Properties

- BODY PT NO (J): index of the body points
- INTEG PT NO (I): index of the integration point for which the computed parameters are printed
- WALL TEMPERATURE, °R (TW): temperature of the wall
- WALL ENTHALPY, Btu/lbm (HW): enthalpy of the flow at the wall temperature
- WALL DENSITY, lbm/ft<sup>3</sup> (ROW): density of the flow at the wall temperature

- WALL VISCOSITY, lbm/ft-s (VISW): viscosity at the wall
- RECOVERY ENTHALPY, Btu/lbm (HR): recovery enthalpy,  

$$h_r = h_e + r(h_t - h_e)$$
- RECOVERY FACTOR (HECOV): recovery factor,  $r$
- SENSBL CONV HEAT FLUX, Btu/ft<sup>2</sup>-s
- CF/2: skin friction coefficient divided by two,  

$$C_f/2 = \tau_w / \rho_e u_e^2$$
- B-PRIME THERMOCHEM: dimensionless blowing parameter,  

$$B' \equiv (\rho v)_w / M$$
 due to ablation only, where  $M$  is the mass transfer coefficient
- RECOVERY ENTHALPY, Btu/lbm:  $h_r \equiv h_e + r(h_t - h_e)$  where  $h_t$  is the total enthalpy,  $h_e$  is the edge enthalpy, and  $r$  is the recovery factor
- HEAT TRANS COEFFICIENT, lbm/ft<sup>2</sup>-s:  $H = \rho_e u_e C_h = \frac{\dot{q}_w}{h_r - h_w}$ ,  
 where  $C_h$  is the Stanton number and  $\dot{q}_w$  is the surface heat flux

#### Viscous Flow -- Edge Properties Table

- BODY PT NO (J): index of the body parts
- INTEG PT NO (I): index of the integration point for which the computed parameters are printed
- STREAM LENGTH, in. (S): stream length along the nosetip surface from the stagnation point to the integration points
- VELOCITY, ft/s (UE): velocity at the edge of the boundary layer
- MACH NO (HCAM): Mach number at the edge of the boundary layer
- ENTHALPY, Btu/lbm (HE): enthalpy at the edge of the boundary layer

- TEMPERATURE,  $^{\circ}\text{R}$  (TE): temperature at the edge of the boundary layer
- DENSITY,  $\text{lbm/ft}^3$  (ROE): density at the edge of the boundary layer
- VISCOSITY,  $\text{lbm/ft-s}$  (VISE): viscosity at the edge of the boundary layer
- UNIT RE NO,  $1/\text{ft}$  (URE): unit Reynolds number at the edge of the boundary layer

#### Viscous Flow -- Boundary Layer Solution Table

- BODY PT NO (J): index of the body points
- INTEG PT NO (I): index of the integration point for which the computed parameters are printed
- STREAM LENGTH, in. (S): stream length along the nosetip surface from the stagnation point to the integration points
- MOMENTUM THICKNESS, mil (THE): momentum thickness  $\theta$  of the boundary layer

$$\theta = \int_0^{\delta} \frac{\rho u}{\rho_e u_e} \left( 1 - \frac{u}{u_e} \right) dy$$

where  $\delta$  is the momentum boundary layer thickness and  $y$  is the radial distance from the centerline. For a more general definition of  $\theta$  (also  $\phi$  and  $\delta^*$ ) see Reference 1).

- ENERGY THICKNESS, mil (PHI): energy thickness  $\phi$  of the boundary layer

$$\phi = \int_0^{\delta\phi} \frac{\rho u}{\rho_e u_e} \left( \frac{h_{te} - h_t}{h_{te} - h_w} \right) dy$$

where  $h_t$  is the total enthalpy and  $\delta_\phi$  is thickness of the energy boundary layer

- SHAPE FACTOR (HSF): boundary layer shape factor,  $H = \delta^*/\theta$
- MOM THICK RE NO (RETH): Reynolds number based on the momentum thickness

$$Re_\theta = \frac{\rho_e u_e \theta}{\mu_e}$$

- ENERGY THICK RE NO (REPH): Reynolds number based on the energy thickness,

$$Re_\phi = \frac{\rho_e u_e \phi}{\mu_e}$$

- HEAT TRANS COEFFICIENT,  $lbm/ft^2s$  (RUCH): heat transfer coefficient,  $H = \rho_e u_e C_h = \dot{q}_w / (h_r - h_w)$   
where  $C_h$  is the Stanton number and  $\dot{q}_w$  is the wall heat flux

- REYNOLDS ANAL FAC (RAF): Reynolds analogy factor

$$C_h / (1/2) C_f,$$

where  $C_f/2 = \tau_w / (\rho_e u_e^2)$  is the friction factor and  $\tau_w$  is the wall shear

- INTERMITTENCY (ADML): boundary layer intermittency factor  $f$ ,  
where  $0 \leq f \leq 1$  for flow ranging from fully laminar to fully turbulent regime
- TRANSITION PARAMETER: Anderson nosetip transition parameter,

$$TP \equiv Re_\theta \left( \frac{k}{\theta} \frac{1}{4} \right)^{0.7}$$

where  $\psi \equiv 0.1 B' + 0.9 (1 + 0.25 B')$   $\rho_e / \rho_w$

### Viscous Flow -- Curved Shock and Roughness Effects Table

- BODY PT NO (J): index of the body points
- INTEG PT NO (L): index of the integration point for which the computer parameters are printed
- STREAM LENGTH, in. (S): stream length along the nosetip surface from the stagnation point to the integration points
- EDGE ENTROPY, Btu/lbm -  $^{\circ}$ R (ENTR): entropy at the edge of the boundary layer
- EDGE STREAMLINE LOCATION AT SHOCK, in. (YBAR): radial coordinate of the point of intersection of the boundary layer edge streamline with shock wave
- EDGE MASS FLUX AUGMENTATION (ROUE): ratio of the boundary layer edge mass flux,  $\rho_e u_e$  to that for a normal shock
- ROUGHNESS, mil (RUF): surface effective sand grain roughness height
- HEAT TRANSFER AUGMENTATION (RUF SMT): augmentation of the heat transfer coefficient due to:
  - transition proximity for the laminar portion, and
  - surface roughness effects for the turbulent portion of the boundary layer

#### BODY GEOMETRY AND BOUNDARY LAYER RESULTS

This table includes information for all of the u and w locations where the information is saved (TBU and TBZ arrays, see Table 3, input).

- STAGNATION POINT LOCATION: Cartesian coordinates and the normalized surface coordinates of the stagnation point



- MINIMUM Z-COORD LOCATION: Cartesian coordinates and the normalized surface coordinates of the point with the minimum z-coordinate
- SURFACE COORDINATES: non-normalized u and w locations of the points
- CARTESIAN COORDINATES: Cartesian coordinates of the points
- RECOVERY ENTHALPY (same as boundary layer output)
- SURFACE PRESSURE (same as edge pressure in boundary layer)
- HEAT TRANS COEFFICIENT (same as boundary layer output)
- INDUCED PRESSURE: pressure calculated using the boundary displacement thickness (atm)
- SKIN FRICTION: skin friction coefficient,  $C_f/2$
- B-PRIME THERMOCHEM (same as boundary layer output)
- SURFACE TEMPERATURE (same as boundary layer output)

#### AERODYNAMIC COEFFICIENTS

This table is printed if the aerodynamic coefficients are calculated (NF(35)  $\neq$  0 and NF(36)  $\neq$  0). The output includes the lift-to-drag ratio, the center of pressure, and the x, y, and z components of: (1) drag, (2) lift, (3) total force, (4) inviscid force, (5) viscous forces (induced pressure and shear), (6) total moment, (7) inviscid moment, and (8) viscous moments.

#### 4.4.3 SAMPLE PROBLEM

This section presents input listings and selected output page listings for the flight test case. The complete output is shown for the windward and leeward streamlines, while only the first output table is shown for the remaining streamlines.

FLIGHT CALCULATION MACH=16.2 ALPHA=9.0 10.4/6.0 BICONIC w/ YAW STAU.

01 GENERAL CONSTANTS

0	1	1	6	0	2	2	4	-1	-1	0
0.08333	560.			0.0		0.0	41.0			
415.48	81.86									

02 ENVIRONMENT TABLE

389.87	0.074868	15609.	5.0	22
180.0	179.7151	179.1897	178.6070	178.2586
176.8858	176.4636	176.0602	175.0483	173.4933
90.	70.	50.	30.	10.
				0.0

03 GEOMETRY TABLE

0.92	10.4	1.0	4.1764	2	1
5 2 2 1 1 4					
4 4 4 4 7					
4.1764	0.0	4.9303	0.9049	10.4	
4.9303	0.9049	31.3304	5.7502		
31.3304	5.7502	80.2864	10.8457		

10.8457	11.0471	11.2986	11.5000	10.7331	10.9315	11.1300	11.2384
10.2502	10.4397	10.6293	10.8187	9.4614	9.6363	9.8113	9.9862
0.0	0.0	0.0	0.0	1.8752	1.9094	1.9446	1.9792
3.6945	3.7628	3.8311	3.8994	5.4614	5.5034	5.6033	5.7032
80.2864	82.2031	84.1197	86.0364	80.2864	82.2031	84.1197	86.0364
80.2864	82.2031	84.1197	86.0364	80.2864	82.2031	84.1197	86.0364
9.4614	9.6363	9.8113	9.9862	7.9372	8.0788	8.2255	8.3721
6.0042	6.1152	6.2262	6.3372	4.2500	4.2500	4.2500	4.2500
5.4035	5.5034	5.6033	5.7032	7.4697	7.6078	7.7459	7.8840
9.0921	9.2601	9.4283	9.5963	10.1349	10.3511	10.5669	10.7819
80.2864	82.2031	84.1197	86.0364	80.2864	82.2031	84.1197	86.0364
80.2864	82.2031	84.1197	86.0364	80.2864	82.2031	84.1197	86.0364
4.2500	4.2500	4.2500	4.2500	4.2500	4.2500	4.2500	4.2500
4.2500	4.2500	4.2500	4.2500	4.2500	4.2500	4.2500	4.2500
10.1349	10.3511	10.5669	10.7819	10.1349	10.4309	10.7257	11.0194
10.1349	10.5106	10.8846	11.2568	10.1349	10.5904	11.0434	11.4943
80.2864	82.2031	84.1197	86.0364	80.2864	82.2031	84.1197	86.0364
80.2864	82.2031	84.1197	86.0364	80.2864	82.2031	84.1197	86.0364
4.2500	4.2500	4.2500	4.2500	1.3333	1.3333	1.3333	1.3333
-1.3333	-1.3333	-1.3333	-1.3333	-4.2500	-4.2500	-4.2500	-4.2500
10.1349	10.5904	11.0434	11.4943	10.8138	11.2418	11.6696	12.0971
10.8138	11.2418	11.6696	12.0971	10.1349	10.5904	11.0434	11.4943
80.2864	82.2031	84.1197	86.0364	80.2864	82.2031	84.1197	86.0364
80.2864	82.2031	84.1197	86.0364	80.2864	82.2031	84.1197	86.0364
4.2500	4.2500	4.2500	4.2500	-4.2500	-4.2500	-4.2500	-4.2500
-4.2500	-4.2500	-4.2500	-4.2500	-4.2500	-4.2500	-4.2500	-4.2500
10.1349	10.5904	11.0434	11.4943	10.1349	10.5106	10.8846	11.2568
10.1349	10.4309	10.7257	11.0194	10.1349	10.3511	10.5669	10.7819
80.2864	82.2031	84.1197	86.0364	80.2864	82.2031	84.1197	86.0364
80.2864	82.2031	84.1197	86.0364	80.2864	82.2031	84.1197	86.0364
-4.2500	-4.2500	-4.2500	-4.2500	-6.0042	-6.1152	-6.2262	-6.3372
-7.9322	-8.0788	-8.2255	-8.3721	-9.4614	-9.6363	-9.8113	-9.9862
10.1349	10.3511	10.5669	10.7819	9.0921	9.2601	9.4283	9.5963
7.4697	7.6078	7.7459	7.8840	5.4035	5.5034	5.6033	5.7032
80.2864	82.2031	84.1197	86.0364	80.2864	82.2031	84.1197	86.0364
80.2864	82.2031	84.1197	86.0364	80.2864	82.2031	84.1197	86.0364
-9.4614	-9.6363	-9.8113	-9.9862	-10.2502	-10.4397	-10.6293	-10.8187
-10.7331	-10.9315	-11.1300	-11.3284	-10.8457	-11.0471	-11.2496	-11.4500



3-D MOMENTUM ENERGY INTEGRAL TECHNIQUE

\*\*\*\*\*

\*\*\*\*\* I N P U T \*\*\*\*\*

FLIGHT CALCULATION MACH=16.2 ALPHA=5.0 10.4/6.0 BICNIC W/ YAW STAR.

--- GENERAL PROGRAM FLAGS ---

PLOT OUTPUT FLAG	NF(12) = 0
PRINT OUTPUT FLAG	NF(13) = 1
TRANSITION CRITERIA FLAG	NF(15) = 6
CARDON TRANS. CRIT. FLAG	NF(16) = 0
GAS PROPERTY FLAG	IRG = 1
ENTROPY SWALLOWING FLAG	IFNTRP = 4
BLOWING CORRECTION FLAG	JBLM = 0

SCALE FACTOR	0.0033
INITIAL WALL TEMPERATURE (DEG R)	560.0000

# 3-D MOMENTUM ENERGY INTEGRAL TECHNIQUE

## --- GENERAL ENVIRONMENT ---

PRESSURE (ATM)	TEMPERATURE (DEG F)	VELOCITY (FPS)	ALPHA (DEG)
0.075	387.87	15609.00	5.00

NUMBER OF STREAMLINES = 22

STREAMLINE IDENTIFYING ANGLES ARE

180.00	179.74	179.19
176.06	175.05	173.49
10.00	0.0	

177.26	176.89	176.44
70.00	50.00	30.00

--- ROPU GENYETNY ---

NPATCH (1) = 4 4 4 4 7

$\text{ZBRT}(A) = 0.493037 \times 0.904900 + 0.313300 + 0.575020 + 0.1$	0.0	0.0
---	-----	-----

2RT181 = 0.313300+02	0.575020+01	0.802860+02	0.108960+02	0.0	0.0
----------------------	-------------	-------------	-------------	-----	-----

0.0	0.210+000.	410+000.	590+000.0	0.200+000.-	400+000.	570+000.0	0.180+000.	360+000.	510+000.0	0.150+000.	270+000.0
0.0	0.0	0.0	0.0	0.0	0.550-010.	110+000.	150+000.0	0.110+000.	210+000.	270+000.0	0.150+000.
0.420+010.	420+010.	430+010.	440+010.	420+010.	440+010.	430+010.	440+010.	420+010.	430+010.	440+010.	420+010.

	0.150+000.290+000.420+009.0	0.110+006.210+000.290+000.0	0.550-010.110+000.150+000.0	0.780-000.540+000.0.780-000.
0.0.0				
0.150+000.290+000.420+000.0	0.180+000.360+000.510+000.0	0.200+000.400+000.570+000.0	0.210+000.410+000.550+000.	
0.420+010.630+010.640+010.640+010.	0.200+010.430+010.460+010.420+010.620+010.640+010.640+010.	0.420+010.620+010.640+010.640+010.640+010.640+010.	0.620+010.640+010.640+010.640+010.640+010.640+010.	

[illegible]

0.0	-0.150+00-	0.290+00-	0.420+00.0	-0.180+00-	0.360+00-	0.510+00.0	-0.700+00-	0.400+00-	0.570+00.0	-0.210+00-	0.410+00-	0.540+00.0
0.0	0.150+00.0	0.290+00.0	0.420+00.0	0.110+00.0	0.210+00.0	0.290+00.0	0.550+01.0	0.110+00.0	0.150+00.0	0.560+00.0	0.110+00.0	0.140+00.0
0.0	0.150+00.0	0.290+00.0	0.420+00.0	0.200+01.0	0.420+01.0	0.440+01.0	0.200+01.0	0.420+01.0	0.270+01.0	0.420+01.0	0.270+01.0	0.440+01.0
0.0	0.200+01.0	0.420+01.0	0.440+01.0	0.200+01.0	0.420+01.0	0.440+01.0	0.200+01.0	0.420+01.0	0.440+01.0	0.200+01.0	0.420+01.0	0.440+01.0









3-D MOMENTUM ENERGY INTEGRAL TECHNIQUE

---MATERIAL PROPERTIES---

\*\*\*\*\* MATERIAL NUMBER 1 \*\*\*\*\*

--- SURFACE ROUGHNESS ---

ROUGHNESS HEIGHT FOR TRANSITION	K-LAM = 0.230 (MIL)
ROUGHNESS HEIGHT FOR TURBULENT HEATING	K-TURN = 2.000 (MIL)
LAMINAR HEATING AUGMENTATION FLAG	JROUGH = 1

--- PARAMETERS IN BLOWING CORRECTION TO TRANSFER COEFFICIENTS ---

LAMINAR SHEAR PARAMETER	(HLS) = 0.5000
LAMINAR HEATING PARAMETER	(HLH) = 0.5000
TURBULENT SHEAR PARAMETER	(HTS) = 0.3500
TURBULENT HEATING PARAMETER	(BTH) = 0.3500

3-D MOMENTUM ENERGY INTEGRAL TECHNIQUE

\*\*\*\*\* MATERIAL NUMBER 2 \*\*\*\*\*

--- SURFACE ROUGHNESS ---

ROUGHNESS HEIGHT FOR TRANSITION	K-LAM = 0.230 (MIL)
ROUGHNESS HEIGHT FOR TURBULENT HEATING	K-TURN = 2.000 (MIL)
LAMINAR HEATING AUGMENTATION FLAG	JROUGH = 1

--- PARAMETERS IN BLOWING CORRECTION TO TRANSFER COEFFICIENTS ---

LAMINAR SHEAR PARAMETER	(HLS) = 0.5000
LAMINAR HEATING PARAMETER	(HLH) = 0.5000
TURBULENT SHEAR PARAMETER	(HTS) = 0.3500
TURBULENT HEATING PARAMETER	(BTH) = 0.3500

## 3-D MOMENTUM ENERGY INTEGRAL TECHNIQUE

--- INVISCID DATA ---

AMINF = 1.62000+01 ALPHA = 5.00000+00 MUAT = 36 NDAI = 11

Z = 0.0

M	PHDAT	RB	RBZ	WATH	OMEGA	SF
1	3.1470+00	0.0	5.5710+08	0.0	0.0	3.1420+00
2	3.1370+00	0.0	5.5710+08	0.0	4.1800-04	3.1370+00
3	3.1320+00	0.0	5.5710+08	0.0	8.4300-04	3.1370+00
4	3.1270+00	0.0	5.5710+08	0.0	1.2700-03	3.1270+00
5	3.1220+00	0.0	5.5710+08	0.0	1.7300-03	3.1270+00
6	3.1170+00	0.0	5.5710+08	0.0	2.1900-03	3.1170+00
7	3.1110+00	0.0	5.5710+08	0.0	2.7470-03	3.1110+00
8	3.1050+00	0.0	5.5710+08	0.0	3.3310-03	3.1050+00
9	3.1000+00	0.0	5.5710+08	0.0	3.7810-03	3.1000+00
10	3.0940+00	0.0	5.5710+08	0.0	4.3200-03	3.0940+00
11	3.0870+00	0.0	5.5710+08	0.0	4.9110-03	3.0870+00
12	3.0800+00	0.0	5.5710+08	0.0	5.5770-03	3.0800+00
13	3.0730+00	0.0	5.5710+08	0.0	6.2110-03	3.0730+00
14	3.0650+00	0.0	5.5710+08	0.0	6.9480-03	3.0650+00
15	3.0550+00	0.0	5.5710+08	0.0	7.8020-03	3.0550+00
16	3.0440+00	0.0	5.5710+08	0.0	8.8450-03	3.0440+00
17	3.0280+00	0.0	5.5710+08	0.0	1.0240-02	3.0280+00
18	2.9950+00	0.0	5.5710+08	0.0	1.3200-02	2.9950+00
19	2.9670+00	0.0	5.5710+08	0.0	1.5640-02	2.9670+00
20	2.7430+00	0.0	5.5710+08	0.0	3.0880-02	2.7930+00
21	2.6180+00	0.0	5.5710+08	0.0	4.5070-02	2.6180+00
22	2.4430+00	0.0	5.5710+08	0.0	5.7820-02	2.4430+00
23	2.2640+00	0.0	5.5710+08	0.0	6.8740-02	2.2690+00
24	2.0940+00	0.0	5.5710+08	0.0	7.7500-02	2.0940+00
25	1.9200+00	0.0	5.5710+08	0.0	8.3850-02	1.9200+00
26	1.7450+00	0.0	5.5710+08	0.0	8.7620-02	1.7450+00
27	1.5710+00	0.0	5.5710+08	0.0	8.8720-02	1.5710+00
28	1.3960+00	0.0	5.5710+08	0.0	8.7110-02	1.3960+00
29	1.2220+00	0.0	5.5710+08	0.0	8.2940-02	1.2220+00
30	1.0470+00	0.0	5.5710+08	0.0	7.6270-02	1.0470+00
31	8.7270-01	0.0	5.5710+08	0.0	6.7340-02	8.7270-01
32	6.9810-01	0.0	5.5710+08	0.0	5.6420-02	6.9810-01
33	5.2360-01	0.0	5.5710+08	0.0	4.3440-02	5.2360-01
34	3.4910-01	0.0	5.5710+08	0.0	2.9960-02	3.4910-01
35	1.7450-01	0.0	5.5710+08	0.0	1.5200-02	1.7450-01
36	0.0	0.0	5.5710+08	0.0	0.0	0.0

OUTPUT DELETED

# 3-D MOMENTUM ENERGY INTEGRAL TECHNIQUE

FLIGHT CALCULATION MACH=16.2 ALPHA=5.0 10.4/R.O. RICONIC W/ YAW STAR.

MACH NO VELOCITY ANGLE OF UNIT RE NO  
(FT/SEC) ATTACK (L/FT)  
16.20 15609.00 5.00 1.24330+07

FLUID PROPERTIES		PRESSURE (ATM)	TEMPERATURE (DEGR)	DENSITY (LBM/FT3)	ENTHALPY (BTU/LBM)	ENTROPY (BTU/LBM-DEGR)	ISENTROPIC EXPOONENT
FREESTREAM NORMAL SHOCK STAGNATION		0.075	389.870	0.007617	93.27	1.7140	1.187
		24.619	10654.924	0.076593	4210.82	2.4869	1.181
		25.964	10743.801	0.080024	4958.94	2.4869	1.181

# 3-D MOMENTUM ENERGY INTEGRAL TECHNIQUE

STREAMLINE NO.	BODY PT NO	INTEG PT NO	BETA (DEG)	SONIC POINT LOCATION			TRANSITION POINT LOCATION			WALL TEMPERATURE (DEGR)	R-PRIME THERM CHGM	REFLECTIV EMISSIVITY (100/100)	HEAT TRANS COEFFICIENT (100/100)
				S			S						
				X	Y	Z	X	Y	Z				
1			0.0	0.554	-0.591	0.000	0.215	10.026	-7.510	0.000	0.445		
	1	1	3.44900-03	-0.00				25.9465	7249.34	3.44900-01		4054.04	1.15000000
	2	7	1.26680-02	0.00				25.9467	7171.29	3.26310-01		4051.71	0.87700-01
	3	9	5.34410-02	0.00				23.7139	7091.79	3.11340-01		4039.09	0.87700-01
	4	11	1.21770-01	0.00				20.3347	7014.63	3.04320-01		4011.57	0.87700-01
	5	13	2.15090-01	0.00				16.0331	6892.57	2.93780-01		4076.48	0.87700-01
	6	15	3.27540-01	0.00				11.6360	6736.40	2.79120-01		4030.46	0.87700-01
	7	17	4.58900-01	0.00				7.6666	6515.20	2.61410-01		4177.00	0.87700-01
	8	19	6.04800-01	0.00				4.7233	6224.40	2.45770-01		4121.33	0.87700-01
	9	21	7.53900-01	0.00				2.7776	5639.60	2.47500-01		4679.37	1.00100-01
	10	23	1.38910+00	0.00				2.1242	5187.81	2.31440-01		4554.40	1.16710-01
	11	25	2.39530+00	0.00				1.6723	4879.31	2.20160-01		4613.11	0.90850-01
	12	27	3.66200+00	0.00				1.4446	4678.09	2.29110-01		4589.40	0.77000-01
	13	29	5.02540+00	0.00				1.4037	4610.19	2.27890-01		4572.75	0.77000-01
	14	31	6.37810+00	0.00				1.4565	4616.10	2.28940-01		4556.53	0.77000-01
	15	33	7.67020+00	0.00				1.5530	4652.25	2.29080-01		4539.50	0.77000-01
	16	35	8.88090+00	0.00				1.6706	4678.66	2.29210-01		4520.79	0.90850-01
	17	37	1.00090+01	0.00				1.7941	4981.27	2.30590-01		4516.51	1.00100-01
	18	39	1.10670+01	0.00				1.9121	5536.27	2.47270-01		4539.28	1.77000-01
	19	41	1.20770+01	0.00				2.0110	5846.03	2.73730-01		4567.95	2.70590-01
	20	43	1.30600+01	0.00				2.0824	5962.86	2.83670-01		4571.25	3.13450-01
	21	45	1.40340+01	0.00				2.1223	5979.70	2.86970-01		4566.21	3.32770-01
	22	47	1.50160+01	0.00				2.1352	5987.65	2.88100-01		4553.10	3.40270-01
	23	49	1.60230+01	0.00				2.1282	5981.27	2.88030-01		4561.08	3.47700-01
	24	51	1.70570+01	0.00				2.1104	5976.25	2.87620-01		4524.93	3.47800-01
	25	53	1.81600+01	0.00				2.0883	5969.41	2.87050-01		4517.53	3.42910-01
	26	55	1.93090+01	0.00				2.0659	5962.07	2.86610-01		4506.54	3.41300-01
	27	57	2.05270+01	0.00				2.0460	5955.42	2.85800-01		4497.27	3.39800-01
	28	59	2.18010+01	0.00				2.0366	5950.70	2.85400-01		4488.50	3.36240-01
	29	61	2.31650+01	0.00				2.0304	5946.50	2.85100-01		4484.15	3.38230-01
	30	63	2.45670+01	0.00				2.0286	5941.63	2.84520-01		4476.49	3.37700-01
	31	65	2.60560+01	0.00				2.0298	5941.65	2.84250-01		4471.51	3.37230-01
	32	67	2.76920+01	0.00				1.2941	5647.25	2.63760-01		4487.10	2.70020-01
	33	69	3.00440+01	0.00				0.9179	5394.10	2.50450-01		4475.50	1.66430-01
	34	71	3.31990+01	0.00				0.8720	5369.41	2.45800-01		4466.08	1.61350-01
	35	73	3.71000+01	0.00				0.8983	5405.43	2.51560-01		4453.12	1.60620-01
	36	75	4.19850+01	0.00				0.8935	5407.58	2.51300-01		4448.11	1.60300-01
	37	77	4.73830+01	0.00				0.8985	5408.13	2.51770-01		4446.17	1.70000-01
	38	79	5.30670+01	0.00				0.9231	5424.21	2.52610-01		4446.11	1.77700-01
	39	81	5.88130+01	0.00				0.9478	5438.51	2.52710-01		4446.24	1.90300-01
	40	83	6.45200+01	0.00				0.9787	5456.68	2.53710-01		4446.57	1.77440-01
	41	85	7.01900+01	0.00				1.0176	5479.29	2.54640-01		4447.27	1.84700-01
	42	87	7.58820+01	0.00				1.0511	5496.72	2.55300-01		4447.96	1.88300-01
	43	89	8.16410+01	0.00				1.0669	5501.63	2.55670-01		4448.63	1.89100-01
	44	91	8.74800+01	0.00				1.0670	5501.56	2.55670-01		4448.66	1.99900-01

# 3-D MOMENTUM ENERGY INTEGRAL TECHNIQUE

VISCOS FLOW - EDGE PROPERTIES  
\*\*\*\*\*

BODY PT NO (J)	INTEG PT NO (I)	STREAM LENGTH INCH (S)	VELOCITY FT/SEC (UE)	MACH NO (MACH)	ENTHALPY BTU/LBM (HE)	TEMPERATURE DEG R (TE)	DENSITY LBM/FT3 (PDE)	VISCOSITY LBM/FT-SFC (VISE)	INIT PF NO I/FT (UPEC)
1	1	0.0	0.0	0.0	4958.9	10743.8	4.0020E-02	9.9760E-05	0.0
2	7	0.0729	1266.2	0.2486	4274.9	10491.9	1.9760E-02	9.9400E-05	1.0100E-04
3	9	0.2333	2411.0	0.4771	4422.9	10543.7	7.4700E-02	9.9430E-05	1.0430E-04
4	11	0.3936	3729.4	0.7500	4681.2	10750.3	6.6140E-02	9.9460E-05	2.5500E-04
5	13	0.5540	5027.8	1.0763	4454.1	9824.2	5.5790E-02	9.9460E-05	2.9470E-04
6	15	0.7164	6275.8	1.3373	4172.4	9243.4	4.7540E-02	9.9460E-05	2.9810E-04
7	17	0.8747	7468.4	1.6588	3465.0	8596.0	3.0510E-02	9.9460E-05	2.9850E-04
8	19	1.0351	8498.8	1.9753	3516.5	7937.9	2.0630E-02	9.9460E-05	2.9410E-04
9	21	1.1891	9258.5	2.2371	3247.0	7410.0	1.3150E-02	7.4100E-05	1.6010E-04
10	23	1.8348	9784.4	2.6267	3045.5	7094.8	1.0620E-02	7.3550E-05	1.4140E-04
11	25	2.8579	10293.5	2.6156	2862.9	6804.4	8.8200E-03	7.1200E-05	1.2750E-04
12	27	4.1457	10642.2	2.7514	2697.1	6608.2	7.4110E-03	6.9470E-05	1.2100E-04
13	29	5.5319	10880.7	2.8453	2594.6	6487.9	7.0860E-03	6.8520E-05	1.2520E-04
14	31	6.9072	11106.9	2.9350	2445.3	6390.8	8.1690E-03	6.7580E-05	1.3750E-04
15	33	8.2208	11339.5	3.0299	2391.0	6285.6	9.2160E-03	6.6580E-05	1.5610E-04
16	35	9.4517	11589.5	3.1157	2276.5	6168.8	1.0150E-02	6.5680E-05	1.7940E-04
17	37	10.5985	11844.0	3.2495	2157.4	6032.2	1.1250E-02	6.4740E-05	2.0750E-04
18	39	11.6748	12114.9	3.3774	2027.8	5876.8	1.2440E-02	6.3850E-05	2.3980E-04
19	41	12.7015	12395.1	3.5218	1890.7	5678.8	1.3670E-02	6.1200E-05	2.7680E-04
20	43	13.7003	12685.5	3.6833	1745.2	5457.2	1.4870E-02	5.9370E-05	3.1780E-04
21	45	14.6907	12967.4	3.8622	1600.8	5185.1	1.6050E-02	5.7250E-05	3.6170E-04
22	47	15.6898	13249.9	4.0563	1458.2	4893.4	1.7200E-02	5.4980E-05	4.1470E-04
23	49	16.7132	13590.7	4.2676	1324.2	4570.8	1.8400E-02	5.2710E-05	4.7200E-04
24	51	17.7748	13723.5	4.4974	1197.7	4237.6	1.9720E-02	4.9910E-05	5.4230E-04
25	53	18.8857	13932.0	4.7467	1082.6	3897.7	2.1240E-02	4.7220E-05	6.2710E-04
26	55	20.0545	14125.2	5.0123	974.3	3572.1	2.2940E-02	4.4570E-05	7.2710E-04
27	57	21.2874	14285.7	5.2727	883.3	3287.1	2.4750E-02	4.2150E-05	8.3890E-04
28	59	22.5880	14433.7	5.5462	798.4	3031.5	2.6830E-02	3.9870E-05	9.7270E-04
29	61	23.9584	14541.0	5.7806	736.3	2801.0	2.8750E-02	3.7970E-05	1.1010E-03
30	63	25.3929	14635.4	6.0101	681.3	2614.6	3.0770E-02	3.6280E-05	1.2410E-03
31	65	26.9137	14716.4	6.2279	633.8	2453.5	3.2780E-02	3.4790E-05	1.3840E-03
32	68	28.5601	14777.7	6.4610	773.0	2923.7	1.7560E-02	3.9060E-05	4.5080E-04
33	71	30.4355	14656.1	6.8467	669.2	2572.3	1.6040E-02	3.5490E-05	5.7480E-04
34	75	34.1076	14829.4	6.5836	567.1	2219.7	1.5540E-02	3.2570E-05	7.0550E-04
35	80	38.1200	14995.5	7.2409	468.2	1861.2	1.9140E-02	2.9000E-05	9.8080E-04
36	86	42.9459	15074.6	7.6265	420.7	1689.0	2.0700E-02	2.7200E-05	1.1580E-03
37	93	48.3709	15104.3	7.7871	407.8	1624.1	2.1740E-02	2.6510E-05	1.3070E-03
38	100	54.0846	15111.7	7.8299	398.3	1607.3	2.2780E-02	2.6370E-05	1.4500E-03
39	107	59.8626	15112.6	7.8353	397.8	1605.2	2.3670E-02	2.6310E-05	1.5500E-03
40	114	65.5005	15110.2	7.8207	399.2	1611.0	2.4100E-02	2.6370E-05	1.6510E-03
41	121	71.3024	15102.6	7.7770	403.8	1627.9	2.4800E-02	2.6550E-05	1.7410E-03
42	128	77.0252	15093.4	7.7264	409.4	1646.0	2.5100E-02	2.6770E-05	1.8770E-03
43	135	82.8164	15087.8	7.6762	412.7	1660.2	2.5400E-02	2.6900E-05	1.9300E-03
44	137	83.0364	15087.7	7.6957	412.8	1660.4	2.5400E-02	2.6900E-05	1.9300E-03

# 3-D MOMENTUM ENERGY INTEGRAL TECHNIQUE

## VISCOS FLOW - WALL AND R. L. RECOVERY PROPERTIES

BODY PT NO (J)	INTEG PT NO (I)	STREAM LENGTH INCH (S)	WALL TEMPERATURE DEG R (TW)	WALL ENTHALPY BTU/LHM (HW)	WALL DENSITY LHM/FT3 (RW)	WALL VISCOSITY LHM/FT-SEC (VISM)	RECOVERY ENTHALPY BTU/LHM (HP)	RECOVERY FACTOR (RECOV)	SENSBL COMV HEAT FLUX BTU/FT2-SEC	REF/2
1	1	0.0	7249.3	2626.4	1.3500-01	7.2640-05	4958.9	0.8367	2.7030E-03	1.0000E-03
2	7	0.6729	7171.3	2575.4	1.3430-01	7.2030-05	4953.7	0.8367	1.4913E-03	7.2440-03
3	9	0.2333	7091.6	2531.6	1.2670-01	7.1440-05	4940.0	0.8367	1.6540E-03	3.9540-03
4	11	0.3936	7016.6	2500.9	1.0980-01	7.0430-05	4913.6	0.8367	1.5060E-03	2.7370-03
5	13	0.5540	6899.6	2461.9	8.8000-02	7.0170-05	4876.5	0.8367	1.3110E-03	2.2780-03
6	15	0.7144	6734.4	2401.2	6.5440-02	6.9050-05	4810.5	0.8367	1.0800E-03	2.0710-03
7	17	0.8747	6515.2	2307.1	4.4640-02	6.7500-05	4773.0	0.8367	8.5570E-02	1.9500-03
8	19	1.0351	6228.4	2169.4	2.8900-02	6.5410-05	4723.3	0.8367	6.4250E-02	1.8940-03
9	21	1.1891	5639.6	1838.9	1.9110-02	6.0790-05	4678.3	0.8367	5.1170E-02	1.7080-03
10	23	1.8348	5187.8	1607.2	1.4040-02	5.7270-05	4646.4	0.8367	3.5480E-02	1.0340-03
11	25	2.8579	4479.3	1457.6	1.3510-02	5.4880-05	4613.3	0.8367	2.8470E-02	1.0100-03
12	27	4.1457	4678.1	1375.0	1.2190-02	5.3340-05	4589.5	0.8367	2.4670E-02	4.6710-03
13	29	5.5319	4610.4	1346.4	1.2030-02	5.2810-05	4572.8	0.8367	2.1470E-02	4.0700-03
14	31	6.9072	4618.1	1348.3	1.2450-02	5.2810-05	4556.5	0.8367	2.1470E-02	5.5470-03
15	33	8.2208	4652.2	1362.7	1.3180-02	5.3140-05	4539.5	0.8367	2.1470E-02	5.1800-03
16	35	9.4517	4606.7	1380.3	1.4040-02	5.3480-05	4520.8	0.8367	2.5310E-02	5.4370-03
17	37	10.5985	4981.4	1498.9	1.6180-02	5.5660-05	4514.5	0.8367	2.1230E-02	5.4140-03
18	39	11.6748	5536.2	1802.2	1.3410-02	6.0040-05	4519.3	0.8367	2.4850E-02	9.4770-03
19	41	12.7015	5856.0	2007.0	1.3150-02	6.2670-05	4568.0	0.8367	6.0400E-02	1.7100-03
20	43	13.7003	5942.8	2068.4	1.3370-02	6.3190-05	4571.2	0.8367	7.8650E-02	1.3000-03
21	45	14.6907	5973.2	2088.9	1.3510-02	6.3640-05	4564.2	0.8367	8.2250E-02	1.2300-03
22	47	15.6898	5982.7	2095.2	1.3590-02	6.3720-05	4553.1	0.8367	8.2370E-02	1.1600-03
23	49	16.7132	5981.3	2094.6	1.3550-02	6.3710-05	4541.1	0.8367	8.2400E-02	1.1600-03
24	51	17.7748	5976.2	2091.9	1.3450-02	6.3670-05	4528.9	0.8367	8.2380E-02	1.0490-03
25	53	18.8857	5969.4	2088.1	1.3370-02	6.3620-05	4517.5	0.8367	8.2380E-02	9.7530-03
26	55	20.0545	5962.1	2084.0	1.3200-02	6.3560-05	4506.5	0.8367	8.2380E-02	8.8770-03
27	57	21.2874	5955.4	2080.1	1.3100-02	6.3510-05	4497.3	0.8367	8.2380E-02	8.0400-03
28	59	22.5580	5950.7	2077.7	1.3020-02	6.3470-05	4488.5	0.8367	8.2380E-02	7.3700-03
29	61	23.5584	5946.5	2074.4	1.3020-02	6.3440-05	4482.2	0.8367	8.2380E-02	6.7970-03
30	63	25.1999	5943.6	2072.4	1.3010-02	6.3410-05	4476.5	0.8367	8.2380E-02	6.2740-03
31	65	26.9137	5941.8	2070.9	1.3030-02	6.3400-05	4471.5	0.8367	8.2380E-02	5.9750-03
32	68	28.5601	5942.2	1910.8	8.8000-03	6.1080-05	4472.2	0.8367	8.2380E-02	7.1490-03
33	71	30.5355	5933.5	1770.4	6.5400-03	5.9100-05	4475.5	0.8367	8.2380E-02	6.5470-03
34	75	34.1076	5369.1	1777.3	6.2400-03	5.8910-05	4464.0	0.8367	8.2380E-02	6.5470-03
35	80	38.1200	5405.4	1780.5	6.4240-03	5.9210-05	4453.1	0.8367	8.2380E-02	6.5470-03
36	86	42.9459	5403.6	1779.4	6.3640-03	5.9190-05	4448.1	0.8367	8.2380E-02	6.5470-03
37	93	48.3700	5408.3	1782.6	6.4230-03	5.9230-05	4446.4	0.8367	8.2380E-02	6.5470-03
38	100	54.0446	5424.2	1791.4	6.5750-03	5.9460-05	4444.1	0.8367	8.2380E-02	6.5470-03
39	107	59.8626	5438.5	1799.0	6.7300-03	5.9470-05	4446.2	0.8367	8.2380E-02	6.5470-03
40	114	65.6005	5456.7	1808.9	6.9230-03	5.9620-05	4446.6	0.8367	8.2380E-02	6.5470-03
41	121	71.3024	5479.3	1821.2	7.1640-03	5.9800-05	4447.2	0.8367	8.2380E-02	6.5470-03
42	128	77.0252	5496.7	1830.4	7.3730-03	5.9930-05	4448.0	0.8367	8.2380E-02	6.5470-03
43	135	82.8164	5501.6	1837.4	7.4770-03	5.9970-05	4448.4	0.8367	8.2380E-02	6.5470-03
44	137	83.0364	5501.6	1832.3	7.4730-03	5.9930-05	4448.4	0.8367	8.2380E-02	6.5470-03

# 3-D MOMENTUM ENERGY INTEGRAL TECHNIQUE

VISCOUS FLOW - BOUNDARY LAYER SOLUTION  
\*\*\*\*\*

BODY PT NO	INTEG PT NO	STREAM LENGTH INCH (SI)	MOMENTUM THICKNESS MIL (THE)	ENERGY THICKNESS MIL (PHI)	SHAPE FACTOR (HSF)	WGM THICK PE NO (RETH)	ENERGY THICK PE NO (REPH)	HEAT TRANS COEFFICIENT LHM/FT <sup>2</sup> -SEC (PUCH)	PRANDTL ANAL FAC (RAF)	INTER- MITTENCY (ADML)	TRANSITION PARAMETER (TP)
1	1	0.0	0.204	0.395	1.431	0.0	0.0	1.1590+00	0.8387	0.0	0.0
2	7	0.0729	0.313	0.496	1.418	2.6310+01	4.1760+01	8.3730-01	1.1511	0.0	30.161
3	9	0.2333	0.379	0.659	1.423	5.7760+01	1.0050+02	6.8640-01	0.9663	0.0	58.036
4	11	0.3936	0.401	0.731	1.454	8.5500+01	1.5580+02	6.2410-01	0.9045	0.0	81.540
5	13	0.5540	0.446	0.841	1.513	1.0970+02	2.0660+02	5.6300-01	0.8576	0.0	95.158
6	15	0.7144	0.529	1.017	1.589	1.3130+02	2.5270+02	5.4470-01	0.8244	0.0	98.756
7	17	0.8747	0.658	1.296	1.682	1.4730+02	2.8990+02	3.6450-01	0.7706	0.0	92.296
8	19	1.0351	0.870	1.739	1.763	1.6030+02	3.1740+02	2.5160-01	0.7561	0.0	80.158
9	21	1.1891	1.256	2.381	1.691	1.6750+02	3.1760+02	1.8020-01	0.7756	0.0	66.798
10	23	1.8348	1.864	3.021	1.601	2.1960+02	3.5600+02	1.1620-01	1.0804	0.0	68.496
11	25	2.8579	2.497	3.658	1.558	2.6530+02	3.8870+02	9.0850-02	1.2345	0.0	67.981
12	27	4.1457	2.944	4.100	1.510	2.9700+02	4.1360+02	7.6800-02	1.3371	0.0	64.091
13	29	5.5319	3.094	4.186	1.538	3.2240+02	4.3680+02	7.2750-02	1.3947	0.0	0.0
14	31	6.9072	3.048	4.061	1.574	3.4940+02	4.6550+02	7.3670-02	1.4197	0.0	0.0
15	33	8.2208	2.902	3.838	1.628	3.7760+02	4.9940+02	7.6760-02	1.4250	0.0	0.0
16	35	9.4517	2.729	3.599	1.692	4.0850+02	5.3870+02	8.0580-02	1.4194	0.09	0.0
17	37	10.5985	2.599	3.501	1.970	4.6940+02	6.0540+02	1.0360-01	1.3319	0.19	0.0
18	39	11.6748	2.794	3.901	2.639	5.6300+02	7.7960+02	1.7700-01	1.2398	0.39	0.0
19	41	12.7015	3.414	4.666	3.581	7.8770+02	1.0770+03	2.7060-01	1.2000	0.70	0.0
20	43	13.7003	4.118	5.369	4.175	1.0900+03	1.4220+03	3.1360-01	1.1914	0.89	0.0
21	45	14.6907	4.692	5.927	4.726	1.4270+03	1.7960+03	3.3230-01	1.1918	0.93	0.0
22	47	15.6898	5.121	6.345	5.286	1.7680+03	2.1910+03	3.6070-01	1.1908	0.94	0.0
23	49	16.7132	5.418	6.639	5.901	2.1150+03	2.6160+03	3.6370-01	1.1898	0.94	0.0
24	51	17.7148	5.604	6.823	6.594	2.5330+03	3.0830+03	3.6480-01	1.1884	0.94	0.0
25	53	18.8857	5.701	6.903	7.383	2.9770+03	3.6050+03	3.6780-01	1.1874	0.97	0.0
26	55	20.0545	5.727	6.875	8.271	3.4700+03	4.1810+03	3.6410-01	1.1875	0.97	0.0
27	57	21.2874	5.751	6.875	9.197	4.0200+03	4.8060+03	3.6390-01	1.1883	0.98	0.0
28	59	22.5680	5.718	6.786	10.223	4.6320+03	5.4980+03	3.6320-01	1.1889	0.98	0.0
29	61	23.9584	5.743	6.758	11.154	5.2700+03	6.2010+03	3.6320-01	1.1902	0.98	0.0
30	63	25.3999	5.757	6.722	12.107	5.9550+03	6.9530+03	3.6370-01	1.1911	0.99	0.0
31	65	26.9137	5.703	6.693	13.052	6.6960+03	7.7410+03	3.6370-01	1.1900	0.99	0.0
32	68	28.5401	10.560	12.597	9.969	5.7270+03	6.8320+03	2.7000-01	1.2108	0.99	0.0
33	71	30.9355	12.260	15.208	11.124	5.8770+03	7.2840+03	1.6450-01	1.2098	0.99	0.0
34	75	34.1076	11.079	13.733	13.174	6.5500+03	8.1190+03	1.6140-01	1.2104	0.99	0.0
35	80	38.1200	9.344	11.400	16.324	7.7070+03	9.4070+03	1.6240-01	1.2126	0.99	0.0
36	86	42.9459	9.010	10.755	18.260	8.9630+03	1.0380+04	1.6040-01	1.2176	0.99	0.0
37	93	48.3700	9.156	10.694	19.113	9.5390+03	1.1140+04	1.6060-01	1.2224	0.99	0.0
38	100	54.0864	9.465	10.849	19.378	9.5310+03	1.1820+04	1.7060-01	1.2279	0.99	0.0
39	107	59.8826	9.850	11.137	19.436	1.1040+04	1.2600+04	1.7650-01	1.2279	0.99	0.0
40	114	65.6005	10.213	11.429	19.398	1.1750+04	1.3150+04	1.8010-01	1.2294	1.00	0.0
41	121	71.3024	10.574	11.715	19.220	1.2490+04	1.3780+04	1.8470-01	1.2294	1.00	0.0
42	128	77.0252	10.938	12.135	18.985	1.3070+04	1.4630+04	1.8830-01	1.2297	1.00	0.0
43	135	82.8164	11.516	12.673	18.820	1.3720+04	1.5160+04	1.8910-01	1.2297	1.00	0.0
44	137	83.0364	11.537	12.697	18.817	1.3750+04	1.5180+04	1.8910-01	1.2297	1.00	0.0



# 3-D MOMENTUM ENERGY INTEGRAL TECHNIQUE

## ----- VISCIOUS FLOW - CURVED SHOCK AND ROUGHNESS EFFECTS -----

BODY PT NO	INTEG PT NO	STREAM LENGTH INCH (S)	CURVED SHOCK EFFECTS		EDGE MASS FLUX AUGMENTATION		SURFACE ROUGHNESS EFFECTS		FINISHNESS REYNOLDS NO
			EDGE ENTROPY BTU/LBM-DEG R (ENTR)	EDGE STREAMLINE LOCATION AT SHOCK INCH (YSTR)	(RUE)	(RUE)	ROUGHNESS MIL (RUE)	HEAT TRANSFER AUGMENTATION (RUE)	
1	1	0.0	2.48688	0.0	1.0000	0.2300	1.0000	1.0000	0.0
2	7	0.0729	2.48523	0.0094	1.5197	0.2300	1.0000	1.0000	2.4450000
3	9	0.2333	2.48379	0.0242	1.1260	0.2300	1.0000	1.0000	3.9510000
4	11	0.3936	2.48113	0.0375	1.1331	0.2300	1.0000	1.0000	4.5470000
5	13	0.5540	2.47766	0.0490	1.1220	0.2300	1.0000	1.0000	4.5710000
6	15	0.7144	2.47374	0.0585	1.1162	0.2300	1.0000	1.0000	4.1320000
7	17	0.8747	2.46734	0.0657	1.1069	0.2300	1.0000	1.0000	3.4570000
8	19	1.0351	2.46789	0.0699	1.0942	0.2300	1.0000	1.0000	2.4400000
9	21	1.1891	2.47363	0.0711	1.0572	0.2300	1.0000	1.0000	2.0210000
10	23	1.8348	2.46704	0.0887	1.0772	0.2300	1.0000	1.0000	1.3740000
11	25	2.8579	2.45755	0.1108	1.1072	0.2300	1.0000	1.0000	1.1100000
12	27	4.1457	2.44723	0.1350	1.1371	0.2300	1.0000	1.0000	9.8100001
13	29	5.5319	2.43363	0.1620	1.1827	0.2300	1.0000	1.0000	9.4770001
14	31	6.9072	2.41567	0.1918	1.2489	0.2300	1.0000	1.0000	9.1150001
15	33	8.2208	2.39384	0.2241	1.3338	0.2300	1.0000	1.0000	1.0740000
16	35	9.4517	2.36984	0.2586	1.4353	0.2300	1.0000	1.0000	1.0400000
17	37	10.5985	2.34449	0.3102	1.5493	0.2300	1.0000	1.0000	2.1240000
18	39	11.6748	2.31779	0.4115	1.6774	0.2300	1.0000	1.0000	6.1170000
19	41	12.7015	2.28998	0.5579	1.8219	0.2300	1.0000	1.0000	1.1460001
20	43	13.7003	2.26161	0.7209	1.9811	0.2300	1.0000	1.0000	1.4940001
21	45	14.6907	2.23335	0.8881	2.1579	0.2300	1.0000	1.0000	1.6590001
22	47	15.6898	2.20528	1.0591	2.3512	0.2300	1.0000	1.0000	1.7570001
23	49	16.7132	2.17723	1.2370	2.5688	0.2300	1.0000	1.0000	1.8700001
24	51	17.7748	2.14895	1.4258	2.8167	0.2300	1.0000	1.0000	1.9970001
25	53	18.8857	2.12065	1.6306	3.1008	0.2300	1.0000	1.0000	2.1340001
26	55	20.0545	2.09282	1.8537	3.4208	0.2300	1.0000	1.0000	2.2870001
27	57	21.2874	2.06594	2.0998	3.7548	0.2300	1.0000	1.0000	2.4570001
28	59	22.5880	2.04060	2.3706	4.1273	0.2300	1.0000	1.0000	2.6470001
29	61	23.9544	2.01740	2.6629	4.5460	0.2300	1.0000	1.0000	2.8570001
30	63	25.3949	1.99673	2.9810	5.0142	0.2300	1.0000	1.0000	3.0970001
31	65	26.9137	1.97817	3.3308	5.5396	0.2300	1.0000	1.0000	3.3770001
32	67	28.5601	1.96204	3.7140	6.1266	0.2300	1.0000	1.0000	3.7070001
33	71	30.9355	1.94773	4.1462	6.7866	0.2300	1.0000	1.0000	4.0970001
34	75	34.1076	1.93079	4.6262	7.5469	0.2300	1.0000	1.0000	4.5470001
35	80	38.1200	1.91559	5.1635	8.4869	0.2300	1.0000	1.0000	5.0770001
36	86	42.9459	1.90079	5.7663	9.6338	0.2300	1.0000	1.0000	5.6970001
37	93	48.3700	1.88693	6.4376	10.9277	0.2300	1.0000	1.0000	6.4170001
38	100	54.0846	1.87320	7.21302	12.5633	0.2300	1.0000	1.0000	7.21302
39	107	59.8626	1.86000	8.11393	14.5637	0.2300	1.0000	1.0000	8.11393
40	114	65.6005	1.84730	9.13000	16.9283	0.2300	1.0000	1.0000	9.13000
41	121	71.3024	1.83516	10.2646	19.6285	0.2300	1.0000	1.0000	10.2646
42	128	77.0232	1.82356	13.8246	22.6785	0.2300	1.0000	1.0000	13.8246
43	135	82.8164	1.81246	15.6881	26.4733	0.2300	1.0000	1.0000	15.6881
44	137	83.0364	1.80181	15.7613	26.4727	0.2300	1.0000	1.0000	15.7613

## 3-D MOMENTUM ENERGY INTEGRAL TECHNIQUE

STREAMLINE NO.	BODY PT NO	INTEG PT NO	BETA (DEG)	SONIC POINT LOCATION				TRANSITION POINT LOCATION				R-PT TIME	RECOVERY ENTHALPY (BTU/LBM)	HEAT TRANS COEFFICIENT (1/PM-F <sup>1/2</sup> -SEC)
				S	X	Y	Z	S	X	Y	Z			
2	1	1	0.26	0.554	-0.591	0.002	0.215	10.026	-2.500	0.026	9.445	4958.94	1.1589D+09	
	2	7										4953.71	8.2727D-01	
	3	9										4919.98	6.8638D-01	
	4	11										4913.57	6.2433D-01	
	5	13										4876.48	5.6297D-01	
	6	15										4830.46	4.4671D-01	
	7	17										4777.00	3.4846D-01	
	8	19										4723.31	2.5157D-01	
	9	21										4679.30	1.8015D-01	
	10	23										4646.37	1.1119D-01	
	11	25										4613.30	9.0845D-02	
	12	27										4589.48	7.6791D-02	
	13	29										4572.74	7.2732D-02	
	14	31										4556.51	7.3748D-02	
	15	33										4539.48	7.6710D-02	
	16	35										4520.78	8.0544D-02	
	17	37										4514.50	1.0251D-01	
	18	39										4519.19	1.7682D-01	
	19	41										4567.90	2.7021D-01	
	20	43										4571.24	3.1305D-01	
	21	45										4564.22	3.2192D-01	
	22	47										4553.12	3.4033D-01	
	23	49										4541.14	3.4733D-01	
	24	51										4524.01	3.6362D-01	
	25	53										4517.62	3.6762D-01	
	26	55										4506.62	3.4122D-01	
	27	57										4497.33	3.1965D-01	
	28	59										4488.54	3.3864D-01	
	29	61										4482.18	3.3783D-01	
	30	63										4476.50	3.3727D-01	
	31	65										4471.50	3.3687D-01	
	32	68										4487.19	2.1077D-01	
	33	71										4475.12	1.6391D-01	
	34	75										4463.99	1.6048D-01	
	35	80										4453.09	1.6861D-01	
	36	86										4448.02	1.6876D-01	
	37	93										4446.24	1.6976D-01	
	38	100										4446.00	1.7277D-01	
	39	107										4446.11	1.7528D-01	
	40	114										4446.41	1.7862D-01	
	41	121										4446.01	1.8208D-01	
	42	128										4447.60	1.8645D-01	
	43	135										4448.06	1.8707D-01	
	44	137										4448.05	1.8707D-01	

### 3-D MOMENTUM ENERGY INTEGRAL TECHNIQUE

OUTPUT DELETED

# 3-D MOMENTUM ENERGY INTEGRAL TECHNIQUE

STREAMLINE NO.	BETA (DEG)	SONIC POINT LOCATION			TRANSITION POINT LOCATION			R-PRIME THFPMXCHM	RECOVERY ENTHALPY (BTU/LBM)	HEAT TRANS COEFFICIENT (LHM/FT <sup>2</sup> -SEC)	
		S	X	Y	Z	S	X				Y
6	2.11	0.554	-0.591	0.020	0.215	10.026	-2.491	0.207	9.345		
BODY PT NO	INTEG PT NO	STREAMLINE NO.	LOCATION PHI (DEG)	METRIC COEFFICIENT	BODY ANGLE (DEG)	EDGE PRESSURE (ATM)	WALL TEMPERATURE (DEGR)				
1	1	3.4498D-03	-0.00	0.0	90.00	25.9665	7249.37	3.4807D-01	4958.94	1.1501D+03	
2	7	1.2668D-02	1.08	7.6987D-02	85.46	25.5665	7171.38	3.2635D-01	4953.70	8.3749D-01	
3	9	5.3441D-02	1.63	2.3689D-01	75.46	23.7132	7091.09	3.1116D-01	4939.58	6.8442D-01	
4	11	1.2177D-01	1.82	3.9321D-01	65.29	20.3335	7016.54	3.0431D-01	4913.57	6.2401D-01	
5	13	2.1504D-01	1.92	5.3653D-01	55.17	16.0317	6898.85	2.9365D-01	4876.47	5.4215D-01	
6	15	3.2754D-01	1.99	6.6055D-01	45.02	11.6376	6734.01	2.7905D-01	4810.45	4.4435D-01	
7	17	4.5890D-01	2.04	7.6541D-01	35.08	7.6655	6510.57	2.6137D-01	4776.98	3.4603D-01	
8	19	6.0460D-01	2.08	8.4710D-01	25.09	4.7225	6227.34	2.3964D-01	4723.31	2.5118D-01	
9	21	7.5390D-01	2.11	9.0073D-01	15.23	2.7712	5637.80	2.4741D-01	4679.13	1.7980D-01	
10	23	1.3891D+00	2.26	1.0878D+00	15.40	2.1188	5185.99	2.3143D-01	4644.70	1.1605D-01	
11	25	2.3953D+00	2.50	1.4203D+00	15.40	1.6704	4876.44	2.3015D-01	4613.24	9.0630D-02	
12	27	3.6620D+00	2.81	1.9050D+00	15.39	1.4413	4674.64	2.2929D-01	4589.38	7.6565D-02	
13	29	5.0254D+00	3.17	2.5256D+00	15.39	1.3990	4605.66	2.2897D-01	4572.62	7.2435D-02	
14	31	6.3781D+00	3.58	3.2734D+00	15.39	1.4486	4611.96	2.2896D-01	4556.50	7.2309D-02	
15	33	7.6702D+00	4.03	4.1304D+00	15.39	1.5450	4646.59	2.2905D-01	4539.77	6.8367D-02	
16	35	8.8809D+00	4.50	5.0887D+00	15.38	1.6601	4690.90	2.2919D-01	4520.67	6.0164D-02	
17	37	1.0009D+01	5.00	6.1388D+00	15.38	1.7810	4974.01	2.3057D-01	4514.37	5.0784D-01	
18	39	1.1067D+01	5.51	7.2704D+00	15.37	1.8966	5526.16	2.4637D-01	4538.92	1.7516D-01	
19	41	1.2077D+01	6.04	8.5022D+00	15.37	1.9946	5847.47	2.7300D-01	4567.55	2.6748D-01	
20	43	1.3060D+01	6.59	9.8457D+00	15.36	2.0649	5936.73	2.8308D-01	4571.13	3.1048D-01	
21	45	1.4034D+01	7.17	1.1304D+01	15.35	2.1052	5968.01	2.8654D-01	4564.27	3.2949D-01	
22	47	1.5016D+01	7.76	1.2904D+01	15.35	2.1187	5977.77	2.8769D-01	4553.26	3.3813D-01	
23	49	1.6023D+01	8.38	1.4661D+01	15.34	2.1124	5978.71	2.8794D-01	4541.37	3.4124D-01	
24	51	1.7067D+01	9.02	1.6598D+01	15.33	2.0945	5973.03	2.8745D-01	4529.93	3.4157D-01	
25	53	1.8163D+01	9.68	1.8736D+01	15.32	2.0717	5965.53	2.8685D-01	4517.93	3.4058D-01	
26	55	1.9309D+01	10.37	2.1050D+01	15.31	2.0470	5957.03	2.8605D-01	4506.43	3.3865D-01	
27	57	2.0527D+01	11.09	2.3591D+01	15.30	2.0246	5948.59	2.8528D-01	4497.67	3.3632D-01	
28	59	2.1801D+01	11.85	2.6445D+01	15.29	2.0081	5943.68	2.8490D-01	4488.82	3.3431D-01	
29	61	2.3149D+01	12.66	2.9721D+01	15.27	1.9968	5938.14	2.8436D-01	4482.75	3.3276D-01	
30	63	2.4567D+01	13.52	3.3394D+01	15.25	1.9892	5933.83	2.8389D-01	4476.55	3.3203D-01	
31	65	2.6054D+01	14.43	3.7513D+01	15.24	1.9843	5930.12	2.8367D-01	4471.42	3.3195D-01	
32	67	2.7682D+01	15.42	4.1987D+01	10.82	1.9822	5926.02	2.8346D-01	4466.35	3.3155D-01	
33	70	3.0044D+01	16.81	4.7740D+01	10.78	0.8836	5924.06	2.8346D-01	4461.43	3.3093D-01	
34	74	3.3199D+01	18.76	5.6193D+01	10.73	0.8317	5924.06	2.8346D-01	4457.46	3.3061D-01	
35	79	3.7190D+01	21.49	6.8172D+01	10.65	0.8454	5924.06	2.8346D-01	4452.46	3.3029D-01	
36	85	4.1989D+01	25.17	8.4494D+01	10.52	0.8208	5924.06	2.8346D-01	4446.58	3.3002D-01	
37	91	4.7383D+01	29.80	1.0854D+02	10.34	0.7786	5924.06	2.8346D-01	4442.64	3.2974D-01	
38	98	5.3067D+01	35.17	1.3542D+02	10.08	0.7431	5924.06	2.8346D-01	4437.61	3.2945D-01	
39	105	5.8413D+01	41.27	1.6925D+02	9.74	0.6911	5924.06	2.8346D-01	4432.64	3.2917D-01	
40	112	6.4570D+01	47.95	2.0510D+02	9.34	0.6310	5924.06	2.8346D-01	4427.64	3.2889D-01	
41	119	7.0190D+01	55.22	2.4590D+02	8.82	0.5350	5924.06	2.8346D-01	4422.64	3.2861D-01	
42	126	7.5882D+01	63.18	2.9274D+02	8.22	0.5667	5924.06	2.8346D-01	4417.64	3.2833D-01	
43	133	8.1641D+01	69.98	3.4747D+02	7.40	1.4248	5924.06	2.8346D-01	4412.64	3.2805D-01	
44	135	8.1860D+01	70.04	4.0363D+02	7.02	1.3171	5924.06	2.8346D-01	4407.64	3.2777D-01	

OUTPUT DELETED

### 3-D MOMENTUM ENERGY INTEGRAL TECHNIQUE

OUT PUT DELETED

### 3-0 MOMENTUM ENERGY INTEGRAL TECHNIQUE

[illegible]

OUTPUT DELETED

# 3-D MOMENTUM ENERGY INTEGRAL TECHNIQUE

STREAMLINE NO.	BODY PT NO	INTEG PT NO	BETA (DEG)	SONIC POINT LOCATION			TRANSITION POINT LOCATION			WALL TEMPERATURE (DEGR)	EDGE PRESSURE (ATM)	BODY ANGLE (DEG)	METRIC COEFFICIENT	STREAMLINE LOCATION PHI (DEG)	Z (IN)	RECOVERY ENTHALPY (BTU/LB-R)	HEAT TRANS COEFFICIENT (LB/FT <sup>2</sup> -SEC)
				S	X	Y	S	X	Y								
15			50.00	0.582	-0.410	0.426	0.215	12.876	0.604	2.920	12.077						
1	1	1	3.44980-03	-0.00	0.0		90.00	25.9645	7233.31	3.43070-01	4958.94		0.0			1.06660-00	
2	2	7	1.26680-02	28.13	9.59720-02		84.76	25.4663	7151.97	3.21340-01	4951.07		9.59720-02			7.83640-01	
3	3	9	5.34410-02	39.99	2.57680-01		73.99	23.3210	7081.62	3.10060-01	4936.89		2.57680-01			6.75250-01	
4	4	11	1.21770-01	43.98	4.12540-01		63.67	19.7099	6990.69	3.07530-01	4908.68		4.12540-01			4.09560-01	
5	5	13	2.15090-01	46.08	5.53590-01		53.51	15.2932	6875.68	2.94580-01	4882.27		5.53590-01			5.27050-01	
6	6	15	3.27540-01	47.46	6.74750-01		43.31	10.9328	6700.62	2.76100-01	4872.27		6.74750-01			4.28840-01	
7	7	17	4.58400-01	48.47	7.75940-01		33.33	7.0529	6470.04	2.57960-01	4766.73		7.75940-01			3.29580-01	
8	8	19	6.04800-01	49.30	8.53740-01		23.31	4.3232	6172.39	2.35950-01	4714.37		8.53740-01			2.36810-01	
9	9	21	7.53900-01	50.00	9.03520-01		13.42	2.4775	5563.29	2.44760-01	4669.18		9.03520-01			1.67400-01	
10	10	23	1.34910+00	52.86	1.06480+00		13.39	1.8668	5077.68	2.31040-01	4635.57		1.06480+00			1.07400-01	
11	11	25	2.39530+00	57.49	1.33720+00		13.05	1.4289	4736.56	2.29630-01	4601.83		1.33720+00			8.04520-02	
12	12	27	3.66200+00	63.71	1.69890+00		12.61	1.1289	4467.90	2.28540-01	4574.65		1.69890+00			6.35470-02	
13	13	29	5.02540+00	69.42	2.11530+00		12.11	0.9728	4200.71	2.27870-01	4553.59		2.11530+00			5.45660-02	
14	14	31	6.37810+00	75.55	2.50760+00		11.61	0.8762	4176.71	2.27350-01	4536.67		2.50760+00			4.86430-02	
15	15	33	7.57020+00	81.56	2.88140+00		11.10	0.8041	4075.55	2.26950-01	4521.54		2.88140+00			4.41770-02	
16	16	35	8.88040+00	87.14	3.29540+00		10.61	0.7451	3983.50	2.26570-01	4508.51		3.29540+00			4.02840-02	
17	17	37	1.00090+01	92.34	3.65810+00		10.15	0.6932	3895.19	2.26200-01	4497.21		3.65810+00			3.65660-02	
18	18	39	1.10670+01	97.14	3.70120+00		9.73	0.6477	3819.74	2.25900-01	4487.21		3.70120+00			3.27480-02	
19	19	41	1.20770+01	101.68	3.86740+00		9.33	0.6064	3740.20	2.25570-01	4478.38		3.86740+00			2.91430-02	
20	20	43	1.30800+01	105.87	4.01060+00		8.99	0.5710	3674.12	2.25320-01	4468.65		4.01060+00			2.61830-02	
21	21	45	1.40340+01	110.19	4.17610+00		8.64	0.5346	3598.60	2.25200-01	4457.64		4.17610+00			2.34190-02	
22	22	47	1.50160+01	113.97	4.18750+00		8.34	0.5072	4145.26	2.24920-01	4450.51		4.18750+00			2.08160-02	
23	23	49	1.60230+01	118.01	4.29610+00		8.03	0.4777	4247.77	2.24820-01	4441.28		4.29610+00			1.86500-02	
24	24	51	1.70670+01	121.30	4.26900+00		7.74	0.4519	4331.66	2.24820-01	4431.28		4.26900+00			1.67160-02	
25	25	53	1.81660+01	125.67	4.29770+00		7.47	0.4298	4372.15	2.24910-01	4421.28		4.29770+00			1.50510-02	
26	26	55	1.93090+01	129.87	4.28720+00		7.18	0.4051	4375.08	2.24900-01	4411.28		4.28720+00			1.36540-02	
27	27	57	2.05220+01	133.32	4.23060+00		6.94	0.3895	4387.72	2.24950-01	4401.28		4.23060+00			1.24900-02	
28	28	59	2.18010+01	137.11	4.08020+00		6.73	0.3731	4376.26	2.24910-01	4391.28		4.08020+00			1.15030-02	
29	29	61	2.31490+01	140.94	4.16680+00		6.50	0.3577	4344.40	2.24940-01	4381.28		4.16680+00			1.07070-02	
30	30	63	2.45670+01	144.08	3.86800+00		6.33	0.3486	4336.76	2.24930-01	4371.28		3.86800+00			0.99020-02	
31	31	65	2.60560+01	147.59	3.73490+00		6.16	0.3394	4302.73	2.24920-01	4361.28		3.73490+00			0.92020-02	
32	32	67	2.76820+01	151.00	3.89410+00		6.02	0.3241	4301.73	2.24910-01	4351.28		3.89410+00			0.85020-02	
33	33	69	3.00440+01	154.64	2.94090+00		5.87	0.2253	3966.38	2.24800-01	4341.28		2.94090+00			0.78020-02	
34	34	71	3.31990+01	160.11	3.45420+00		5.74	0.2151	3900.12	2.24770-01	4331.28		3.45420+00			0.71020-02	
35	35	73	3.71900+01	163.34	2.12060+00		5.62	0.1979	3821.23	2.24740-01	4321.28		2.12060+00			0.64020-02	
36	36	75	4.19450+01	167.27	2.52160+00		5.50	0.1872	3747.72	2.24710-01	4311.28		2.52160+00			0.57020-02	
37	37	77	4.73830+01	170.50	1.87700+00		5.38	0.1736	3637.60	2.24680-01	4301.28		1.87700+00			0.50020-02	
38	38	79	5.30670+01	171.27	1.27700+00		5.26	0.1554	3581.04	2.24650-01	4291.28		1.27700+00			0.43020-02	
39	39	81	5.88130+01	171.73	1.25660+00		5.14	0.1415	3547.78	2.24620-01	4281.28		1.25660+00			0.36020-02	
40	40	83	6.45200+01	172.02	1.26620+00		5.02	0.1315	3506.19	2.24590-01	4271.28		1.26620+00			0.29020-02	
41	41	85	7.01900+01	172.70	1.27190+00		4.90	0.1233	3464.04	2.24560-01	4261.28		1.27190+00			0.22020-02	
42	42	87	7.58420+01	172.33	1.28380+00		4.78	0.1162	3421.87	2.24530-01	4251.28		1.28380+00			0.15020-02	
43	43	89	8.16410+01	172.65	1.27490+00		4.66	0.1104	3379.73	2.24500-01	4241.28		1.27490+00			0.08020-02	
44	44	91	8.18660+01	172.44	1.26500+00		4.54	0.1104	4458.71	2.24470-01	4231.28		1.26500+00			0.01020-02	

OUTPUT DELETED

### 3-1) MOMENTUM ENERGY INTEGRAL TECHNIQUE

STREAMLINE NO.	BETA (DEG)	SONIC POINT LOCATION				TRANSITION POINT LOCATION				R-PRIME TEMPMICHEM	R-RECOVERY ENTHALPY (RTU/LBM)	HEAT TRANS COEFFICIENT (LRM/FT-SEC)
		LOCATION				LOCATION						
		S	X	Y	Z	S	X	Y	Z			
22	180.00	0.554	0.457	0.000	0.122	8.997	2.285	0.000	8.276			
BODY PT NO	INTEG PT NO	STREAMLINE Z (IN)	LOCATION PHI (DEG)	METRIC COEFFICIENT	BODY ANGLE (DEG)	EDGE PRESSURE (ATM)	WALL TEMPERATURE (DEGR)					
1	1	3.44980-03	-0.00	0.0	90.00	25.9645	7179.37	3.27760-01	4958.96	8.43200-01		
2	7	1.26680-02	180.00	2.21440-01	75.46	23.7139	7080.18	3.08440-01	4940.10	6.46560-01		
3	9	5.34410-02	180.00	3.75220-01	65.46	20.3347	7019.90	3.05110-01	4913.69	6.20840-01		
4	11	1.21770-01	180.00	5.17350-01	55.10	16.0331	6902.23	2.94340-01	4876.59	5.46640-01		
5	13	2.15080-01	180.00	6.41450-01	45.18	11.6340	6737.82	2.79790-01	4830.42	4.48040-01		
6	15	3.27540-01	180.00	7.42570-01	35.03	7.6666	6516.99	2.61700-01	4777.00	3.47670-01		
7	17	4.58900-01	180.00	8.27030-01	25.08	4.7273	6229.66	2.39920-01	4723.34	2.52040-01		
8	19	6.04800-01	180.00	8.76490-01	15.09	2.7097	5886.56	2.19920-01	4667.67	1.77330-01		
9	21	7.53400-01	180.00	9.04140-01	5.23	1.4916	5188.67	2.07800-01	4628.00	1.17430-01		
10	23	1.38910+00	180.00	9.57580-01	5.40	1.1745	4627.97	2.09330-01	4603.05	7.27610-02		
11	25	2.39530+00	180.00	1.07190+00	5.40	0.9185	4286.18	2.27860-01	4577.21	5.31120-02		
12	27	3.66200+00	180.00	1.07470+00	5.40	0.7010	3968.88	2.26570-01	4552.21	3.89340-02		
13	29	5.02540+00	180.00	1.13200+00	5.40	0.5620	3723.05	2.25580-01	4534.15	2.99620-02		
14	31	6.37810+00	180.00	1.16780+00	5.40	0.4876	3552.04	2.24870-01	4522.47	2.47150-02		
15	33	7.67020+00	180.00	1.18900+00	5.40	0.4436	3429.99	2.24350-01	4514.69	2.14160-02		
16	35	8.88080+00	180.00	1.20000+00	5.40	0.4145	3444.56	2.24670-01	4516.86	2.27370-02		
17	37	1.00000+01	180.00	1.20410+00	5.40	0.3941	3623.35	2.25520-01	4529.08	2.65080-02		
18	39	1.10670+01	180.00	1.20320+00	5.40	0.3702	3758.32	2.26270-01	4562.22	3.07510-02		
19	41	1.20770+01	180.00	1.19860+00	5.40	0.3479	3867.83	2.26880-01	4556.46	3.47350-02		
20	43	1.30600+01	180.00	1.19100+00	5.40	0.3591	3951.62	2.27350-01	4566.46	3.73880-02		
21	45	1.40340+01	180.00	1.18080+00	5.40	0.3523	4015.98	2.27770-01	4576.78	3.98460-02		
22	47	1.50160+01	180.00	1.16810+00	5.40	0.3469	4065.19	2.27980-01	4585.87	4.17140-02		
23	49	1.60230+01	180.00	1.15280+00	5.40	0.3428	4103.14	2.28200-01	4597.87	4.31960-02		
24	51	1.70670+01	180.00	1.13480+00	5.40	0.3397	4132.20	2.28360-01	4609.94	4.43480-02		
25	53	1.81600+01	180.00	1.11410+00	5.40	0.3376	4155.78	2.28400-01	4617.18	4.52750-02		
26	55	1.93090+01	180.00	1.09060+00	5.40	0.3363	4172.56	2.28580-01	4612.68	4.60990-02		
27	57	2.05220+01	180.00	1.06640+00	5.40	0.3357	4184.58	2.28650-01	4617.52	4.64690-02		
28	59	2.18010+01	180.00	1.03570+00	5.40	0.3357	4197.45	2.28690-01	4621.76	4.67100-02		
29	61	2.31430+01	180.00	1.00690+00	5.40	0.3362	4196.89	2.28710-01	4625.68	4.68670-02		
30	63	2.45670+01	180.00	9.72750-01	5.40	0.3373	4198.65	2.28720-01	4628.76	4.69940-02		
31	65	2.60560+01	180.00	9.38400-01	5.40	0.3388	4197.31	2.28700-01	4631.56	4.70980-02		
32	68	2.76820+01	180.00	8.96910-01	1.00	0.2488	3972.17	2.27930-01	4614.57	3.72530-02		
33	71	3.00440+01	180.00	8.22640-01	1.00	0.2548	3950.98	2.27780-01	4616.70	3.65890-02		
34	75	3.31490+01	180.00	7.37000-01	1.00	0.2527	3937.85	2.27720-01	4616.31	3.58090-02		
35	80	3.71960+01	180.00	6.58130-01	1.00	0.2752	3861.04	2.27410-01	4616.16	3.30600-02		
36	86	4.19890+01	180.00	6.02710-01	1.00	0.2708	3757.07	2.27010-01	4610.70	2.94970-02		
37	93	4.73430+01	180.00	5.73410-01	1.00	0.1877	3660.04	2.26650-01	4604.83	2.65030-02		
38	100	5.30670+01	180.00	5.66780-01	1.00	0.1683	3572.94	2.26360-01	4600.19	2.39110-02		
39	107	5.88130+01	180.00	5.74680-01	1.00	0.1546	3500.74	2.26070-01	4598.00	2.19870-02		
40	114	6.45200+01	180.00	5.91160-01	1.00	0.1466	3464.70	2.25860-01	4598.24	2.05370-02		
41	121	7.01490+01	180.00	6.12810-01	1.00	0.1377	3406.18	2.25720-01	4597.55	1.95770-02		
42	128	7.58820+01	180.00	6.38000-01	1.00	0.1333	3379.82	2.25620-01	4601.87	1.89310-02		
43	135	8.16410+01	180.00	6.66080-01	0.99	0.1306	3358.52	2.25540-01	4605.63	1.84160-02		
44	137	8.18600+01	180.00	6.67200-01	0.99	0.1306	3359.03	2.25540-01	4605.62	1.84200-02		



## 3-D MOMENTUM ENERGY INTEGRAL TECHNIQUE

## VISCOS FLOW - EDGE PROPERTIES

BDY PT NO	INTEG PT NO	STREAM LENGTH INCH (S)	VELOCITY F/SEC (UF)	MACH NO (MCAI)	ENTHALPY BTU/LBM (HE)	TEMPERATURE DEG R (TE)	DENSITY LRM/FT <sup>3</sup> (RNF)	VISCOSITY LRM/FT-SEC (VISE)	UNIT PE NO 1/FT (IPE)
1	1	0.0	0.0	0.0	4958.9	10743.8	8.0020-02	9.9740-05	0.0
2	7	0.2335	2403.3	0.4756	4843.6	10544.7	7.4700-02	9.8400-05	1.8240+06
3	9	0.3438	3724.6	0.7490	4681.9	10251.4	6.6150-02	9.6410-05	2.8550+06
4	11	0.5542	5024.5	1.0355	4456.8	9825.2	5.4780-02	9.3470-05	2.9650+06
5	13	0.7146	6277.0	1.3376	4172.1	9258.9	4.2540-02	8.9460-05	2.9870+06
6	15	0.8749	7468.3	1.6588	3845.1	8596.1	3.0510-02	8.4860-05	2.6850+06
7	17	1.0353	8498.5	1.9752	3516.6	7938.1	2.0630-02	7.8190+05	2.0190+06
8	19	1.1957	9449.5	2.3014	3175.7	7318.8	1.3050-02	7.5290-05	1.6380+06
9	21	1.3496	10072.3	2.5387	2932.9	6869.8	7.7230-03	7.1930-05	1.0810+06
10	23	1.4954	10445.2	2.6816	2780.1	6642.8	6.3380-03	7.0120-05	9.6410+05
11	25	3.0184	10817.7	2.8358	2621.9	6415.3	5.1780-03	6.8750-05	8.2070+05
12	27	4.3062	11166.3	2.9875	2468.9	6197.3	4.1330-03	6.6410-05	8.0600+05
13	29	5.6425	11411.6	3.1012	2358.3	6036.7	3.4290-03	6.5040-05	6.0160+05
14	31	7.0678	11567.4	3.1760	2286.8	5936.0	3.0400-03	6.4170-05	5.8850+05
15	33	8.3814	11670.0	3.2260	2239.1	5867.5	2.8100-03	6.3580-05	5.1570+05
16	35	9.6123	11740.3	3.2607	2206.3	5817.1	2.6530-03	6.3170-05	4.0310+05
17	37	10.7591	11792.3	3.2867	2181.8	5780.0	2.5630-03	6.2780-05	4.7690+05
18	39	11.8354	11831.6	3.3066	2163.3	5752.0	2.4610-03	6.2430-05	4.6490+05
19	41	12.8620	11861.7	3.3216	2149.0	5730.6	2.3990-03	6.2350-05	4.5560+05
20	43	13.8609	11884.6	3.3333	2138.2	5714.1	2.3500-03	6.2320-05	4.4820+05
21	45	14.8512	11901.4	3.3420	2130.2	5701.6	2.3110-03	6.2270-05	4.4270+05
22	47	15.8503	11913.4	3.3482	2124.5	5692.5	2.2800-03	6.2140-05	4.3770+05
23	49	16.8738	11921.0	3.3523	2120.9	5686.3	2.2560-03	6.2090-05	4.3320+05
24	51	17.9354	11924.9	3.3545	2119.0	5682.6	2.2380-03	6.2060-05	4.2990+05
25	53	19.0462	11925.4	3.3550	2118.8	5681.2	2.2240-03	6.2050-05	4.2740+05
26	55	20.2150	11923.0	3.3541	2119.9	5681.7	2.2150-03	6.2060-05	4.2550+05
27	57	21.4480	11918.1	3.3519	2127.2	5683.9	2.2100-03	6.2080-05	4.2420+05
28	59	22.7484	11911.1	3.3486	2125.6	5687.6	2.2080-03	6.2120-05	4.2330+05
29	61	24.1190	11902.2	3.3443	2129.8	5692.5	2.2040-03	6.2140-05	4.2290+05
30	63	25.5605	11891.6	3.3392	2136.9	5698.6	2.2120-03	6.2210-05	4.2280+05
31	65	27.0742	11879.2	3.3333	2140.7	5705.8	2.2180-03	6.2280-05	4.2320+05
32	68	28.7206	12202.6	3.5017	1985.2	5680.9	1.7080-03	6.0340-05	3.6520+05
33	71	31.0960	12210.6	3.5045	1981.3	5680.8	1.7540-03	6.0360-05	3.5570+05
34	75	34.2682	12260.5	3.5303	1956.9	5649.7	1.7560-03	6.0090-05	3.5790+05
35	80	38.2806	12329.4	3.5688	1923.1	5397.2	1.6520-03	5.9650-05	3.6150+05
36	86	43.1064	12409.5	3.6151	1883.5	5332.9	1.5020-03	5.9120-05	3.1520+05
37	93	48.5305	12523.5	3.6807	1826.8	5247.9	1.3640-03	5.8400-05	3.0510+05
38	100	54.2451	12609.9	3.7324	1793.4	5180.3	1.2430-03	5.7530-05	2.9250+05
39	107	60.0232	12650.5	3.7586	1762.9	5135.5	1.1400-03	5.6400-05	2.8100+05
40	114	65.7610	12646.8	3.7598	1764.7	5141.1	1.0740-03	5.4900-05	2.6710+05
41	121	71.4630	12623.7	3.7495	1776.4	5141.1	1.0240-03	5.3460-05	2.5260+05
42	128	77.1858	12583.9	3.7246	1796.5	5158.4	9.8610-04	5.2770-05	2.3710+05
43	135	82.9769	12520.1	3.6966	1828.4	5190.6	9.5610-04	5.8040-05	2.0670+05
44	137	83.1969	12516.8	3.6947	1830.1	5192.7	9.5670-04	5.8060-05	2.0630+05

# 3-D MOMENTUM ENERGY INTEGRAL TECHNIQUE

VISCOS FLOW - WALL AND R. I. RECOVERY PROPERTIES

BODY PT NO	INTCG PT NO	STREAM LENGTH INCH (SI)	WALL TEMPERATURE DEG F (TM)	WALL ENTHALPY BTU/LBM (HM)	WALL DENSITY LBM/FT <sup>3</sup> (KMW)	WALL VISCOSITY LBM/FT-SEC (VISM)	RECOVERY ENTHALPY BTU/LBM (HRI)	RECOVERY FACTOR (PFCNV)	SENSBL CFMV HEAT FLUX BTU/FT <sup>2</sup> -SEC	CF/2
1	1	0.0	7179.4	2578.6	1.3470-01	7.2090-05	4958.9	0.8367	2.0070+03	1.0005+00
2	7	0.2335	7080.2	2523.6	1.2670-01	7.1350-05	4940.1	0.8367	1.4040+03	2.5400-03
3	9	0.3938	7019.9	2503.2	1.0970-01	7.0960-05	4911.7	0.8367	1.5100+03	2.5110-03
4	11	0.5542	6902.2	2463.7	8.7950-02	7.0190-05	4876.6	0.8367	1.3100+03	2.3040-03
5	13	0.7146	6737.8	2403.6	6.5390-02	6.9080-05	4830.4	0.8367	1.0970+03	2.0750-03
6	15	0.8749	6517.0	2308.4	4.6440-02	6.7520-05	4777.0	0.8367	8.5810+02	1.7670-03
7	17	1.0353	6227.6	2170.2	2.9890-02	6.5420-05	4723.3	0.8367	6.4150+02	1.0770-03
8	19	1.1957	5886.6	1995.3	1.7680-02	6.2810-05	4667.7	0.8367	4.7300+02	2.0700-03
9	21	1.3696	5188.7	1619.3	1.1750-02	5.7330-05	4628.0	0.8367	3.5100+02	2.0450-03
10	23	1.5954	4628.0	1356.9	1.0030-02	5.2950-05	4603.0	0.8367	2.3420+02	1.0760-03
11	25	3.0184	4284.2	1218.2	8.4910-03	5.0270-05	4577.2	0.8367	1.7860+02	8.2950-04
12	27	4.3062	3468.9	1113.0	6.7950-03	4.7830-05	4552.7	0.8367	1.3390+02	7.0990-04
13	29	5.6925	3723.1	1030.4	5.9620-03	4.5880-05	4534.1	0.8367	1.0500+02	6.2370-04
14	31	7.0676	3552.0	974.0	5.4220-03	4.4480-05	4522.5	0.8367	8.7700+01	5.5360-04
15	33	8.3814	3430.0	934.1	5.1150-03	4.3450-05	4514.7	0.8367	7.6680+01	5.0270-04
16	35	9.6123	3466.6	945.0	4.7310-03	4.3730-05	4516.9	0.8367	7.9410+01	5.5370-04
17	37	10.7591	3623.4	995.8	4.2980-03	4.5060-05	4529.1	0.8367	9.3080+01	7.0450-04
18	39	11.8354	3758.3	1042.4	3.9890-03	4.6160-05	4542.2	0.8367	1.0760+02	9.4860-04
19	41	12.8620	3867.8	1080.7	3.7570-03	4.7050-05	4554.9	0.8367	1.1940+02	9.7400-04
20	43	13.8609	3951.6	1110.0	3.5900-03	4.7720-05	4566.5	0.8367	1.2920+02	1.0840-03
21	45	14.8512	4016.0	1132.6	3.4690-03	4.8230-05	4576.8	0.8367	1.3710+02	1.1770-03
22	47	15.8503	4065.4	1150.0	3.3700-03	4.8590-05	4585.9	0.8367	1.4330+02	1.2430-03
23	49	16.8738	4103.1	1163.3	3.2990-03	4.8820-05	4593.9	0.8367	1.4920+02	1.2980-03
24	51	17.9354	4132.2	1173.5	3.2460-03	4.9150-05	4600.9	0.8367	1.5200+02	1.3620-03
25	53	19.0462	4155.8	1181.8	3.2070-03	4.9360-05	4607.2	0.8367	1.5490+02	1.3760-03
26	55	20.2150	4172.6	1187.7	3.1820-03	4.9470-05	4612.7	0.8367	1.5730+02	1.4020-03
27	57	21.4480	4184.6	1192.0	3.1670-03	4.9570-05	4617.5	0.8367	1.5900+02	1.4230-03
28	59	22.7480	4192.5	1194.8	3.1610-03	4.9630-05	4621.8	0.8367	1.6010+02	1.4310-03
29	61	24.1190	4196.9	1196.3	3.1610-03	4.9660-05	4625.5	0.8367	1.6070+02	1.4350-03
30	63	25.5605	4198.7	1196.9	3.1710-03	4.9680-05	4628.8	0.8367	1.6090+02	1.4360-03
31	65	27.0742	4197.3	1196.4	3.1870-03	4.9670-05	4631.5	0.8367	1.6080+02	1.4360-03
32	68	28.7206	3972.2	1116.8	2.6690-03	4.7860-05	4614.6	0.8367	1.3010+02	1.5250-03
33	71	31.0960	3951.0	1109.3	2.5500-03	4.7670-05	4616.7	0.8367	1.2760+02	1.3910-03
34	75	34.2682	3937.9	1104.6	2.5370-03	4.7590-05	4618.3	0.8367	1.2610+02	1.3680-03
35	80	38.2806	3861.0	1077.0	2.4100-03	4.6960-05	4614.2	0.8367	1.1690+02	1.1670-03
36	86	43.1064	3757.4	1039.4	2.2210-03	4.6110-05	4610.7	0.8367	1.0530+02	1.1070-03
37	93	48.5305	3660.0	1004.1	2.0370-03	4.5310-05	4604.8	0.8367	9.5430+01	1.0770-03
38	100	54.2451	3572.9	976.3	1.8670-03	4.4590-05	4600.2	0.8367	8.6720+01	1.0660-03
39	107	60.6232	3500.7	953.7	1.7670-03	4.3990-05	4598.9	0.8367	8.0130+01	1.0510-03
40	114	65.7610	3446.7	936.1	1.6440-03	4.3530-05	4598.2	0.8367	7.5210+01	1.0380-03
41	121	71.4630	3406.2	923.9	1.6030-03	4.3200-05	4594.6	0.8367	7.1960+01	1.0260-03
42	128	77.1858	3379.8	915.6	1.5630-03	4.2940-05	4601.8	0.8367	6.9710+01	1.0150-03
43	135	82.9769	3358.5	908.9	1.5340-03	4.2700-05	4605.4	0.8367	6.8050+01	1.0050-03
44	137	83.1969	3359.0	909.1	1.5410-03	4.2710-05	4605.6	0.8367	6.8080+01	1.0050-03

# 3-D MOMENTUM ENERGY INTEGRAL TECHNIQUE

## VISCOUS FLOW - BOUNDARY LAYER SOLUTION

BODY PT NO	INTEG PT NO	STREAM LENGTH INCH	MOMENTUM THICKNESS MIL	ENERGY THICKNESS MIL	SHAPE FACTOR	MIN THICK RE NO	ENERGY THICK RE NO	HEAT TRANS COEFFICIENT LBM/FT <sup>2</sup> -SEC	REYNOLDS ANAL FAC	INTER- MITTENT	TRANSITION PARAMETER
(J)	(I)	(S)	(THE)	(PHI)	(HSF)	(RETH)	(REFPH)	(PICKH)	(PAF)	(AIML)	(TP)
1	1	0.0	0.286	0.552	1.421	0.0	0.0	8.4320-01	0.8392	0.0	0.0
2	7	0.2335	0.396	0.659	1.470	6.0170+01	1.0020+02	6.6460-01	1.0457	0.0	58.746
3	9	0.3538	0.398	0.723	1.460	8.4760+01	1.5390+02	6.2980-01	0.9096	0.0	81.199
4	11	0.5342	0.444	0.834	1.514	1.0900+02	2.0470+02	5.4660-01	0.8618	0.0	94.890
5	13	0.7146	0.525	1.007	1.590	1.3050+02	2.5030+02	4.4610-01	0.8286	0.0	94.523
6	15	0.8749	0.657	1.290	1.682	1.4710+02	2.8860+02	3.4760-01	0.7830	0.0	92.236
7	17	1.0353	0.878	1.735	1.763	1.6030+02	3.1670+02	2.5200-01	0.7547	0.0	80.131
8	19	1.1957	1.234	2.469	1.822	1.6840+02	3.3710+02	1.7730-01	0.7083	0.0	65.219
9	21	1.3496	1.913	3.658	1.674	1.7240+02	3.2970+02	1.1740-01	0.7312	0.0	51.619
10	23	1.9954	2.772	4.685	1.496	2.1410+02	3.6860+02	7.2760-02	1.0229	0.0	53.023
11	25	3.0194	4.037	6.217	1.409	2.7610+02	4.2520+02	5.3110-02	1.1431	0.0	52.953
12	27	4.3062	5.596	8.294	1.326	3.2400+02	5.2310+02	3.8940-02	1.1484	0.0	50.678
13	29	5.6925	7.194	10.434	1.254	3.6060+02	5.2310+02	2.9440-02	1.2778	0.0	0.0
14	31	7.0678	8.571	12.218	1.199	3.9180+02	5.5930+02	2.6710-02	1.2686	0.0	0.0
15	33	8.3814	9.769	13.783	1.157	4.1980+02	5.9230+02	2.1420-02	1.3095	0.0	0.0
16	35	9.6123	10.870	15.332	1.246	4.4670+02	6.3000+02	2.2230-02	1.2890	0.05	0.0
17	37	10.7591	12.076	17.125	1.457	4.8000+02	6.8060+02	2.6600-02	1.2592	0.17	0.0
18	39	11.8354	13.421	19.051	1.650	5.2000+02	7.3810+02	3.0750-02	1.2445	0.28	0.0
19	41	12.8620	14.902	21.093	1.816	5.6580+02	8.0080+02	3.4380-02	1.2378	0.38	0.0
20	43	13.8609	16.521	23.244	1.955	6.1700+02	8.6810+02	3.7390-02	1.2354	0.47	0.0
21	45	14.8512	18.284	25.524	2.068	6.7160+02	9.4040+02	3.9800-02	1.2352	0.55	0.0
22	47	15.8503	20.202	27.947	2.161	7.3600+02	1.0180+03	4.1710-02	1.2358	0.62	0.0
23	49	16.8738	22.298	30.545	2.236	8.0490+02	1.1030+03	4.3200-02	1.2370	0.68	0.0
24	51	17.9354	24.596	33.356	2.299	8.8120+02	1.1950+03	4.4350-02	1.2387	0.73	0.0
25	53	19.0462	27.125	36.408	2.356	9.6620+02	1.2970+03	4.5240-02	1.2395	0.77	0.0
26	55	20.2150	29.915	39.731	2.402	1.0610+03	1.4090+03	4.5920-02	1.2401	0.81	0.0
27	57	21.4480	32.993	43.360	2.437	1.1660+03	1.5330+03	4.6410-02	1.2407	0.84	0.0
28	59	22.7486	36.382	47.322	2.463	1.2830+03	1.6690+03	4.6710-02	1.2415	0.86	0.0
29	61	24.1190	40.101	51.636	2.480	1.4130+03	1.8200+03	4.6860-02	1.2423	0.89	0.0
30	63	25.5605	44.163	56.316	2.491	1.5560+03	1.9840+03	4.6890-02	1.2431	0.91	0.0
31	65	27.0742	48.254	61.362	2.495	1.7020+03	2.1640+03	4.6800-02	1.2421	0.92	0.0
32	68	28.7206	62.762	63.140	2.614	1.8050+03	2.3020+03	3.7250-02	1.2425	0.93	0.0
33	71	31.0960	70.542	92.781	2.673	2.0480+03	2.7460+03	3.6380-02	1.2286	0.94	0.0
34	75	34.2682	83.921	109.553	2.667	2.5030+03	3.2670+03	3.5930-02	1.2206	0.96	0.0
35	80	38.2806	104.916	136.766	2.687	2.9860+03	3.8970+03	3.3040-02	1.2183	0.97	0.0
36	86	43.1064	131.033	171.247	2.704	3.4620+03	4.4980+03	2.9530-02	1.2149	0.98	0.0
37	93	48.5305	155.034	205.222	2.760	3.7790+03	5.0030+03	2.6500-02	1.2050	0.98	0.0
38	100	54.2451	176.237	235.154	2.799	3.9900+03	5.3110+03	2.3030-02	1.2059	0.98	0.0
39	107	60.0232	193.386	259.085	2.805	4.0710+03	5.4540+03	2.1900-02	1.2136	0.98	0.0
40	114	65.7610	207.163	277.255	2.780	4.0730+03	5.4780+03	2.0540-02	1.2165	0.98	0.0
41	121	71.4630	218.020	290.585	2.746	4.0810+03	5.4600+03	1.9590-02	1.2176	0.98	0.0
42	128	77.1858	226.630	300.089	2.703	4.0590+03	5.3750+03	1.8910-02	1.2193	0.98	0.0
43	135	82.9759	234.274	308.005	2.665	4.0260+03	5.2740+03	1.8410-02	1.2212	0.98	0.0
44	137	83.1969	234.275	307.612	2.642	4.0270+03	5.2910+03	1.8420-02	1.2213	0.98	0.0

# 3-D MOMENTUM ENERGY INTEGRAL TECHNIQUE

## VISCIOUS FLOW - CURVED SHOCK AND ROUGHNESS EFFECTS

			CURVED SHOCK EFFECTS		EDGE MASS FLUX AUGMENTATION		SURFACE ROUGHNESS EFFECTS		ROUGHNESS		HEAT TRANSFER AUGMENTATION		PIUGHNESS	
BODY PT NO	INTEG PT NO	STREAM LENGTH INCH (SI)	EDGE ENTROPY BTU/LRM-DEG R (ENTR)	EDGE STREAMLINE LOCATION AT SHOCK INCH (YBAR)	(RDEF)	M/L (RUF)	(PUFSMT)	(RFRP)	M/L (RUF)	(PUFSMT)	(RFRP)	M/L (RUF)	(PUFSMT)	PIUGHNESS RFRPLUS MO
1	1	0.0	2.4868	0.0	1.0000	0.2300	1.0000	0.0	0.2300	1.0000	0.0	0.2300	1.0000	3.7400E+00
2	7	0.2335	2.4836	0.0242	1.1920	0.2300	1.0000	3.7400E+00	0.2300	1.0000	3.7400E+00	0.2300	1.0000	4.5440E+00
3	9	0.3938	2.4812	0.0368	1.1315	0.2300	1.0000	4.5710E+00	0.2300	1.0000	4.5710E+00	0.2300	1.0000	4.5710E+00
4	11	0.5542	2.4773	0.0483	1.1211	0.2300	1.0000	4.1340E+00	0.2300	1.0000	4.1340E+00	0.2300	1.0000	3.4540E+00
5	13	0.7146	2.4737	0.0579	1.1145	0.2300	1.0000	2.6440E+00	0.2300	1.0000	2.6440E+00	0.2300	1.0000	1.9740E+00
6	15	0.8749	2.4703	0.0647	1.1049	0.2300	1.0000	1.4770E+00	0.2300	1.0000	1.4770E+00	0.2300	1.0000	9.8810E-01
7	17	1.0353	2.4670	0.0692	1.0948	0.2300	1.0000	7.8780E-01	0.2300	1.0000	7.8780E-01	0.2300	1.0000	6.4060E-01
8	19	1.1957	2.4639	0.0711	1.0841	0.2300	1.0000	5.3830E-01	0.2300	1.0000	5.3830E-01	0.2300	1.0000	4.7670E-01
9	21	1.3496	2.47910	0.0700	1.0746	0.2300	1.0000	4.3760E-01	0.2300	1.0000	4.3760E-01	0.2300	1.0000	4.0520E-01
10	23	1.4954	2.47514	0.0797	1.0380	0.2300	1.0000	3.7670E-01	0.2300	1.0000	3.7670E-01	0.2300	1.0000	3.5120E-01
11	25	3.0184	2.46956	0.0917	1.0532	0.2300	1.0000	3.2830E-01	0.2300	1.0000	3.2830E-01	0.2300	1.0000	3.0670E-01
12	27	4.3062	2.46643	0.1006	1.0606	0.2300	1.0000	2.8640E-01	0.2300	1.0000	2.8640E-01	0.2300	1.0000	2.6640E-01
13	29	5.6925	2.46473	0.1071	1.0616	0.2300	1.0000	2.4640E-01	0.2300	1.0000	2.4640E-01	0.2300	1.0000	2.2640E-01
14	31	7.0678	2.46333	0.1122	1.0647	0.2300	1.0000	2.0640E-01	0.2300	1.0000	2.0640E-01	0.2300	1.0000	1.8640E-01
15	33	8.3814	2.46218	0.1164	1.0672	0.2300	1.0000	1.6640E-01	0.2300	1.0000	1.6640E-01	0.2300	1.0000	1.4640E-01
16	35	9.6123	2.46125	0.1244	1.0686	0.2300	1.0000	1.2640E-01	0.2300	1.0000	1.2640E-01	0.2300	1.0000	1.0640E-01
17	37	10.7591	2.46052	0.1377	1.0696	0.2300	1.0000	0.8640E-01	0.2300	1.0000	0.8640E-01	0.2300	1.0000	0.6640E-01
18	39	11.8354	2.45948	0.1511	1.0704	0.2300	1.0000	0.4640E-01	0.2300	1.0000	0.4640E-01	0.2300	1.0000	0.2640E-01
19	41	12.8620	2.45961	0.1644	1.0709	0.2300	1.0000	0.0640E-01	0.2300	1.0000	0.0640E-01	0.2300	1.0000	0.0000
20	43	13.8609	2.45939	0.1773	1.0711	0.2300	1.0000	0.0000	0.2300	1.0000	0.0000	0.2300	1.0000	0.0000
21	45	14.8512	2.45934	0.1900	1.0708	0.2300	1.0000	0.0000	0.2300	1.0000	0.0000	0.2300	1.0000	0.0000
22	47	15.8503	2.45943	0.2024	1.0704	0.2300	1.0000	0.0000	0.2300	1.0000	0.0000	0.2300	1.0000	0.0000
23	49	16.8738	2.45964	0.2166	1.0698	0.2300	1.0000	0.0000	0.2300	1.0000	0.0000	0.2300	1.0000	0.0000
24	51	17.9354	2.45996	0.2268	1.0686	0.2300	1.0000	0.0000	0.2300	1.0000	0.0000	0.2300	1.0000	0.0000
25	53	19.0462	2.46037	0.2386	1.0674	0.2300	1.0000	0.0000	0.2300	1.0000	0.0000	0.2300	1.0000	0.0000
26	55	20.2150	2.46087	0.2504	1.0661	0.2300	1.0000	0.0000	0.2300	1.0000	0.0000	0.2300	1.0000	0.0000
27	57	21.4480	2.46144	0.2623	1.0646	0.2300	1.0000	0.0000	0.2300	1.0000	0.0000	0.2300	1.0000	0.0000
28	59	22.7486	2.46205	0.2741	1.0630	0.2300	1.0000	0.0000	0.2300	1.0000	0.0000	0.2300	1.0000	0.0000
29	61	24.1190	2.46272	0.2858	1.0613	0.2300	1.0000	0.0000	0.2300	1.0000	0.0000	0.2300	1.0000	0.0000
30	63	25.5605	2.46342	0.2974	1.0595	0.2300	1.0000	0.0000	0.2300	1.0000	0.0000	0.2300	1.0000	0.0000
31	65	27.0742	2.46416	0.3075	1.0576	0.2300	1.0000	0.0000	0.2300	1.0000	0.0000	0.2300	1.0000	0.0000
32	67	28.7206	2.46480	0.3100	1.0559	0.2300	1.0000	0.0000	0.2300	1.0000	0.0000	0.2300	1.0000	0.0000
33	69	31.0960	2.46523	0.3224	1.0542	0.2300	1.0000	0.0000	0.2300	1.0000	0.0000	0.2300	1.0000	0.0000
34	71	34.2682	2.46577	0.3371	1.0525	0.2300	1.0000	0.0000	0.2300	1.0000	0.0000	0.2300	1.0000	0.0000
35	73	38.2806	2.46646	0.3510	1.0508	0.2300	1.0000	0.0000	0.2300	1.0000	0.0000	0.2300	1.0000	0.0000
36	75	43.1064	2.46711	0.3627	1.0491	0.2300	1.0000	0.0000	0.2300	1.0000	0.0000	0.2300	1.0000	0.0000
37	77	48.5305	2.46771	0.3713	1.0474	0.2300	1.0000	0.0000	0.2300	1.0000	0.0000	0.2300	1.0000	0.0000
38	79	54.2451	2.46836	0.3789	1.0457	0.2300	1.0000	0.0000	0.2300	1.0000	0.0000	0.2300	1.0000	0.0000
39	81	60.0232	2.46898	0.3860	1.0440	0.2300	1.0000	0.0000	0.2300	1.0000	0.0000	0.2300	1.0000	0.0000
40	83	65.7610	2.46957	0.3929	1.0423	0.2300	1.0000	0.0000	0.2300	1.0000	0.0000	0.2300	1.0000	0.0000
41	85	71.4630	2.47014	0.3993	1.0406	0.2300	1.0000	0.0000	0.2300	1.0000	0.0000	0.2300	1.0000	0.0000
42	87	77.1858	2.47069	0.4075	1.0389	0.2300	1.0000	0.0000	0.2300	1.0000	0.0000	0.2300	1.0000	0.0000
43	89	82.9769	2.47129	0.4155	1.0372	0.2300	1.0000	0.0000	0.2300	1.0000	0.0000	0.2300	1.0000	0.0000
44	91	88.1969	2.47189	0.4159	1.0355	0.2300	1.0000	0.0000	0.2300	1.0000	0.0000	0.2300	1.0000	0.0000

# 3-D MOMENTUM ENERGY INTEGRAL TECHNIQUE

## BODY GEOMETRY AND SURFACE QUANTITY RESULTS

STAGNATION POINT LOCATION				
MINIMUM Z-COORD. LOCATION				
SURFACE COORDINATES (INCH)				
X (IN)	Y (IN)	Z (IN)	U	V
-0.0780	0.0000	0.0000	0.0000	0.0000
0.0	0.0	0.0	0.0	0.0
SURFACE COORDINATES (INCH)				
U	V	X	Y	Z
0.0	0.0	0.0	0.0	-0.000
0.0	0.5	0.313	0.0	0.055
0.5	0.5	0.289	0.120	0.055
1.0	0.5	0.221	0.221	0.055
1.5	0.5	0.120	0.289	0.055
2.0	0.5	0.000	0.313	0.055
2.5	0.5	-0.120	0.289	0.055
3.0	0.5	-0.221	0.221	0.055
3.5	0.5	-0.289	0.120	0.055
4.0	0.5	-0.313	0.000	0.055
0.0	1.0	0.589	0.0	0.213
0.5	1.0	0.546	0.225	0.213
1.0	1.0	0.416	0.416	0.213
1.5	1.0	0.225	0.546	0.213
2.0	1.0	0.0	0.589	0.213
2.5	1.0	-0.225	0.546	0.213
3.0	1.0	-0.416	0.416	0.213
3.5	1.0	-0.546	0.225	0.213
4.0	1.0	-0.589	0.0	0.213
0.0	1.3	0.702	0.0	0.326
0.5	1.3	0.648	0.269	0.326
1.0	1.3	0.497	0.497	0.326
1.5	1.3	0.269	0.648	0.326
2.0	1.3	0.000	0.702	0.326
2.5	1.3	-0.269	0.648	0.326
3.0	1.3	-0.497	0.497	0.326
3.5	1.3	-0.648	0.269	0.326
4.0	1.3	-0.702	0.000	0.326
SURFACE COORDINATES (INCH)				
U	V	X	Y	Z
0.0	0.0	0.0	0.0	0.0
0.0	0.5	0.313	0.0	0.055
0.5	0.5	0.289	0.120	0.055
1.0	0.5	0.221	0.221	0.055
1.5	0.5	0.120	0.289	0.055
2.0	0.5	0.000	0.313	0.055
2.5	0.5	-0.120	0.289	0.055
3.0	0.5	-0.221	0.221	0.055
3.5	0.5	-0.289	0.120	0.055
4.0	0.5	-0.313	0.000	0.055
0.0	1.0	0.589	0.0	0.213
0.5	1.0	0.546	0.225	0.213
1.0	1.0	0.416	0.416	0.213
1.5	1.0	0.225	0.546	0.213
2.0	1.0	0.0	0.589	0.213
2.5	1.0	-0.225	0.546	0.213
3.0	1.0	-0.416	0.416	0.213
3.5	1.0	-0.546	0.225	0.213
4.0	1.0	-0.589	0.0	0.213
0.0	1.3	0.702	0.0	0.326
0.5	1.3	0.648	0.269	0.326
1.0	1.3	0.497	0.497	0.326
1.5	1.3	0.269	0.648	0.326
2.0	1.3	0.000	0.702	0.326
2.5	1.3	-0.269	0.648	0.326
3.0	1.3	-0.497	0.497	0.326
3.5	1.3	-0.648	0.269	0.326
4.0	1.3	-0.702	0.000	0.326
SURFACE COORDINATES (INCH)				
U	V	X	Y	Z
0.0	0.0	0.0	0.0	0.0
0.0	0.5	0.313	0.0	0.055
0.5	0.5	0.289	0.120	0.055
1.0	0.5	0.221	0.221	0.055
1.5	0.5	0.120	0.289	0.055
2.0	0.5	0.000	0.313	0.055
2.5	0.5	-0.120	0.289	0.055
3.0	0.5	-0.221	0.221	0.055
3.5	0.5	-0.289	0.120	0.055
4.0	0.5	-0.313	0.000	0.055
0.0	1.0	0.589	0.0	0.213
0.5	1.0	0.546	0.225	0.213
1.0	1.0	0.416	0.416	0.213
1.5	1.0	0.225	0.546	0.213
2.0	1.0	0.0	0.589	0.213
2.5	1.0	-0.225	0.546	0.213
3.0	1.0	-0.416	0.416	0.213
3.5	1.0	-0.546	0.225	0.213
4.0	1.0	-0.589	0.0	0.213
0.0	1.3	0.702	0.0	0.326
0.5	1.3	0.648	0.269	0.326
1.0	1.3	0.497	0.497	0.326
1.5	1.3	0.269	0.648	0.326
2.0	1.3	0.000	0.702	0.326
2.5	1.3	-0.269	0.648	0.326
3.0	1.3	-0.497	0.497	0.326
3.5	1.3	-0.648	0.269	0.326
4.0	1.3	-0.702	0.000	0.326
SURFACE COORDINATES (INCH)				
U	V	X	Y	Z
0.0	0.0	0.0	0.0	0.0
0.0	0.5	0.313	0.0	0.055
0.5	0.5	0.289	0.120	0.055
1.0	0.5	0.221	0.221	0.055
1.5	0.5	0.120	0.289	0.055
2.0	0.5	0.000	0.313	0.055
2.5	0.5	-0.120	0.289	0.055
3.0	0.5	-0.221	0.221	0.055
3.5	0.5	-0.289	0.120	0.055
4.0	0.5	-0.313	0.000	0.055
0.0	1.0	0.589	0.0	0.213
0.5	1.0	0.546	0.225	0.213
1.0	1.0	0.416	0.416	0.213
1.5	1.0	0.225	0.546	0.213
2.0	1.0	0.0	0.589	0.213
2.5	1.0	-0.225	0.546	0.213
3.0	1.0	-0.416	0.416	0.213
3.5	1.0	-0.546	0.225	0.213
4.0	1.0	-0.589	0.0	0.213
0.0	1.3	0.702	0.0	0.326
0.5	1.3	0.648	0.269	0.326
1.0	1.3	0.497	0.497	0.326
1.5	1.3	0.269	0.648	0.326
2.0	1.3	0.000	0.702	0.326
2.5	1.3	-0.269	0.648	0.326
3.0	1.3	-0.497	0.497	0.326
3.5	1.3	-0.648	0.269	0.326
4.0	1.3	-0.702	0.000	0.326
SURFACE COORDINATES (INCH)				
U	V	X	Y	Z
0.0	0.0	0.0	0.0	0.0
0.0	0.5	0.313	0.0	0.055
0.5	0.5	0.289	0.120	0.055
1.0	0.5	0.221	0.221	0.055
1.5	0.5	0.120	0.289	0.055
2.0	0.5	0.000	0.313	0.055
2.5	0.5	-0.120	0.289	0.055
3.0	0.5	-0.221	0.221	0.055
3.5	0.5	-0.289	0.120	0.055
4.0	0.5	-0.313	0.000	0.055
0.0	1.0	0.589	0.0	0.213
0.5	1.0	0.546	0.225	0.213
1.0	1.0	0.416	0.416	0.213
1.5	1.0	0.225	0.546	0.213
2.0	1.0	0.0	0.589	0.213
2.5	1.0	-0.225	0.546	0.213
3.0	1.0	-0.416	0.416	0.213
3.5	1.0	-0.546	0.225	0.213
4.0	1.0	-0.589	0.0	0.213
0.0	1.3	0.702	0.0	0.326
0.5	1.3	0.648	0.269	0.326
1.0	1.3	0.497	0.497	0.326
1.5	1.3	0.269	0.648	0.326
2.0	1.3	0.000	0.702	0.326
2.5	1.3	-0.269	0.648	0.326
3.0	1.3	-0.497	0.497	0.326
3.5	1.3	-0.648	0.269	0.326
4.0	1.3	-0.702	0.000	0.326
SURFACE COORDINATES (INCH)				
U	V	X	Y	Z
0.0	0.0	0.0	0.0	0.0
0.0	0.5	0.313	0.0	0.055
0.5	0.5	0.289	0.120	0.055
1.0	0.5	0.221	0.221	0.055
1.5	0.5	0.120	0.289	0.055
2.0	0.5	0.000	0.313	0.055
2.5	0.5	-0.120	0.289	0.055
3.0	0.5	-0.221	0.221	0.055
3.5	0.5	-0.289	0.120	0.055
4.0	0.5	-0.313	0.000	0.055
0.0	1.0	0.589	0.0	0.213
0.5	1.0	0.546	0.225	0.213
1.0	1.0	0.416	0.416	0.213
1.5	1.0	0.225	0.546	0.213
2.0	1.0	0.0	0.589	0.213
2.5	1.0	-0.225	0.546	0.213
3.0	1.0	-0.416	0.416	0.213
3.5	1.0	-0.546	0.225	0.213
4.0	1.0	-0.589	0.0	0.213
0.0	1.3	0.702	0.0	0.326
0.5	1.3	0.648	0.269	0.326
1.0	1.3	0.497	0.497	0.326
1.5	1.3	0.269	0.648	0.326
2.0	1.3	0.000	0.702	0.326
2.5	1.3	-0.269	0.648	0.326
3.0	1.3	-0.497	0.497	0.326
3.5	1.3	-0.648	0.269	0.326
4.0	1.3	-0.702	0.000	0.326
SURFACE COORDINATES (INCH)				
U	V	X	Y	Z
0.0	0.0	0.0	0.0	0.0
0.0	0.5	0.313	0.0	0.055
0.5	0.5	0.289	0.120	0.055
1.0	0.5	0.221	0.221	0.055
1.5	0.5	0.120	0.289	0.055
2.0	0.5	0.000	0.313	0.055
2.5	0.5	-0.120	0.289	0.055
3.0	0.5	-0.221	0.221	0.055
3.5	0.5	-0.289	0.120	0.055
4.0	0.5	-0.313	0.000	0.055
0.0	1.0	0.589	0.0	0.213
0.5	1.0	0.546	0.225	0.213
1.0	1.0	0.416	0.416	0.213
1.5	1.0	0.225	0.546	0.213
2.0	1.0	0.0	0.589	0.213
2.5	1.0	-0.225	0.546	0.213
3.0	1.0	-0.416	0.416	0.213
3.5	1.0	-0.546	0.225	0.213
4.0	1.0	-0.589	0.0	0.213
0.0	1.3	0.702	0.0	0.326
0.5	1.3	0.648	0.269	0.326
1.0	1.3	0.497	0.497	0.326
1.5	1.3	0.269	0.648	0.326
2.0	1.3	0.000	0.702	0.326
2.5	1.3	-0.269	0.648	0.326
3.0	1.3	-0.497	0.497	0.326
3.5	1.3	-0.648	0.269	0.326
4.0	1.3	-0.702	0.000	0.326
SURFACE COORDINATES (INCH)				
U	V	X	Y	Z
0.0	0.0	0.0	0.0	0.0
0.0	0.5	0.313	0.0	0.055
0.5	0.5	0.289	0.120	0.055
1.0	0.5	0.221	0.221	0.055
1.5	0.5	0.120	0.289	0.055
2.0	0.5	0.000	0.313	0.055
2.5	0.5	-0.120	0.289	0.055
3.0	0.5	-0.221	0.221	0.055
3.5	0.5	-0.289	0.120	0.055
4.0	0.5	-0.313	0.000	0.055
0.0	1.0	0.589	0.0	0.213
0.5	1.0	0.546	0.225	0.213
1.0	1.0	0.416	0.416	0.213
1.5	1.0	0.225	0.546	0.213
2.0	1.0	0.0	0.589	0.213
2.5	1.0	-0.225	0.546	0.213

# 3-D MOMENTUM ENERGY INTEGRAL TECHNIQUE

0.0	1.5	0.794	0.0	0.456	4724.5	4.7676	6.48470+02	4.7933	0.002	2.4040-01	6235.92
0.5	1.5	0.733	0.304	0.456	4726.7	4.8919	6.56630+02	4.8976	0.002	2.4130-01	6248.94
1.0	1.5	0.562	0.562	0.456	4731.9	5.1465	6.75870+02	5.1521	0.002	2.4340-01	6278.95
1.5	1.5	0.304	0.733	0.456	4740.0	5.5573	7.07700+02	5.5629	0.002	2.4680-01	6325.84
2.0	1.5	0.000	0.794	0.456	4749.8	6.0935	7.49740+02	6.0988	0.002	2.5120-01	6382.97
2.5	1.5	-0.304	0.733	0.456	4759.9	6.6700	7.91500+02	6.6742	0.002	2.5540-01	6436.77
3.0	1.5	-0.562	0.562	0.456	4768.9	7.1979	8.26350+02	7.2030	0.002	2.5870-01	6479.48
3.5	1.5	-0.733	0.304	0.456	4775.5	7.5904	8.50490+02	7.5953	0.012	2.6090-01	6508.14
4.0	1.5	-0.794	0.000	0.456	4778.2	7.7534	8.60770+02	7.7583	0.002	2.6180-01	6519.99
0.0	1.8	0.863	0.0	0.600	4669.4	2.7732	4.79700+02	2.7775	0.002	2.2050-01	5897.38
0.5	1.8	0.796	0.330	0.600	4672.0	2.8488	4.86400+02	2.8531	0.002	2.2140-01	5913.93
1.0	1.8	0.610	0.610	0.600	4678.2	3.0355	5.02290+02	3.0399	0.002	2.2330-01	5951.94
1.5	1.8	0.330	0.796	0.600	4687.7	3.3405	5.27480+02	3.3448	0.002	2.2620-01	6009.10
2.0	1.8	0.000	0.863	0.600	4699.3	3.7454	5.59870+02	3.7497	0.002	2.3000-01	6077.52
2.5	1.8	-0.330	0.796	0.600	4709.0	4.1196	5.91790+02	4.1240	0.002	2.3390-01	6138.33
3.0	1.8	-0.610	0.610	0.600	4717.1	4.4577	6.20170+02	4.4621	0.002	2.3770-01	6188.39
3.5	1.8	-0.796	0.330	0.600	4722.8	4.7128	6.40870+02	4.7171	0.002	2.3940-01	6223.20
4.0	1.8	-0.863	0.000	0.600	4725.0	4.8161	6.49620+02	4.8204	0.002	2.4050-01	6237.46
0.0	2.0	0.905	0.0	0.754	4628.0	1.4916	3.53300+02	1.4935	0.002	2.3280-01	5188.67
0.5	2.0	0.835	0.346	0.754	4630.2	1.5414	3.60420+02	1.5433	0.002	2.3380-01	5214.07
1.0	2.0	0.640	0.640	0.754	4634.5	1.6433	3.76100+02	1.6455	0.002	2.3510-01	5268.49
1.5	2.0	0.346	0.835	0.754	4641.5	1.8107	4.00440+02	1.8137	0.002	2.3750-01	5339.47
2.0	2.0	0.000	0.905	0.754	4651.9	2.0335	4.29930+02	2.0367	0.002	2.4010-01	5425.17
2.5	2.0	-0.346	0.835	0.754	4662.1	2.2870	4.59890+02	2.2900	0.002	2.4280-01	5507.55
3.0	2.0	-0.640	0.640	0.754	4670.5	2.5178	4.85140+02	2.5209	0.002	2.4510-01	5573.69
3.5	2.0	-0.835	0.346	0.754	4676.7	2.6589	5.03400+02	2.6621	0.002	2.4680-01	5620.51
4.0	2.0	-0.905	0.000	0.754	4679.3	2.7774	5.11750+02	2.7806	0.002	2.4750-01	5639.61
0.0	2.2	1.874	0.0	6.034	4525.4	0.5066	9.21460+01	0.5074	0.001	2.2500-01	3555.55
0.5	2.2	1.731	0.717	6.034	4524.5	0.5207	9.73150+01	0.5210	0.001	2.2530-01	3664.92
1.0	2.2	1.325	1.325	6.034	4524.5	0.5603	1.07430+02	0.5612	0.001	2.2570-01	3743.95
1.5	2.2	0.717	1.731	6.034	4527.9	0.6414	1.24230+02	0.6429	0.001	2.2630-01	3885.70
2.0	2.2	0.000	1.874	6.034	4534.8	0.7777	1.44100+02	0.7788	0.001	2.2700-01	4067.97
2.5	2.2	-0.717	1.731	6.034	4543.3	0.9620	1.75920+02	0.9631	0.001	2.2770-01	4255.96
3.0	2.2	-1.325	1.325	6.034	4551.5	1.1741	2.04160+02	1.1751	0.001	2.2830-01	4428.31
3.5	2.2	-1.731	0.717	6.034	4558.0	1.3525	2.25330+02	1.3535	0.001	2.2880-01	4556.23
4.0	2.2	-1.874	-0.000	6.034	4560.7	1.4414	2.35930+02	1.4425	0.011	2.2900-01	4614.65
0.0	2.4	2.843	0.0	11.314	4545.3	0.3764	1.10520+02	0.3775	0.001	2.2680-01	3785.05
0.5	2.4	2.625	1.088	11.314	4549.5	0.3878	9.12190+01	0.3887	0.001	2.2540-01	3593.98
1.0	2.4	2.010	2.010	11.314	4547.8	0.4309	8.74510+01	0.4316	0.001	2.2470-01	3691.74
1.5	2.4	1.088	2.625	11.314	4548.7	0.5374	9.77450+01	0.5382	0.000	2.2520-01	3643.17
2.0	2.4	0.000	2.843	11.314	4546.2	0.7604	1.42040+02	0.7611	0.000	2.2650-01	3958.07
2.5	2.4	-1.088	2.625	11.314	4549.2	0.9588	2.17790+02	1.0565	0.001	2.2830-01	4388.81
3.0	2.4	-2.010	2.010	11.314	4548.3	1.4317	2.99270+02	1.5374	0.001	2.3230-01	4844.24
3.5	2.4	-2.625	1.088	11.314	4532.9	1.7696	4.68240+02	1.7705	0.001	2.4610-01	5404.74
4.0	2.4	-2.843	-0.000	11.314	4546.3	1.9363	5.38480+02	1.9373	0.001	2.5170-01	5614.30

# 3-D MOMENTUM ENERGY INTEGRAL TECHNIQUE

0.0	2.6	3.812	0.0	16.594	5597.7	0.3411	1.50270+02	0.3428	2.2810-01	4119.03
0.5	2.6	3.520	1.459	16.594	4579.6	0.3525	1.49330+02	0.3540	2.2820-01	4109.29
1.0	2.6	2.696	2.696	16.594	4550.4	0.3982	1.57160+02	0.3996	2.2830-01	4163.10
1.5	2.6	1.459	3.520	16.594	4530.5	0.5730	2.42500+02	0.5745	2.3310-01	4400.96
2.0	2.6	0.000	3.812	16.594	4535.6	0.8956	4.09400+02	0.8977	2.4640-01	5072.53
2.5	2.6	-1.459	3.520	16.594	4537.8	1.2334	5.37460+02	1.2349	2.6020-01	5543.96
3.0	2.6	-2.696	2.696	16.594	4537.0	1.6428	6.87140+02	1.6455	2.7370-01	5778.97
3.5	2.6	-3.520	1.459	16.594	4535.7	2.0187	8.07950+02	2.0223	2.8580-01	5951.39
4.0	2.6	-3.812	-0.000	16.594	4536.4	2.1185	8.39270+02	2.1222	2.8780-01	5978.52
0.0	2.8	4.781	0.0	21.874	4627.0	0.3357	1.60110+02	0.3378	2.2870-01	4192.69
0.5	2.8	4.415	1.829	21.874	4600.7	0.3417	1.65200+02	0.3436	2.2880-01	4226.20
1.0	2.8	3.381	3.381	21.874	4565.5	0.3952	2.02750+02	0.3975	2.3040-01	4476.46
1.5	2.8	1.829	4.415	21.874	4533.7	0.6163	3.25850+02	0.6215	2.3970-01	4909.26
2.0	2.8	0.000	4.781	21.874	4509.3	0.8786	4.35780+02	0.8826	2.4880-01	5316.70
2.5	2.8	-1.829	4.415	21.874	4500.9	1.2680	5.80270+02	1.2726	2.6210-01	5565.44
3.0	2.8	-3.381	3.381	21.874	4493.6	1.6574	7.07470+02	1.6625	2.7540-01	5796.17
3.5	2.8	-4.415	1.829	21.874	4488.7	1.9424	7.90200+02	1.9478	2.8360-01	5925.35
4.0	2.8	-4.781	-0.000	21.874	4488.2	2.0363	8.17810+02	2.0418	2.8510-01	5950.47
0.0	2.9	5.266	0.0	24.514	4628.6	0.3372	1.60920+02	0.3395	2.2870-01	4198.58
0.5	2.9	4.862	2.015	24.514	4605.0	0.3379	1.68040+02	0.3403	2.2900-01	4245.19
1.0	2.9	3.723	3.723	24.514	4557.0	0.4167	2.24980+02	0.4197	2.3160-01	4518.05
1.5	2.9	2.015	4.862	24.514	4512.3	0.5866	3.17810+02	0.5906	2.3770-01	4977.14
2.0	2.9	0.000	5.266	24.514	4496.3	0.8074	4.52150+02	0.8120	2.4870-01	5347.32
2.5	2.9	-2.015	4.862	24.514	4488.7	1.2871	5.91580+02	1.2921	2.6240-01	5548.22
3.0	2.9	-3.723	3.723	24.514	4479.1	1.6668	7.10080+02	1.6726	2.7610-01	5809.15
3.5	2.9	-4.862	2.015	24.514	4476.9	1.9300	7.83170+02	1.9361	2.8270-01	5916.90
4.0	2.9	-5.266	-0.000	24.514	4476.7	2.0286	8.11980+02	2.0347	2.8450-01	5943.76
0.0	3.0	5.750	0.0	27.154	4618.1	0.2667	1.36660+02	0.2679	2.2810-01	4018.53
0.5	3.0	5.310	2.200	27.154	4590.8	0.2610	1.41580+02	0.2621	2.2830-01	4053.71
1.0	3.0	4.066	4.066	27.154	4537.2	0.3207	1.88880+02	0.3227	2.2980-01	4326.57
1.5	3.0	2.200	5.310	27.154	4495.7	0.4417	2.58070+02	0.4468	2.3320-01	4676.95
2.0	3.0	0.000	5.750	27.154	4490.8	0.6958	3.70950+02	0.6997	2.4240-01	4979.15
2.5	3.0	-2.200	5.310	27.154	4485.8	0.9679	4.67940+02	0.9727	2.5140-01	5283.36
3.0	3.0	-4.066	4.066	27.154	4481.0	1.1980	5.66160+02	1.2037	2.6070-01	5480.11
3.5	3.0	-5.310	2.200	27.154	4482.7	1.3759	6.00020+02	1.3818	2.6580-01	5671.88
4.0	3.0	-5.750	-0.000	27.154	4484.0	1.4456	6.20900+02	1.4515	2.6770-01	5703.95
0.0	3.1	6.007	0.0	29.602	4616.3	0.2535	1.28120+02	0.2544	2.2780-01	3954.95
0.5	3.1	5.547	2.299	29.602	4574.5	0.2378	1.30620+02	0.2379	2.2800-01	3976.17
1.0	3.1	4.248	4.248	29.602	4518.2	0.2484	1.55210+02	0.2505	2.2880-01	4140.60
1.5	3.1	2.299	5.547	29.602	4490.8	0.3432	2.12680+02	0.3465	2.3180-01	4397.33
2.0	3.1	0.000	6.007	29.602	4486.4	0.4970	2.87740+02	0.5015	2.3640-01	4705.69
2.5	3.1	-2.299	5.547	29.602	4478.0	0.6503	3.53860+02	0.6565	2.4140-01	5014.05
3.0	3.1	-4.248	4.248	29.602	4473.6	0.8016	4.08190+02	0.8104	2.4630-01	5286.50
3.5	3.1	-5.547	2.299	29.602	4474.3	0.9326	4.50920+02	0.9395	2.5080-01	5396.67
4.0	3.1	-6.007	0.000	29.602	4477.7	0.9844	4.69020+02	0.9913	2.5290-01	5440.15

# 3-D MOMENTUM ENERGY INTEGRAL TECHNIQUE

0.0	3.1	6.265	0.0	32.050	4616.5	0.2534	1.26630E+02	0.2544	0.001	2.2770-01	3947.64
0.5	3.1	5.785	2.397	32.050	4567.0	0.2185	1.24800E+02	0.2196	0.001	2.2770-01	3926.51
1.0	3.1	4.430	4.430	32.050	4499.4	0.2051	1.15620E+02	0.2074	0.001	2.2770-01	4007.76
1.5	3.1	2.397	5.785	32.050	4484.0	0.3111	1.98120E+02	0.3148	0.001	2.3120-01	4286.97
2.0	3.1	0.000	6.265	32.050	4476.7	0.4354	2.61120E+02	0.4404	0.001	2.3440-01	4603.08
2.5	3.1	-2.397	5.785	32.050	4469.4	0.5594	3.16990E+02	0.5661	0.001	2.3750-01	4919.20
3.0	3.1	-4.430	4.430	32.050	4465.8	0.6975	3.69000E+02	0.7048	0.001	2.4210-01	5185.17
3.5	3.1	-5.785	2.397	32.050	4468.7	0.8319	4.19200E+02	0.8373	0.001	2.4760-01	5327.02
4.0	3.1	-6.265	0.000	32.050	4468.2	0.8869	4.39780E+02	0.8947	0.001	2.4990-01	5378.02
0.0	3.1	6.522	0.0	34.497	4615.6	0.2470	1.23110E+02	0.2480	0.001	2.2760-01	3912.87
0.5	3.1	6.022	2.496	34.497	4556.0	0.2038	1.19850E+02	0.2052	0.001	2.2770-01	3874.87
1.0	3.1	4.612	4.612	34.497	4488.1	0.1906	1.29890E+02	0.1932	0.001	2.2830-01	3924.93
1.5	3.1	2.496	6.022	34.497	4479.3	0.3035	1.95760E+02	0.3074	0.001	2.3090-01	4250.74
2.0	3.1	0.000	6.522	34.497	4470.5	0.4164	2.51980E+02	0.4217	0.001	2.3410-01	4576.55
2.5	3.1	-2.496	6.022	34.497	4461.7	0.5293	3.04830E+02	0.5359	0.001	2.3590-01	4902.36
3.0	3.1	-4.612	4.612	34.497	4458.7	0.6793	3.65020E+02	0.6867	0.001	2.4140-01	5175.19
3.5	3.1	-6.022	2.496	34.497	4460.1	0.8279	4.20600E+02	0.8307	0.001	2.4740-01	5327.59
4.0	3.1	-6.522	0.000	34.497	4460.5	0.8806	4.42020E+02	0.8877	0.001	2.5120-01	5380.93
0.0	3.2	6.779	0.0	36.945	4614.3	0.2363	1.17500E+02	0.2374	0.001	2.2740-01	3845.76
0.5	3.2	6.260	2.594	36.945	4534.9	0.1866	1.11230E+02	0.1864	0.001	2.2750-01	3813.10
1.0	3.2	4.794	4.794	36.945	4486.7	0.1998	1.35670E+02	0.2075	0.001	2.2860-01	3917.07
1.5	3.2	2.594	6.260	36.945	4475.6	0.3060	1.97040E+02	0.3100	0.001	2.3070-01	4252.44
2.0	3.2	0.000	6.779	36.945	4464.4	0.4172	2.54550E+02	0.4176	0.001	2.3300-01	4587.80
2.5	3.2	-2.594	6.260	36.945	4453.4	0.5184	3.02710E+02	0.5252	0.001	2.3520-01	4923.16
3.0	3.2	-4.794	4.794	36.945	4451.4	0.6902	3.74150E+02	0.6974	0.000	2.4290-01	5194.97
3.5	3.2	-6.260	2.594	36.945	4453.1	0.8383	4.30260E+02	0.8455	0.000	2.4900-01	5350.25
4.0	3.2	-6.779	0.000	36.945	4453.8	0.8967	4.51830E+02	0.9037	0.000	2.5140-01	5403.21
0.0	3.4	7.808	0.0	46.736	4605.5	0.1905	9.66290E+01	0.1918	0.001	2.2670-01	3671.73
0.5	3.4	7.210	2.988	46.736	4511.2	0.1533	1.01330E+02	0.1549	0.001	2.2710-01	3679.07
1.0	3.4	5.521	5.521	46.736	4488.6	0.2229	1.50760E+02	0.2260	0.001	2.2860-01	4001.83
1.5	3.4	2.988	7.210	46.736	4466.0	0.2925	1.96090E+02	0.2971	0.001	2.2940-01	4304.56
2.0	3.4	0.000	7.808	46.736	4443.5	0.3622	2.34650E+02	0.3682	0.000	2.3080-01	4607.29
2.5	3.4	-2.988	7.210	46.736	4438.9	0.5120	3.01860E+02	0.5187	0.000	2.3560-01	4958.15
3.0	3.4	-5.521	5.521	46.736	4442.7	0.6910	3.79000E+02	0.6997	0.000	2.4360-01	5212.74
3.5	3.4	-7.210	2.988	46.736	4445.4	0.8378	4.33010E+02	0.8446	0.000	2.4960-01	5354.20
4.0	3.4	-7.808	0.000	46.736	4446.6	0.8975	4.54170E+02	0.9040	0.000	2.5170-01	5407.65
0.0	3.6	8.838	0.0	56.528	4598.9	0.1594	8.27620E+01	0.1613	0.001	2.2620-01	3529.49
0.5	3.6	8.160	3.382	56.528	4509.3	0.1512	9.81650E+01	0.1539	0.001	2.2690-01	3645.46
1.0	3.6	6.249	6.249	56.528	4474.5	0.1897	1.32300E+02	0.1927	0.001	2.2800-01	3911.72
1.5	3.6	3.382	8.160	56.528	4439.6	0.2262	1.63550E+02	0.2314	0.000	2.2910-01	4177.98
2.0	3.6	0.000	8.837	56.528	4432.2	0.3426	2.26900E+02	0.3486	0.000	2.3070-01	4480.07
2.5	3.6	-3.382	8.160	56.528	4436.9	0.5127	3.03300E+02	0.5188	0.000	2.3490-01	4961.54
3.0	3.6	-6.249	6.249	56.528	4442.0	0.7065	1.81170E+02	0.7126	0.000	2.4370-01	5218.88
3.5	3.6	-8.160	3.382	56.528	4445.0	0.8670	4.40120E+02	0.8729	0.000	2.5010-01	5374.63
4.0	3.6	-8.837	0.000	56.528	4446.2	0.9380	4.64780E+02	0.9438	0.000	2.5270-01	5432.84



# 3-D MOMENTUM ENERGY INTEGRAL TECHNIQUE

0.0	3.8	9.867	6.0	66.319	4598.7	0.1424	7.4182D+01	0.1438	0.001	2.2580-01	3412.50
0.5	3.8	9.110	3.775	66.319	4489.1	0.1295	9.8815D+01	0.1331	0.001	2.2600-01	3614.24
1.0	3.8	6.977	6.977	66.319	4438.6	0.1358	1.0815D+02	0.1402	0.000	2.2760-01	3758.76
1.5	3.8	3.775	9.110	66.319	4430.4	0.2104	1.5616D+02	0.2156	0.000	2.2900-01	4133.93
2.0	3.8	0.000	9.867	66.319	4430.4	0.3368	2.2325D+02	0.3425	0.000	2.3070-01	4464.01
2.5	3.8	-3.775	9.110	66.319	4436.9	0.5130	3.0083D+02	0.5188	0.000	2.3470-01	4949.01
3.0	3.8	-6.977	6.977	66.319	4442.2	0.7256	3.8546D+02	0.7313	0.000	2.4190-01	5229.15
3.5	3.8	-9.110	3.775	66.319	4445.5	0.9103	4.5145D+02	0.9157	0.000	2.5110-01	5401.99
4.0	3.8	-9.867	0.000	66.319	4446.8	0.9911	4.7820D+02	0.9963	0.000	2.5400-01	5461.86
0.0	3.9	10.638	0.0	73.662	4601.0	0.1350	7.0590D+01	0.1363	0.001	2.2570-01	3290.13
0.5	3.9	9.823	4.071	73.662	4451.5	0.1175	9.1035D+01	0.1170	0.001	2.2670-01	3544.66
1.0	3.9	7.523	7.522	73.662	4428.8	0.1346	1.0836D+02	0.1385	0.000	2.2760-01	3757.51
1.5	3.9	4.071	9.823	73.662	4425.0	0.2086	1.5662D+02	0.2134	0.000	2.2910-01	4137.60
2.0	3.9	0.000	10.638	73.662	4430.1	0.3328	2.1985D+02	0.3385	0.000	2.3060-01	4450.64
2.5	3.9	-4.071	9.823	73.662	4437.5	0.5197	2.9926D+02	0.5256	0.000	2.3410-01	4967.90
3.0	3.9	-7.522	7.523	73.662	4442.9	0.7505	3.9012D+02	0.7560	0.000	2.4630-01	5241.71
3.5	3.9	-9.823	4.071	73.662	4446.1	0.9504	4.6708D+02	0.9554	0.000	2.5270-01	5428.14
4.0	3.9	-10.638	0.000	73.662	4447.7	1.0381	4.8981D+02	1.0430	0.000	2.5510-01	5489.93
0.0	5.0	11.500	0.0	81.860	4605.6	0.1303	6.7972D+01	0.1314	0.001	2.2550-01	3351.71
0.5	5.0	10.374	5.044	81.860	4444.4	0.1089	8.3946D+01	0.1122	0.000	2.2670-01	3532.62
1.0	5.0	5.806	9.944	81.860	4427.4	0.1781	1.3900D+02	0.1871	0.000	2.2870-01	4030.77
1.5	5.0	4.250	11.227	81.860	4424.1	0.2934	2.0670D+02	0.3007	0.000	2.3010-01	4449.21
2.0	5.0	0.000	12.172	81.860	4438.3	0.4657	4.4074D+02	0.4716	0.000	2.5010-01	5392.85
2.5	5.0	-4.250	11.227	81.860	4444.4	1.1895	5.3517D+02	1.1950	0.000	2.5780-01	5513.07
3.0	5.0	-5.806	9.944	81.860	4440.7	0.6218	3.3618D+02	0.6297	0.000	2.3790-01	5075.43
3.5	5.0	-10.335	5.044	81.860	4444.4	0.9555	4.5965D+02	0.9603	0.000	2.5170-01	5423.86
4.0	5.0	-11.500	0.000	81.860	4448.4	1.0675	4.9416D+02	1.0721	0.000	2.5550-01	5501.79

# 3-D MOMENTUM ENERGY INTEGRAL TECHNIQUE

## AERODYNAMIC COEFFICIENTS

DRAG COMPONENTS			LIFT COMPONENTS			LIFT/DRAG		CENTER OF PRESSURE 0.14958
X	Y	Z	X	Y	Z	X	Z	
0.00548	0.0	0.06265	0.13958	0.0	-0.01221	2.22776		
TOTAL FORCE			INVISCID PRESSURE			INDUCED PRESSURE		WALL SHEAR
X	Y	Z	X	Y	Z	X	Z	
0.1451	0.0	0.0504	0.1442	0.0	0.0448	0.0005	0.0003	0.0053
TOTAL MOMENT			INVISCID PRESSURE			INDUCED PRESSURE		WALL SHEAR
X	Y	Z	X	Y	Z	X	Z	
0.0	0.0217	0.0	0.0	0.0217	0.0	0.0	0.0	0.0

## SECTION 5

### RESULTS

The two-dimensional version of MEIT has been verified by many comparisons with data and other calculations (References 6 to 10). Therefore, testing of 3DMEIT has been concentrated on data from biconic configurations at angle-of-attack. Three runs from References 27 and 28 were selected as test cases for 3DMEIT. The conditions of these three test cases are summarized in Table 5-1. A demonstration calculation was also done at flight conditions on a biconic configuration with yaw stabilizers. This calculation exercised the ablation model to predict wall temperature and blowing parameters.

Figure 5-1 compares an early zero angle-of-attack heat transfer prediction with the experimental data. In general, this prediction is higher than the data, which is believed to be due to the ideal gas properties used in this calculation. The local calculated stagnation temperature was  $1,982^{\circ}\text{R}$ , which is higher than the measured stilling chamber temperature of  $1,894^{\circ}\text{R}$ . The measured local freestream stagnation temperature was  $1,796^{\circ}\text{R}$  which indicates some losses from the stilling chamber conditions. Therefore, the freestream conditions for the calculations were modified as shown in Table 5-1 to more closely match the measured local stagnation temperature. This resulted in much better agreement with the experimental data, as shown in subsequent comparisons.

Table 5-1. Test Case Conditions

Case	Data Group	Configuration	$p_{\infty}$ (atm)	$T_{\infty}$ (°R)	$V_{\infty}$ (ft/s)	$M_{\infty}$	(deg)	$T_o$ (°R)	Comments
1	Phase V GR 159	14°/7° Biconic 0.5 Rn L = 28.283 in.	0.000681	94.54	4,767	10	0	1,982	Ideal gas, laminar
	Modified								
2	Phase V Groups 96, 97, 136-158	14°/7° Biconic 0.5 Rn L = 28.283 in.	0.001361	94.88	4,775	10	5	1,989	Ideal gas, laminar
	Modified								
3	Phase V Groups 71-75 261-265	10.5°/7° Biconic 0.5 Rn L = 31.006 in.	0.001361	84.14	4,498	10	5	1,764	Ideal gas, turbulent, boundary layer trips
4	Flight	10.4°/6° Biconic 0.92 Rn L = 8	0.005913	98.4	3,890	8	10	1,355	Ideal gas, turbulent, ablation model
4			0.074868	389.97	15,609	16.2	5	10,743	

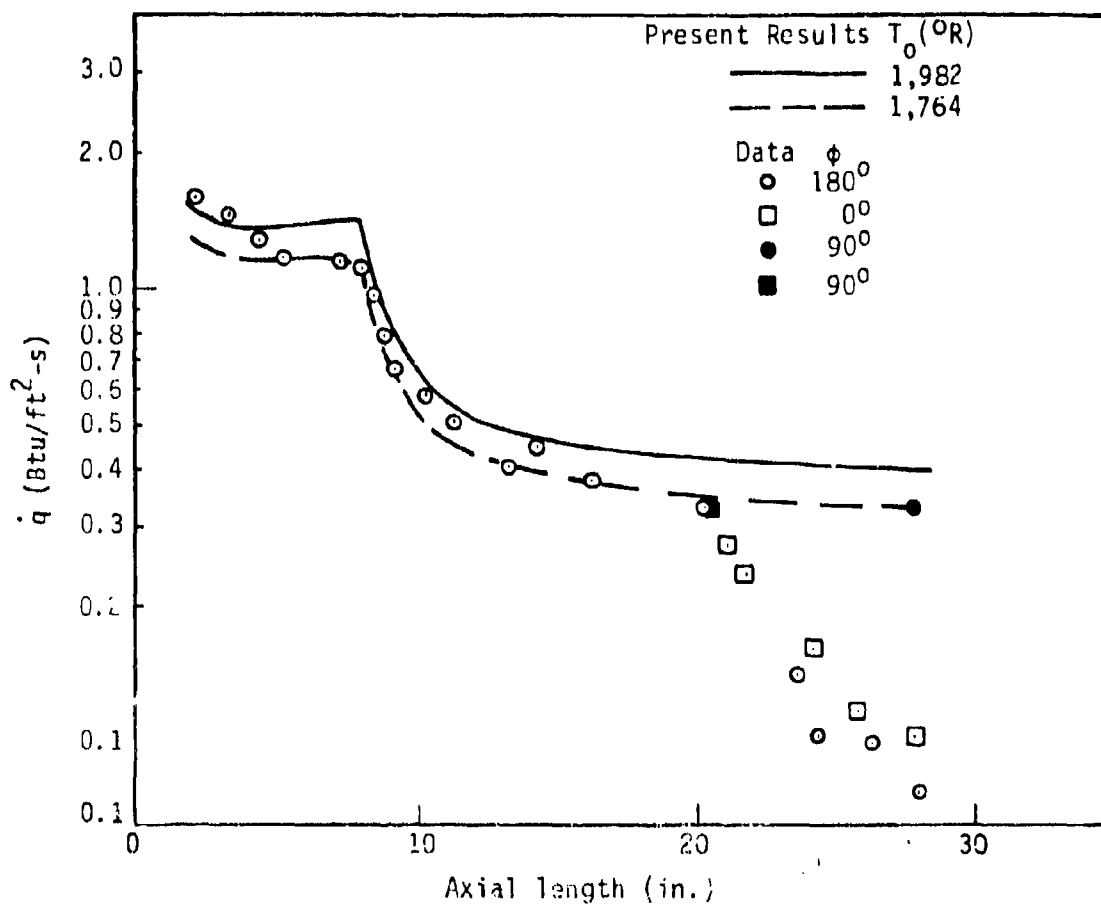


Figure 5-1. Comparison of 3DMEIT with HYTAC Data Group 159, Laminar,  $M = 10$ ,  $\alpha = 0$

Figures 5-2 and 5-3 show the laminar calculation of  $5^\circ$  angle-of-attack. Again, a stagnation temperature of  $1,998^\circ\text{R}$  gives predictions greater than the data. However, with the modified stagnation conditions, the predictions are quite good, except on the leeward side. Figure 5-3 shows that this discrepancy occurs where viscous interactions would be expected to affect the inviscid pressure.

The solution for turbulent flow at  $\alpha = 10^\circ$  is shown in Figures 5-4 through 5-7. Figure 5-4 illustrates the effect of entropy swallowing and shows a significant increase in heating on the windward side compared to isentropic flow. The predictions with entropy swallowing are in good agreement with the experiment.

Like the laminar predictions, those for turbulent flow are poorer on the leeward side. Figures 5-6 and 5-7 compare the inviscid pressure and the experimental data. Again, the inviscid procedure underpredicts the pressure on the forecone and overpredicts the pressure on the aft cone because of viscous interaction effects on the leeward side.

The fourth case is a demonstration of the flight capabilities of 3DMEIT. This case used real gas properties, ablation modeling and a complex configuration with yaw stabilizers on the aft-cone. The patch geometry used in the calculation is shown in Figure 5-8. Figures 5-9 and 5-10 give the heat transfer on this configuration.

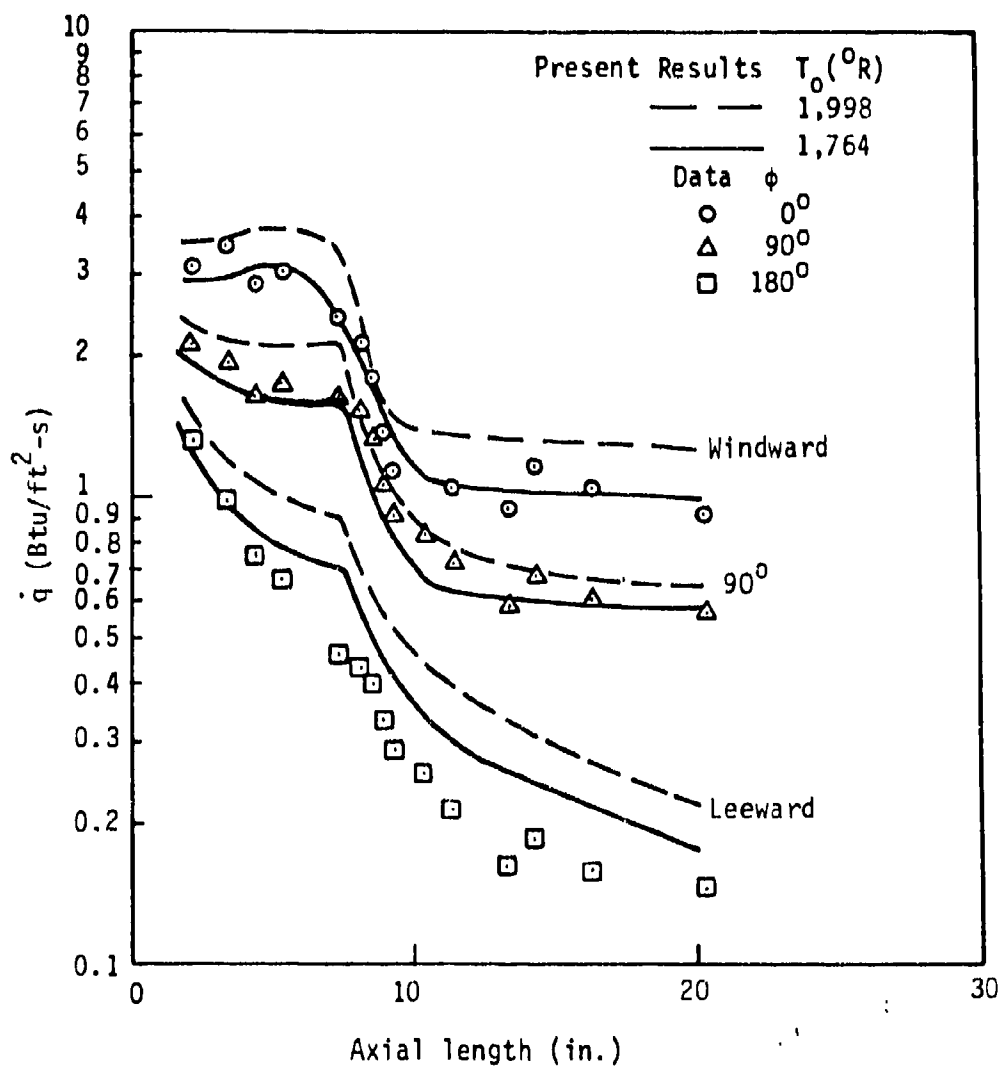


Figure 5-2. Axial Heat Transfer Distributions, Groups 96, 97, 136 to 158 Laminar,  $M = 10$ ,  $\alpha = 5$

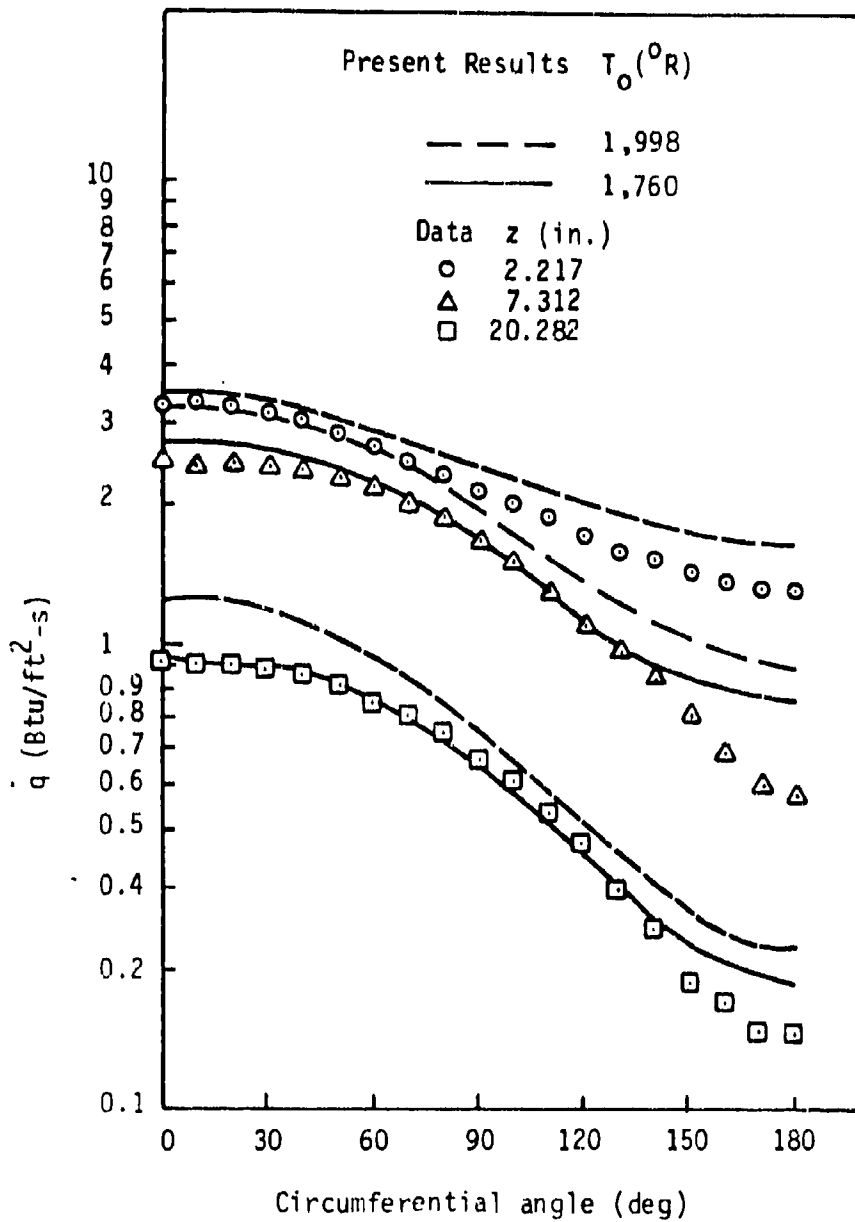


Figure 5-3. Circumferential Heat Transfer Distributions, Groups 96, 97, 136 to 158 Laminar,  $M = 10$ ,  $\alpha = 50$



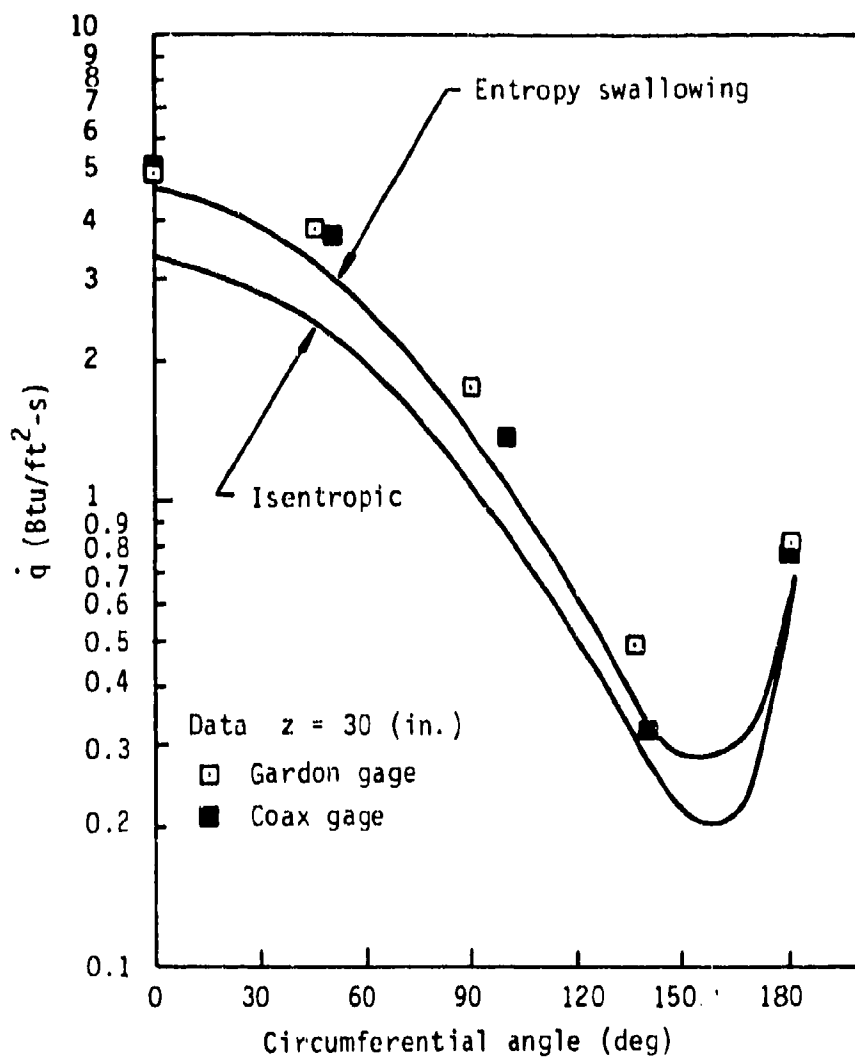


Figure 5-4. Circumferential Heat Transfer Distributions, Phase IV, Turbulent,  $M = 8$ ,  $\alpha = 10^\circ$

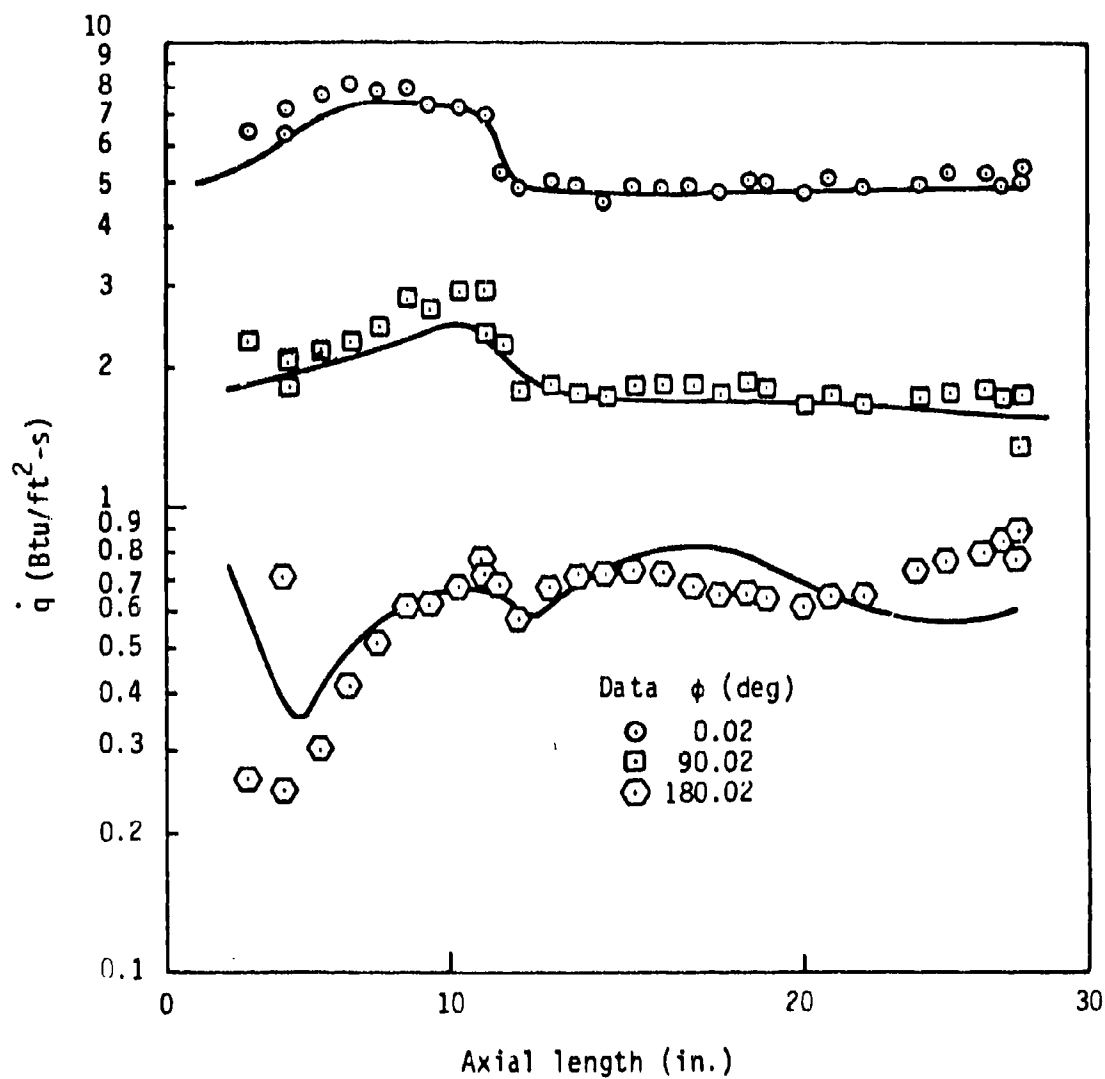


Figure 5-5. Axial Heat Transfer Distributions, Phase IV, Turbulent,  $M = 8$ ,  $\alpha = 100$

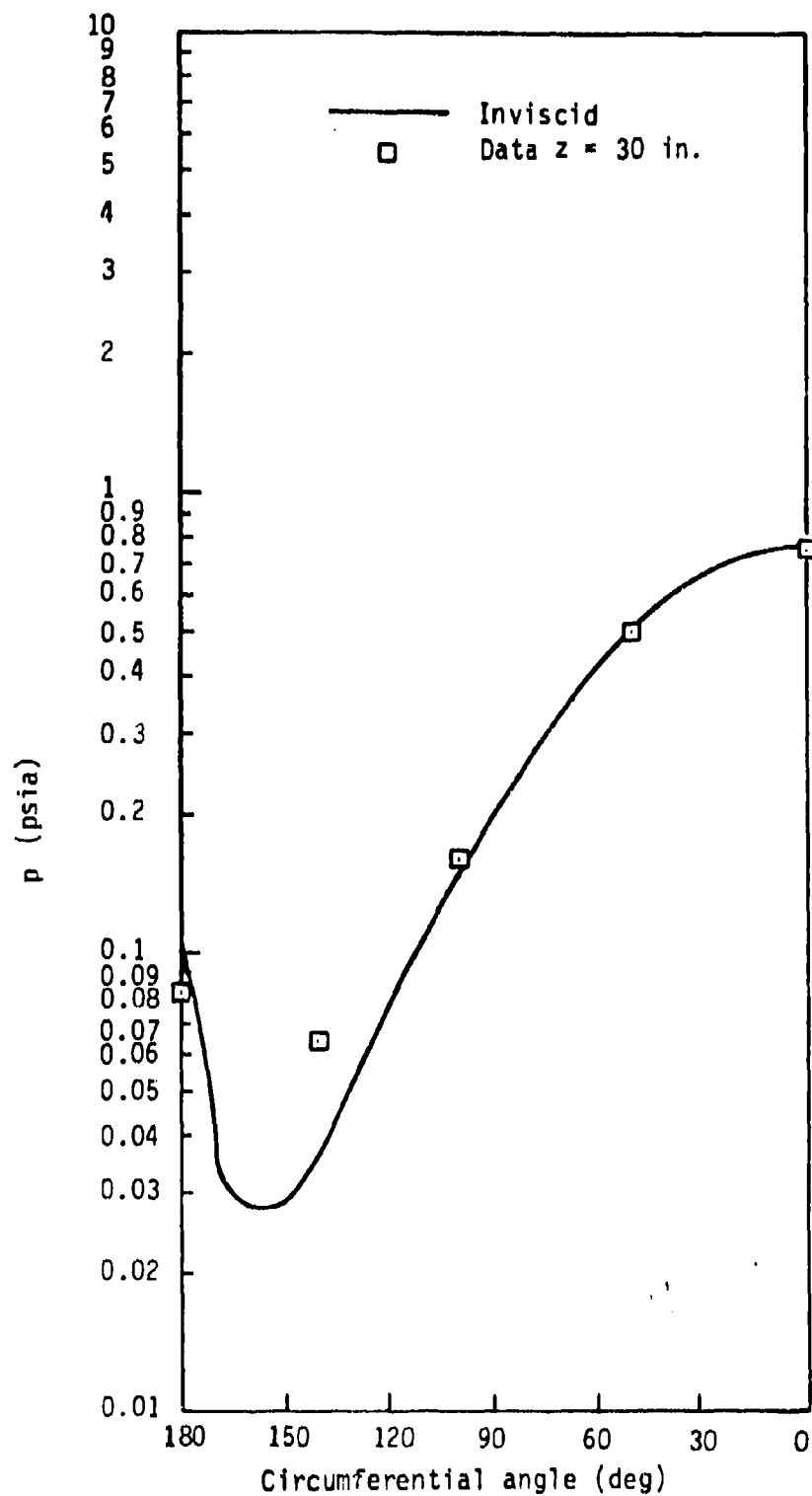


Figure 5-6. Inviscid Surface Pressure Distribution Compared with HYTAC Data,  $M = 8$ ,  $\alpha = 10^\circ$

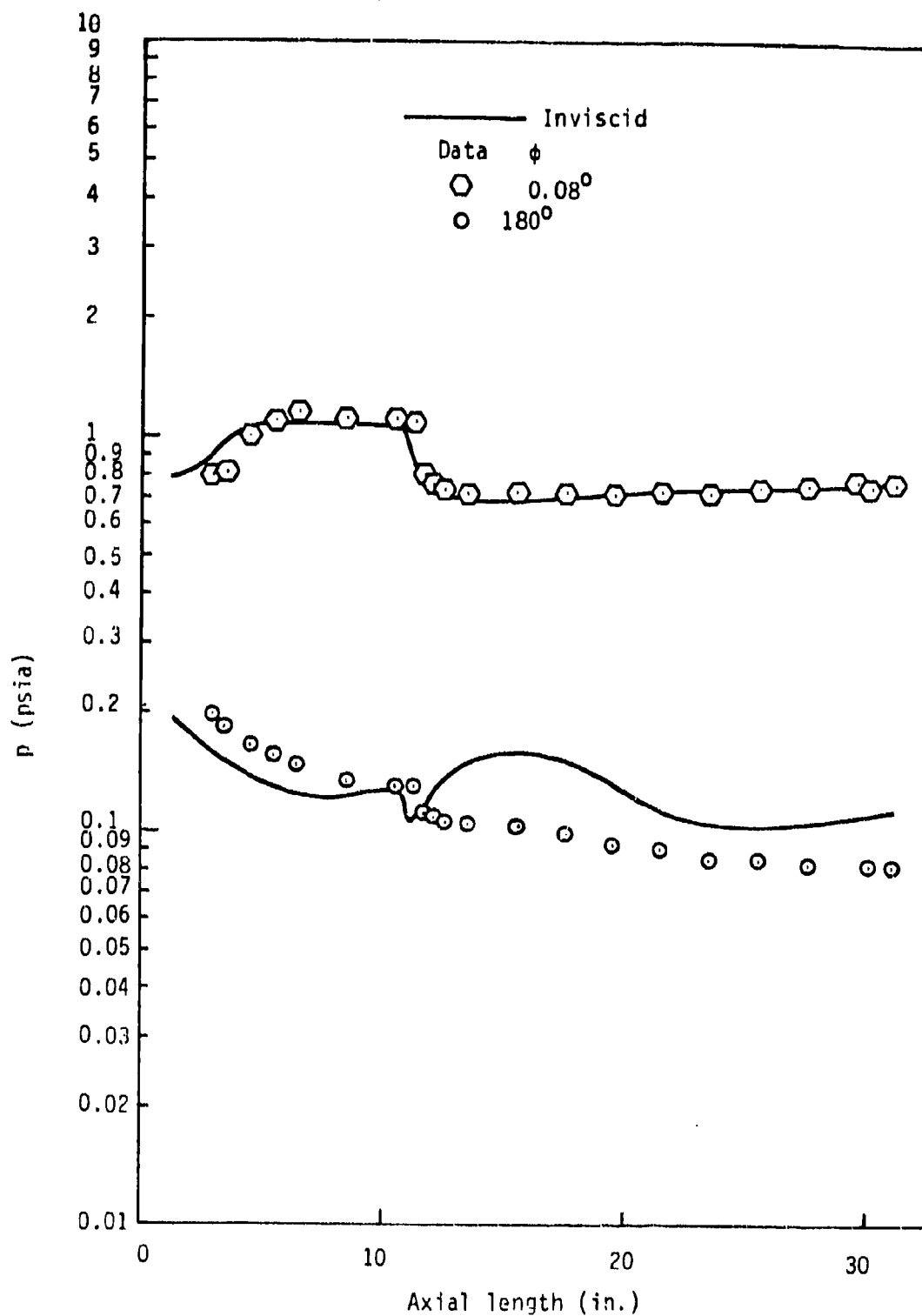


Figure 5-7. Inviscid Surface Pressure Distributions Compared with HYTAC Data,  $M = 8$ ,  $\alpha = 10^\circ$

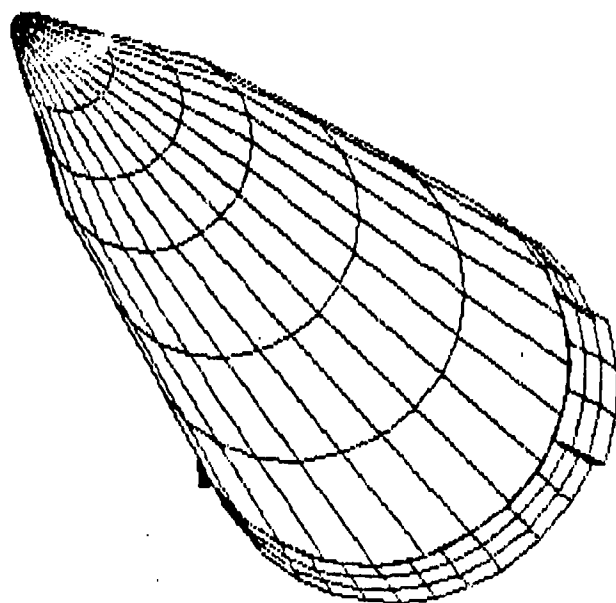


Figure 5-8. Flight Case Geometry with Yaw Stabilizers

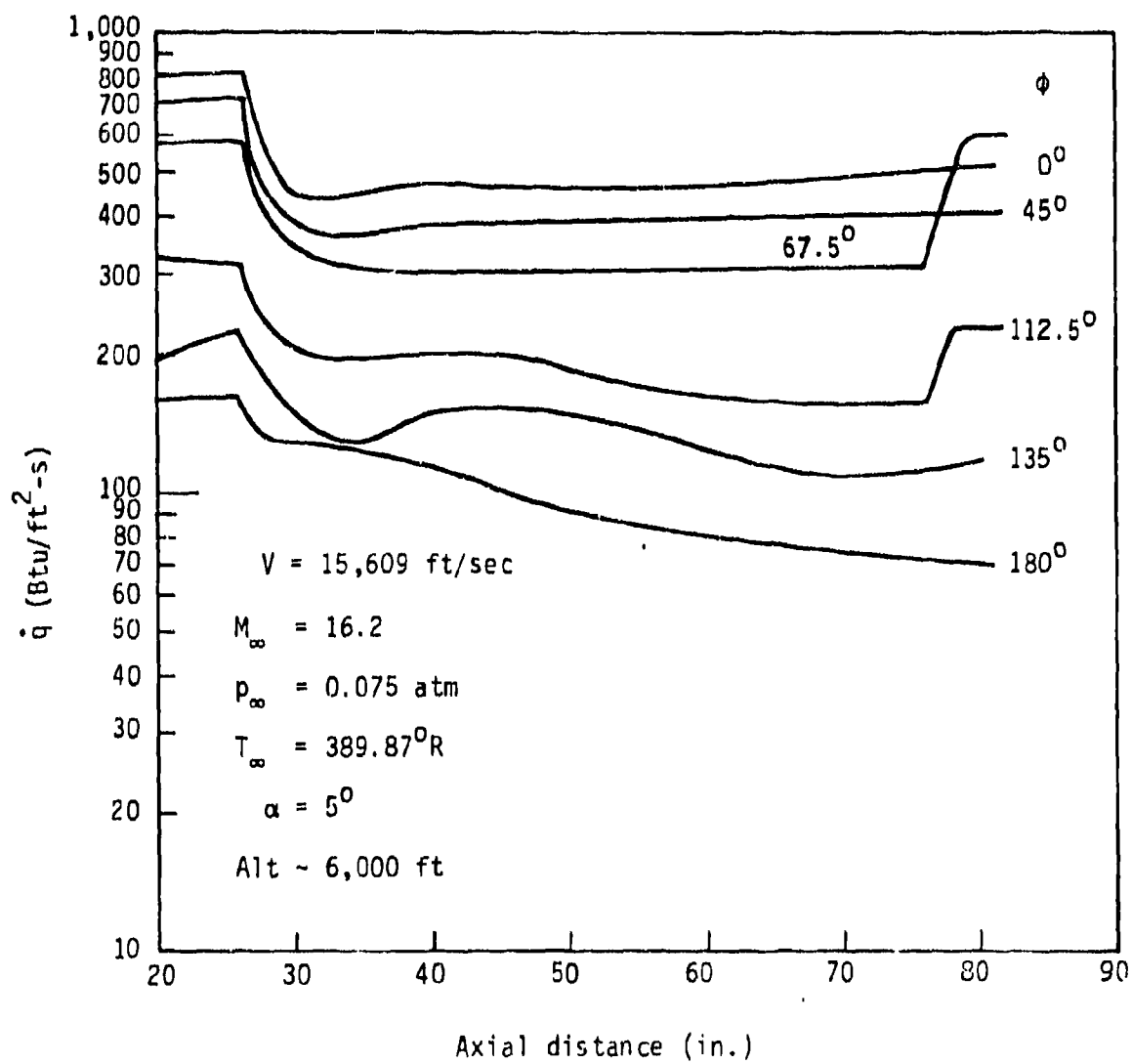


Figure 5-9. Predicted Axial Heating Distributions at Flight Conditions, 10.4/6.0 Biconic with Yaw Stabilizers,  $M = 16.2$ ,  $\alpha = 5^\circ$

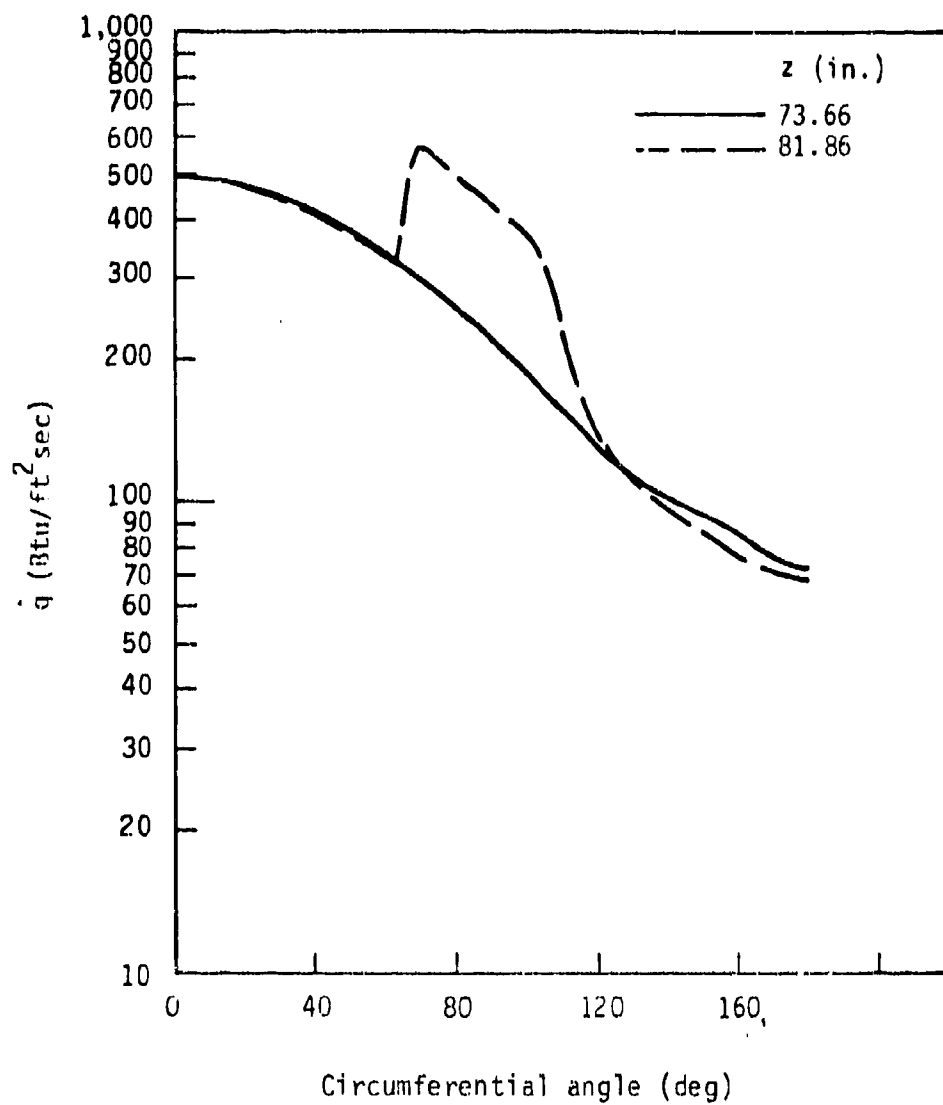


Figure 5-10. Predicted Circumferential Heating Distributions at Flight Conditions, 10.4/6.0 Biconic with Yaw Stabilizers,  $M = 16.2$ ,  $\alpha = 5^\circ$

## SECTION 6

### CONCLUSIONS

This report documents the initial efforts in the development of a coupled inviscid-boundary layer flow field solution procedure specifically designed to treat maneuvering reentry vehicles. The resultant code, which consists of the 3IS inviscid flow field code, a buffer code, and the 3DMEIT integral boundary layer code, can treat equilibrium air thermodynamics, laminar, transitional, or turbulent flows, and models the effects of surface roughness and mass addition from ablating heatshields on the boundary layer flow. Approximate models are provided to automatically determine the wall temperature and mass addition rates over the entire vehicle, for a variety of heatshield materials.

This coupled inviscid-boundary layer flow field procedure represents an extension to the capabilities of such techniques, obtained by making maximum use of the detailed inviscid flow field information available. Specifically, this approach has allowed:

- Direct calculation of the inviscid surface streamlines in the finite-difference inviscid afterbody code (3IS), and
- Accurate definition of the boundary layer edge properties through the use of the detailed inviscid flow field profiles near the wall, rather than using a stream tube mass balance technique (which is difficult to apply to a three-dimensional flow).



The flow field technique resulting from this effort provides a reliable method for engineering predictions of aerodynamic loads and heating on maneuvering reentry vehicles, while being efficient enough (through the use of an integral boundary layer procedure) to allow its routine use in both vehicle design and analysis.

It is recommended that future efforts be conducted to 1) extend the 3DMEIT method for body geometry description in order to enable calculations to be performed at sideslip and 2) allow for an interface between the buffer code and the output of a CM3DT solution in order to treat non-spherical, asymmetric nosetip shapes.

## SECTION 7

### REFERENCES

1. Harris, T. B., "Maneuvering Aerothermal Technology (MAT) Program, Evaluation of Parabolized Navier-Stokes Codes (U)," BMO TR-82- , October 1982 (Secret). ✓
2. Kyriss, C. L. and Harris, T. B., "A Three-Dimensional Flow Field Computer Program for Maneuvering and Ballistic Reentry Vehicles," 10th U. S. Navy Symposium on Aeroballistics, July 1975.
3. Daywitt, J., Brant, D., and Bosworth, F., "Computational Technique for Three-Dimensional Inviscid Flow Fields about Reentry Vehicles, Vol. I. Numerical Analysis," SAMSO TR-79-5, April 1978.
4. Brant, D., Wade, M., and Moran, J., "Computational Technique for Three-Dimensional Inviscid Flow Fields about Reentry Vehicles, Volume II. User's Manual, SAMSO TR-79-5, April 1978.
5. Hall, D. W., "Maneuvering Aerothermal Technology (MAT) Program, Evaluation of Inviscid Afterbody Flow Field Code (U)," BMO TR-82-32, February 1982 (Secret). ✓
6. Abbett, M. J., Dahm, T. J., Brink, D. F., Rafinejad, D., Wolf, C. J., "Passive Nosedip Technology (PANT II) Program, Volume II. Computer User's Manual: ABRES Shape Change Code (ASCC)," Aerotherm Report 76-224, October 1976.
7. Kwong, K., Suchsland, K., and Tong, H., "Momentum/Energy Integral Technique (MEIT) User's Manual," Aerotherm UM-78-86, February 1978.
8. Sandhu, S. S. and Murray, A. L., "Improved Capabilities of the ABRES Shape Change Code (ASCC 79)," Acurex Report TR-79-10/AS, July 1979.
9. Murray, A. L. and Saperstein, J. L., "User's Manual for the Updated ABRES Shape Change Code (ASCC 80)," Reentry Vehicle Technology Program Final Report, Volume 3, Part I, Acurex Report FR-80-38/AS, June 1980.
10. Murray, A. L., Beck, R. A. S., and Saperstein, J. L., "Maneuvering ABRES Shape Change Code (MASCC)," Reentry Vehicle Technology Program Final Report, Volume 3, Part II, BMO/TR-80-52, October 1980.
11. DeJarnette, F. R. and Hamilton, H. H., "Inviscid Surface Streamlines and Heat Transfer on Shuttle-Type Configurations," AIAA Paper No. 72-703, June 1972.
12. Hecht, A. M. and Nestler, D. E., "A Three-Dimensional Boundary-Layer Computer Program for Sphere-Cone Type Reentry Vehicles," AFFDL-TR-78-67, Volume 1, June 1978.

13. Hall, D. W., Dougherty, C. M., and Page, A. B., "Modifications to Inviscid Flow Field Codes," SAI Document No. SAI-067-81R-013, June 1980.
14. Lees, L., "Convective Heat Transfer with Mass Addition and Chemical Reactions," Combustion and Propulsion, Third AGARD Colloquium, Pergamon Press, New York, March 1958.
15. Bartlett, E. and Putz, K., "Heat and Mass Transfer Blowing Corrections for Charring Ablators; Part I: Equal Diffusion Coefficients," Sandia Laboratories Research Report SC-RR-71-0260, November 1971.
16. Costello, F. A., "Mass Transfer Cooling-Laminar Flat Plate Boundary Layer," GE-RESO TFM-8151-012, May 1963.
17. Laganelli, A. L., Fogaroli, R. P., and Martellucci, A., "The Effects of Mass Transfer and Angle of Attack on Hypersonic Turbulent Boundary Layer Characteristics," AFFDL TR-75-35, April 1975.
18. Jackson, M. D. and Baker, D. L., "Surface Roughness Effects, Part I, Experimental Data," Interim Report, PANT Program, Volume III, SAMS0-TR-74-86, June 1974.
19. Personal Communication with M. D. Jackson, ART Stagnation Point Heat Transfer Data, Aerotherm Division/Acurex Corporation, July 1976.
20. Persh, J., "A Procedure for Calculating the Boundary Layer Development in the Region of Transition from Laminar to Turbulent Flow," NAVORD Report 4438, March 1957.
21. Dahm, T. J., "Interim Modeling of Boundary Layers for Shape Change Codes," Interoffice Memorandum, Aerotherm Division/Acurex Corporation, September 1975.
22. Gilbert, L., "Carbon Phenolic Char Growth Study," GE-RESO PIR-FA-74-91-681, August 1974.
23. Fogaroli, R. P., "Carbon Phenolic Ablation at High Pressures," GE-RESO TFM-9151-HTT-061, May 1969.
24. Brant, D. N., "Investigation of Teflon Performance on the MK12 Nostip," GE-RESO PIR-9151-AE-104, December 1973.
25. Hayes, W. D. and Probstein, R. F., Hypersonic Flow Theory, Academic Press, pp. 333-341, 1959.
26. Timmer, H. G., et al., "Ablation Aerodynamics for Slender Reentry Bodies," AFFDL-TR-70-27, March 1970.

27. Carver, D. B., "Heat Transfer, Surface Pressure, and Flow-Field Survey Tests on a Blunt Biconic Model at Mach Number 10 -- Phase V," AEDC-TSR-79-V36, 1979.
28. Carver, D. B., "Heat Transfer, Surface Pressure and Flow-Field Surveys on Conic and Biconic Models with Boundary Layer Trips at Mach Number 8 -- Phases IV and VI," AEDC-TSR-80-V14, 1980.
29. Hall, D. W., "Performance Technology Program (PTP-S II), Volume III: Inviscid Aerodynamic Predictions for Ballistic Reentry Vehicles with Ablated Nosetips," BMO TR-81-1, September 1979.

ACUREX CORPORATION  
ATTN: Chuck Nardo  
485 Clyde Avenue  
Mountain View CA 94040

AEDC/DOT  
Arnold AFS TN 37389

Aerospace Corp  
ATTN: Al Robertson  
P.O. Box 95085  
Los Angeles, CA 90045

AFOSR/NA  
Bolling AFB DC 20332

AFWAL/FIMG  
Wright-Patterson AFB OH 45433

Arete Association  
ATTN: Steve Lubard  
P.O. Box 350  
Encino, CA 91316

AVCO CORPORATION  
ATTN: Noel Thyson  
201 Lowell Street  
Wilmington MA 01887

Ballistic Missile Defense Adv Tech Cntr  
ATTN: Jim Papadopoulos (ATC-M)  
P.O. Box 1500  
Huntsville AL 35807

CALSPAN CORPORATION-AEDC  
ATTN: Billy Griffith  
Arnold AFS TN 37389

General Dynamics - Convair  
ATTN: Archie Gay  
P.O. Box 80847  
San Diego, CA 92138

DWC/AFATL  
Eglin AFB FL 32542

GENERAL ELECTRIC COMPANY/RESO  
ATTN: Robert Neff  
3198 Chestnut Street  
Philadelphia PA 19101

Lockheed Missiles and Space Company  
ATTN: Gerald Chrusciel  
Dept 81-11  
P.O. Box 504  
Sunnyvale, CA 94086

Martin Marietta Corporation  
ATTN: John Carmichael  
P.O. Box 5837  
Orlando FL 32805

MCDONNELL DOUGLAS ASTRONAUTICS COMPANY  
ATTN: Jim Xerikos  
5301 Bolsa Avenue  
Huntington Beach CA 92647

Commander MICON  
U.S. Army Missile Research & Dev Command  
ATTN: R. A. Deep, DRDMI-TDK  
Redstone Arsenal AL 35809

NASA Langley Research Center  
ATTN: Dennis Bushnell  
Hampton VA 23665

NASA Ames Research Center  
ATTN: Paul Cutler  
Moffett Field, CA 94035

Naval Surface Weapons Center  
ATTN: Frank Moore  
Dahlgren VA 22448

Naval Surface Weapons Center  
ATTN: Carson Lyons  
White Oak Laboratory  
Silver Springs MD 20910

PDA ENGINEERING  
ATTN: Jim Dunn  
1560 Brookhollow Drive  
Santa Ana CA 92705

SANDIA LABORATORIES  
ATTN: Al Bustamonte  
P.O. Box 5800  
Albuquerque NM 87185

TRW Defense & Space Systems Group  
ATTN: Jack Ohrenberger, Bldg 4, Rm 1158  
One Space Park  
Redondo Beach CA 90278

TRW/E & DS - Ballistic Missile Div  
ATTN: Tony Lin  
ATTN: Dave Farlow  
P.O. Box 1310  
San Bernardino CA 92402